

# Personalized PCA: Decoupling Shared and Unique Features

Naichen Shi

Raed Al Kontar

*Department of Industrial & Operations Engineering*

*University of Michigan, Ann Arbor*

NAICHENS@UMICH.EDU

ALKONTAR@UMICH.EDU

## Abstract

In this paper, we tackle a significant challenge in PCA: heterogeneity. When data are collected from different sources with heterogeneous trends while still sharing some congruency, it is critical to extract shared knowledge while retaining unique features of each source. To this end, we propose personalized PCA (**PerPCA**), which uses mutually orthogonal global and local principal components to encode both unique and shared features. We show that, under mild conditions, both unique and shared features can be identified and recovered by a constrained optimization problem, even if the covariance matrices are immensely different. Also, we design a fully federated algorithm inspired by distributed Stiefel gradient descent to solve the problem. The algorithm introduces a new group of operations called generalized retractions to handle orthogonality constraints, and only requires global PCs to be shared across sources. We prove the linear convergence of the algorithm under suitable assumptions. Comprehensive numerical experiments highlight **PerPCA**'s superior performance in feature extraction and prediction from heterogeneous datasets. As a systematic approach to decouple shared and unique features from heterogeneous datasets, **PerPCA** finds applications in several tasks including video segmentation, topic extraction, and distributed clustering.

**Keywords:** Principal component analysis, personalization, heterogeneity.

## 1. Introduction

Principal component analysis (PCA) (F.R.S., 1901; Hotelling, 1933) unravels data features by finding a few principal components (PCs) from high dimensional data that best explain a large portion of the variance. Due to its effective feature learning and dimension reduction capability, PCA has seen immense success across various domains, including image processing (Deledalle et al., 2011; Jégou and Chum, 2012), time series modeling (Yang and Shahabi, 2004; Aguilera et al., 1999), bio-information (Reich et al., 2008; Novembre and Stephens, 2008), condition monitoring (Pozo et al., 2018; Li et al., 2018b) and many more.

However, since PCs are data-independent in standard PCA, an underlying assumption is that all data comes from homogeneous distributions. This assumption, however, is often challenged in various scenarios, including the Internet of Things (IoT), where data do not come from a single source but a large number of distinct edge devices (or clients). The edge devices, from smartphones to connected vehicles, usually operate in different environments and conditions (Kontar et al., 2017, 2018). The data collected by edge devices are also subject to changes in external conditions (Kontar et al., 2021) or user preferences (Kulkarni et al., 2020). Thus, it is common for the datasets to contain significant heterogeneity and even conflicting trends while sharing some congruity.

Standard PCA often does not work well when data homogeneity is not guaranteed (Oba et al., 2007; Hong et al., 2021). Few work endeavor to extend PCA philosophy to incorporate data heterogeneity. For example, Heterogeneous PCA (Oba et al., 2007) considers the case where data from different sources have different noise levels. They propose a reweighting technique to alleviate noise heteroscedasticity. Such approach is shown useful in identifying PCs from heteroscedastic noises. However, simply treating the discrepancy among datasets as different levels of noise might be inadequate to understand the intrinsic features within the data and encode both unique and shared features across devices and clients. As such, personalized solutions are needed.

To transmute the heterogeneity from a bane into a blessing, in this work we propose personalized PCA (**PerPCA**) that fits personalized features on each client in addition to common features shared by all clients. In our model, data are driven by several mutually orthogonal global (shared) and local (personalized) PCs. The global PCs model the common patterns among different datasets, while the local PCs model idiosyncratic features of one specific dataset. Global and local PCs work together to fit the observations. Figure 1 is an illustration of using homogeneous PCA and personalized PCA to fit two heterogeneous datasets. As shown in the figure, simply pooling together all data across datasets using homogeneous PCA will fail to encode the unique features within each dataset. This is specifically important when there is significant heterogeneity (see PCs in Homogeneous PCA). In contrast, personalized PCA aims at decoupling unique and shared features so that heterogeneity across data sources is accounted for. Note that, hereon, we will use client, edge device, source and local dataset interchangeably.

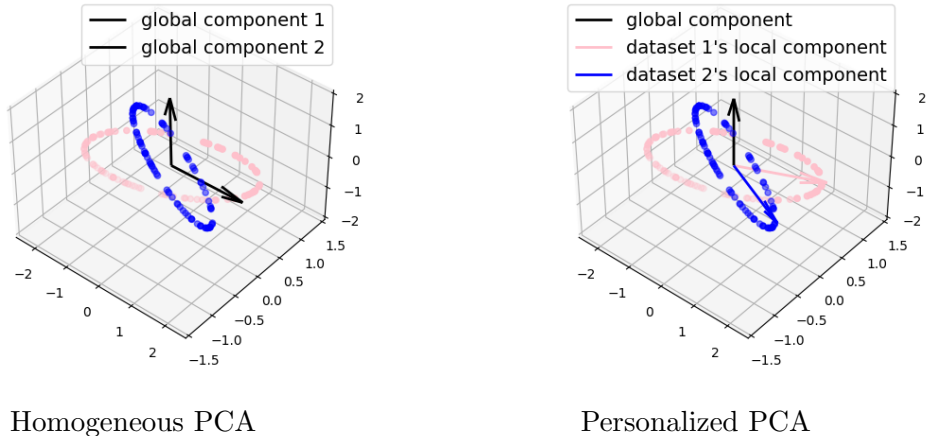


Figure 1: Comparison between homogeneous PCA (standard PCA) and personalized PCA (**PerPCA**). There are two datasets, one colored blue and the other pink. Dots represent the observations. Observations in one dataset are on a 2-dimensional plane. The black arrows represent the global PCs learned, and the colored arrows represent learned local principal components. Homogeneous PCA is the standard PCA on the pooled dataset. We will revisit the example in Sec. 7.

There are several benefits in personalization. Firstly, employing several local PCs to fit individual data patterns enables us to describe immensely heterogeneous trends in datasets accurately. Also, global PCs shared by all data can be estimated more precisely without being effected by disagreeing drifts from different sources. What’s more, disentangling local features from global ones provides a systematic and interpretable approach to analyze the heterogeneity structure of datasets, which is useful in several applications.

To enable personalized PCA, we propose an optimization framework to provably recover both global and local PCs from noisy observations. The objective is to minimize the empirical reconstruction error under orthogonality constraints. The formulation stands on solid theoretical ground: we prove that, under an identifiability condition, the optimal solution can recover the true global and local PCs.

Not only can the PCs be solved, but they can also be solved efficiently. We design an algorithm based on Stiefel manifold gradient descent that can be proved to converge linearly into the global optimum under mild conditions. The algorithm relies on a new operation called generalized retraction to handle the orthogonality constraints. It is worth noting that our algorithm is designed in a *federated manner*, as the need to share raw data or place all data in a central location is circumvented and only the updates of global PCs need to be shared across clients. Compared with centralized PCA where all datasets are uploaded to a central server where PCA is learned on the aggregated dataset, our algorithm reaps the benefits of distributed and federated analytics. Those include, communication, cost, storage and privacy benefits (Kontar et al., 2021). We will show the advantages of **PerPCA** over existing distributed PCA methods in Sec. 2.1.

Furthermore, **PerPCA** proposes a novel paradigm of decoupling shared and unique features. Its applications go beyond simple data dimension reduction. We show that **PerPCA** has remarkable performance in video segmentation and topic extraction tasks. Hence **PerPCA** opens up new possibilities for broader applications.

## 1.1 Main contributions

We summarize our contributions in the following:

- **Modeling:** We propose a personalized PCA model that learns both global and local features. These features can be recovered from observations by solving a nonconvex optimization problem designed to minimize reconstruction error.
- **Consistency:** We find that there exists a simple sufficient condition to ensure the identifiability of the global and local PCs: the maximum eigenvalue of the average of projections into local subspaces should be smaller than 1. We show that, under the identifiability condition, both global and local PCs can be estimated from noisy observations with an error upper bounded by  $O(\frac{1}{n})$ , where  $n$  is the number of observations on each client. As the error decreases to 0 when  $n$  approaches infinity, the error bound essentially implies the consistency of **PerPCA**. The analysis extends conventional matrix perturbation bounds (Bhatia, 1997; Vu et al., 2013) into personalized settings where the change on one client’s covariance matrix can effect the PC estimates on all clients.

- **Algorithm:** We design an algorithm based on Stiefel manifold gradient descent to obtain global and local PC estimates. The major difficulty for the algorithm is handling the orthogonality constraints. To tackle it, we introduce a correction step that relies on a group of operations called *generalized retractions*. A generalized retraction extends retraction in literature (Edelman et al., 1998) as it is defined on the entire  $\mathbb{R}^{d \times r}$  rather than the Stiefel manifold  $St(d, r)$ . In our algorithm, clients only need to share iterates of global PCs, thus preserving privacy and minimizing communication costs.
- **Convergence:** The proposed algorithm has a local linear convergence rate. To our best knowledge, this is the first theoretical guarantee for an algorithm that simultaneously learns global and local PCs. Interestingly, the convergence is faster when local PCs are more heterogeneous. On the technical side, we introduce a novel Lyapunov function to study distributed Stiefel manifold gradient descent with generalized retractions. The convergence analysis also hinges on a new method to derive a lower bound of the minimum eigenvalue of a specific type of positive definite matrices. The lower bound is novel and cannot be inferred from previous works, like the Gershgorin circle theorem. The technical novelties thus enrich existing literature and offer standalone values.
- **Numerical results:** Empirical evidence on both synthetic and real-life datasets confirms **PerPCA**'s ability to decouple shared and unique features. Also, **PerPCA** has exciting applications in video segmentation and topic extraction. For instance, on video segmentation tasks, **PerPCA** has significant advantages over the popular **Robust PCA** (Candes et al., 2011) when heterogeneity patterns are not sparse.

## 1.2 Organization

The paper is organized as follows: we review related work and introduce notations in Sec. 2. In Sec. 3, we propose the formulation of **PerPCA** and link it with constrained optimization. Sec. 4 includes the theoretical analysis on identifiability and consistency. A federated algorithm to solve **PerPCA** is developed in Sec. 5 and its convergence guarantee is established in Sec. 6. Numerical experimentation results are demonstrated in Sec. 7. Finally, Sec. 8 concludes the paper with a brief discussion. Readers mainly interested in implementation and applications of **PerPCA** can focus on Sections 3, 5, and 7.

## 2. Preliminaries

In this section, we will review related work in literature and introduce notations.

### 2.1 Related work

**Structural PCA** Structural PCA attempts to build structural models for data and noise. Research on structural PCA abounds. A seminal algorithm along this line is **Robust PCA** (Candes et al., 2011). The authors point out that traditional PCA is sensitive to noise in the observations, and tackle this issue by decomposing an observation matrix  $\mathbf{Y}$  into a low rank part  $\mathbf{L}$ , and a sparse noise part  $\mathbf{S}$ :  $\mathbf{Y} = \mathbf{L} + \mathbf{S}$ . The low-rank matrix  $\mathbf{L}$  corresponds to the signal, and  $\mathbf{S}$  represents the noise. It turns out that the two parts can be exactly identified under regularity conditions with carefully designed algorithms. **Robust PCA** has

become a useful technique in image denoising and video processing (Bouwman et al., 2018), collaborative filtering (Xu et al., 2012), and many more. Sparse PCA (Zou et al., 2006) adds sparse constraints on the principal components, encouraging each principal component to depend on a minimal number of variables. While these methods are powerful in handling large noise or high dimensional data, they mainly analyze homogeneous data.

Several algorithms are also proposed to leverage variance heterogeneity in different samples. Heterogeneous component analysis (HCA) (Oba et al., 2007) assumes data come from different sources with different levels of noise. To better learn the PCs with heteroscedastic variance, HCA reweights the empirical loss of each observation according to the inverse of its variance so that noisier samples contribute less to the total loss. Hong et al. (2021) calculates the optimal weights in the asymptotic case by considering the signal-to-noise ratio. Though these methods have superior performance compared to uniform weighting PCA, heterogeneity among different sources is only modeled by the noise magnitude.

**Distributed PCA** There has been a recent push to calculate PCs on distributed devices. Oftentimes, the clients/edge devices use their local data to estimate PCs and communicate with a central server to update their estimates. One round of information exchange between clients and the central server is referred to as a communication round. Based on the number of communication rounds between edge devices and the server, research can be roughly divided into two categories (1) those that require only one round of communication and (2) those that require multiple rounds of communication.

For one-shot PCA algorithms, clients estimate PCs from local datasets and send summary statistics to the server. The server then analyzes the aggregated statistics to calculate the PCs of the entire dataset. There are several ways for the server to calculate PCs. Qu et al. (2002) proposes a method to reconstruct the aggregated covariance matrix by averaging the clients’ covariance matrices approximated by a few top PCs. Global PCs can be obtained by solving top eigenvalues of the averaged covariance matrix. `distPCA` (Fan et al., 2019) provides an alternative approach, where the server stacks locally calculated PCs into a large matrix and runs another PCA on the stacked matrix. Liang et al. (2014) uses a similar method, where clients calculate a singular value decomposition (SVD) of the local observation matrix, then send the singular values and singular vectors to the server. The server stacks the scaled singular vectors and runs SVD on the stacked matrix. Federated PCA (Grammenos et al., 2020) considers streaming data applications where edge devices have limited memory budgets. In their work, locally estimated subspaces are hierarchically merged to form the global subspace. Feldman et al. (2013) also focuses on streaming data and reduces large datasets into a small dataset. In spite of the reductions in communication or memory cost, these algorithms are often not guaranteed to recover true PCs exactly. Also, they are build upon homogeneity assumptions and neglect statistical heterogeneity among the distributed datasets.

To obtain more refined estimates of PCs from distributed datasets, a series of works propose to use multiple rounds of communication (Chen et al., 2020; Garber et al., 2017; Huang and Pan, 2020; Alimisis et al., 2021). Among them, Chen et al. (2020) and Garber et al. (2017) design PC updates by shift-and-invert iterations. The shift-and-inverse method (Garber and Hazan, 2015) reformulates inverse power iteration as an unconstrained convex optimization problem and uses gradient-based iterative algorithms to solve it. With similar rationale, Chen et al. (2020) applies the shift-and-invert formulation to distributed settings

and applies distributed Newton methods to solve for the top eigenvector of the covariance matrix. Then the covariance matrix is deflated to calculate the subsequent eigenvectors. Besides shift-and-invert iterations, manifold optimization is also employed for PCA. Huang and Pan (2020) uses distributed Riemann optimization to find top PCs from homogeneous datasets. To further reduce communication costs, Alimisis et al. (2021) combines quantized distributed optimization and Riemannian gradient descent with an exponential map to calculate the leading eigenvectors of the covariance matrix. These methods usually treat the difference among clients’ covariance matrices as errors. Thus when datasets are heterogeneous, the errors are large, and these algorithms can fail to retrieve true PCs.

**Gradient descent on manifolds** The centralized version of gradient descent on manifolds, or Riemannian gradient descent, has been well-studied (Absil et al., 2008; Boumal, 2022). Algorithms based on exponential mappings (Edelman et al., 1998) can achieve convergence rates comparable to their Euclidean counterparts. Since exponential mappings are expensive to compute, there are algorithms that replace them with retractions. (Tang, 2019) presents an elegant framework for analyzing kPCA by Riemannian gradient descent with Cayley retraction. This work proves the local linear convergence of Stiefel gradient descent (St-GD hereon) and also shows that the algorithm can exactly recover the top eigenspaces.

Recent years have also seen advances in distributed manifold optimization. Chen et al. (2021a,b) introduces a simple distributed St-GD algorithm that minimizes a general objective on the manifold. In each round, clients use St-GD on the local objectives and send the updated variables to the server, then the server averages the received update and applies a retraction. The algorithm is guaranteed to converge into stationary points with a sublinear rate.

**PerPCA** also exploit St-GD to solve PCs. However, our algorithm refines simple manifold optimization as it optimizes local and global PCs simultaneously and faces additional orthogonality constraints between global and local PCs. **PerPCA** thus introduces a special correction step to handle such constraints. This is done by defining a new retraction measure we name as a *generalized retraction* defined on the entire  $\mathbb{R}^{d \times r}$  rather than the tangent bundle of Stiefel manifold  $St(d, r)$ .

We should note that among all the algorithms discussed, only **PerPCA** models distributed datasets by global and local PCs. Thus it brings unique advantages in decoupling local and global features from highly heterogeneous datasets. Besides, there are several additional benefits of **PerPCA** in convergence and computation compared with typical existing models. In terms of convergence, **PerPCA** converges into stationary points of the empirical reconstruction loss and is guaranteed to recover true PCs exactly with proper initialization. The algorithm does not involve a computational intensive exponential map and can solve  $k$  PCs at one time. Most importantly, **PerPCA** is fully federated, meaning clients only need to share only few global PCs that encode shared and not unique features. The comparisons of **PerPCA** and several typical PCA algorithm is summarized in Table. 1.

## 2.2 Notations

We first introduce needed notations in this subsection. For a  $d$ -dimensional vector  $\mathbf{x}$ , we use  $\|\mathbf{x}\|$  to denote its 2-norm. The inner product of two vectors is defined as a standard inner

Method	Source	Exact convergence	kPCA	Federated	Personalized
Robust PCA	(Candes et al., 2011)	✓	✓	✗	✗
distPCA	(Fan et al., 2019)	✗	✓	✓	✗
Distri-Eigen	(Chen et al., 2020)	✓	✗	✓	✗
CEDRE	(Huang and Pan, 2020)	✓	✗	✓	✗
PCA by St-GD	(Tang, 2019)	✓	✓	✗	✗
PerPCA	<b>ours</b>	✓	✓	✓	✓

Table 1: Comparison of related work. Metrics included and their definitions are: (i) Exact convergence: the algorithm can recover top subspaces of sample covariance matrix exactly (ii) kPCA: the algorithm can calculate the subspace spanned by top  $k$  PCs, instead of one single component (iii) Federated: the algorithm can be done in a distributed fashion where raw data remains where it is generated on the edge and only focused updates need to be shared across clients (iv) Personalized: the algorithm encodes both shared and unique features across all datasets.

product in Euclidean space:  $\langle \mathbf{x}, \mathbf{y} \rangle = \mathbf{x}^T \mathbf{y}$ . We use  $\mathbf{I}_d$  to denote identity matrix in  $\mathbb{R}^d$ . We sometimes omit the subscript  $d$  if the dimension is clear from the context. For a real matrix  $A \in \mathbb{R}^{m \times n}$ , we use  $\|A\|_F$  to denote its Frobenius norm  $\|A\|_F = \sqrt{\sum_{i=1}^n \sum_{j=1}^m A_{ij}^2}$ ,  $\|A\|_{op}$  to denote its operator norm  $\|A\|_{op} = \max_{\mathbf{v} \in \mathbb{R}^n, \|\mathbf{v}\|=1} \|A\mathbf{v}\|$ . For two matrices  $A, B \in \mathbb{R}^{m \times n}$ , we define their inner product as  $\langle A, B \rangle = \sum_{i=1}^n \sum_{j=1}^m A_{ij} B_{ij} = \text{Tr}(A^T B)$

If  $A \in \mathbb{R}^{n \times n}$  is symmetric positive definite (PSD), it has an eigen-decomposition  $A = \mathbf{U} \mathbf{D} \mathbf{U}^T$ , where  $\mathbf{D}$  is  $n$  by  $n$  diagonal matrix whose diagonal entries are all positive,  $\mathbf{U}$  is a  $n$  by  $n$  unitary matrix. Then for  $p \in \mathbb{R}$ , the  $p$ -th power of  $A$  is defined as  $A^p = \mathbf{U} \mathbf{D}^p \mathbf{U}^T$ . For a square matrix  $A \in \mathbb{R}^{n \times n}$ , we use  $\lambda_{\min}(A)$  and  $\lambda_{\max}(A)$  to denote the minimum and maximum eigenvalue of  $A$ . Similarly, we use  $\lambda_1(A)$ ,  $\lambda_2(A)$ , ...,  $\lambda_n(A)$  to denote  $n$  eigenvalues of  $A$  in the descending order. We use  $\|A\|_{op}$  and  $\lambda_{\max}(A)$  interchangeably when  $A$  is symmetric PSD.

For a matrix  $A \in \mathbb{R}^{m \times n}$ , we use  $\text{vec}(A) \in \mathbb{R}^{mn}$  to denote its vectorization, i.e. the vector formed by concatenating all the column vectors in  $A$ .  $\text{col}(A)$  is the linear subspace spanned by all column vectors of  $A$ . For two matrices  $A, B \in \mathbb{R}^{m \times n}$ , we use  $A \oplus B$  to denote the direct sum of  $A$  and  $B$ . For two matrices  $A \in \mathbb{R}^{m_1 \times n_1}$  and  $B \in \mathbb{R}^{m_2 \times n_2}$ , we use  $A \otimes B$  to denote the direct product. These definitions are standard in literature.

For a matrix  $A \in \mathbb{R}^{m \times n}$ , we use  $A_{i_1:i_2, j_1:j_2}$  to denote the submatrix of  $A$  formed by picking the  $i_1, i_1 + 1 \dots i_2$ -th row and  $j_1, j_1 + 1 \dots j_2$ -th column of  $A$ . For two matrices  $A \in \mathbb{R}^{m \times n_1}$  and  $B \in \mathbb{R}^{m \times n_2}$ ,  $[A, B] \in \mathbb{R}^{m \times (n_1 + n_2)}$  is defined as the concatenation of  $A$  and  $B$  by row.

### 3. What is PerPCA?

#### 3.1 Motivation

Suppose we have  $N$  clients (i.e. data sources), each with an unlabeled dataset  $\{\mathbf{Y}_{(i)}\}_{i=1}^N$ , where  $\mathbf{Y}_{(i)}$  is a  $d$  by  $n_i$  matrix.  $d$  is the dimension of data, and  $n_i$  is the number of datapoints on client  $i$ . The datasets  $\{\mathbf{Y}_{(i)}\}_{i=1}^N$  have commonalities, but also possess client-level distinctive features. The task is to find a few low dimensional common and unique features that best characterize the observations from the high dimensional data  $\{\mathbf{Y}_{(i)}\}_{i=1}^N$ .

Standard PCA uses a small number of principal components (PCs) to explain all the variations in  $\{\mathbf{Y}_{(i)}\}_{i=1}^N$ . Such treatment ignores the client-to-client difference in the observations. The present IoT system usually consists of distributed edge devices (clients) that operate on extremely heterogeneous environments. It is thus important to consider different features on different clients. As a more capacious description of the data, we consider the model where local observations are driven by  $r_1$  global PCs and  $r_{2,(i)}$  local PCs. More specifically, on device  $i$ , the observation  $\mathbf{y}_{(i)}$  is generated from

$$\mathbf{y}_{(i)} \sim \sum_{q=1}^{r_1} \phi_{(i),q} \mathbf{u}_q + \sum_{q=1}^{r_{2,(i)}} \varphi_{(i),q} \mathbf{v}_{(i),q} + \boldsymbol{\epsilon}_{(i)} \quad (1)$$

where  $\phi_{(i),q}$ 's and  $\varphi_{(i),q}$ 's are coefficients, or scores in PCA terminology.  $\mathbf{u}_q$ 's are global PCs,  $\mathbf{v}_{(i),q}$ 's are local PCs, and  $\boldsymbol{\epsilon}_{(i)}$  are i.i.d. noise vectors.  $r_1$  is the number of global PCs, and  $r_{2,(i)}$  is the number of local PCs on client  $i$ . We allow  $\mathbf{v}_{(i),q}$ 's to be client-dependent, while enforcing  $\mathbf{u}_q$ 's to remain the same across all clients. Naturally,  $\mathbf{u}_q$ 's encode the information shared by all participants, while  $\mathbf{v}_{(i),q}$ 's can describe distinctive patterns on each client.

Similar to standard PCA, different principal components need to be orthonormal:

$$\begin{cases} \mathbf{u}_{q_1}^T \mathbf{u}_{q_2} = \delta_{q_1,q_2} \\ (\mathbf{v}_{(i),q_1})^T \mathbf{v}_{(i),q_2} = \delta_{q_1,q_2}, \forall q_1, q_2, \forall i = 1, \dots, N \end{cases} \quad (2)$$

where  $\delta_{q_1,q_2}$  is the Kronecker delta. In addition to (2), we further require that the global and local features are orthogonal:

$$\mathbf{u}_{q_1}^T \mathbf{v}_{(i),q_2} = \delta_{q_1,q_2}, \forall i = 1, \dots, N \quad (3)$$

The orthogonality constraints imply that global and local PCs are independent, thus can potentially be decoupled.

(1) is an interpretable linear model that naturally incorporates both common and individual features on different clients. It is useful in applications where disentangling global and local features is important. The development of IoT and recent advancements in federated and distributed analytics presents numerous such applications including time series data, image and video data, and language data. We will show the efficacy of (1) on several examples.

### 3.2 Method

The task of **PerPCA** is to recover global and local PCs from observations  $\{\mathbf{Y}_{(i)}\}_{i=1}^N$ . We can write global and local PCs into matrix form:

$$\begin{cases} \mathbf{U} = [\mathbf{u}_1, \dots, \mathbf{u}_{r_1}] \\ \mathbf{V}_{(i)} = [\mathbf{v}_{(i),1}, \dots, \mathbf{v}_{(i),r_{2,(i)}}] \end{cases} \quad (4)$$

and solve for  $\mathbf{U}$  and  $\mathbf{V}_{(i)}$ 's by minimizing the empirical reconstruction loss:

$$\begin{aligned} \min_{\mathbf{U}, \{\mathbf{V}_{(i)}\}_{i=1, \dots, N}} \quad & \frac{1}{2} \sum_{i=1}^N \frac{1}{n_i} \left\| \mathbf{Y}_{(i)} - \hat{\mathbf{Y}}_{(i)} \right\|_F^2 \\ \text{subject to} \quad & \mathbf{U}^T \mathbf{U} = \mathbf{I}, \mathbf{V}_{(i)}^T \mathbf{V}_{(i)} = \mathbf{I}, \mathbf{V}_{(i)}^T \mathbf{U} = \mathbf{0}, \forall i \end{aligned} \quad (5)$$

where  $\hat{\mathbf{Y}}_{(i)}$  is the statistical fit for client  $i$ 's data given PCs  $\mathbf{U}$  and  $\mathbf{V}_{(i)}$ :

$$\hat{\mathbf{Y}}_{(i)} = \mathbf{U} \mathbf{U}^T \mathbf{Y}_{(i)} + \mathbf{V}_{(i)} \mathbf{V}_{(i)}^T \mathbf{Y}_{(i)} \quad (6)$$

Intuitively, in (5), we look for the PCs so that the predicted  $\hat{\mathbf{Y}}_{(i)}$  can best fit the distributed datasets. The objective (5) has another interpretation: by some algebra, we can transform the objective (5) into:

$$\begin{aligned} \max_{\mathbf{U}, \{\mathbf{V}_{(i)}\}_{i=1, \dots, N}} \quad & \frac{1}{2} \sum_{i=1}^N \left[ \text{Tr}(\mathbf{U}^T \mathbf{S}_{(i)} \mathbf{U}) + \text{Tr}(\mathbf{V}_{(i)}^T \mathbf{S}_{(i)} \mathbf{V}_{(i)}) \right] \\ \text{subject to} \quad & \mathbf{U}^T \mathbf{U} = \mathbf{I}, \mathbf{V}_{(i)}^T \mathbf{V}_{(i)} = \mathbf{I}, \mathbf{V}_{(i)}^T \mathbf{U} = \mathbf{0}, \forall i \end{aligned} \quad (7)$$

where  $\mathbf{S}_{(i)}$  is defined as the data covariance matrix:

$$\mathbf{S}_{(i)} = \frac{1}{n_i} \mathbf{Y}_{(i)} \mathbf{Y}_{(i)}^T$$

From (7), it is clear that **PerPCA** attempts to find global and local low dimensional subspaces that best align with the data covariance matrix. We will study objective (7) from here on.

For simplicity, we introduce

$$f_i(\mathbf{U}, \mathbf{V}_{(i)}) = \frac{1}{2} \text{Tr}(\mathbf{U}^T \mathbf{S}_{(i)} \mathbf{U}) + \frac{1}{2} \text{Tr}(\mathbf{V}_{(i)}^T \mathbf{S}_{(i)} \mathbf{V}_{(i)}) \quad (8)$$

and

$$f(\mathbf{U}, \{\mathbf{V}_{(i)}\}) = \sum_{i=1}^N f_i(\mathbf{U}, \mathbf{V}_{(i)}) \quad (9)$$

Then (7) transforms to maximizing  $f$  under orthonormality constraints. Notice that though  $f$  and  $f_i$ 's are convex, the constraint in (7) is nonconvex, thus the problem is also nonconvex.

The nonconvex formulation (7) appears difficult to analyze and solve. In the following sections, we will delve into the identifiability and optimization of (7). Fortunately, our results show that under minimal conditions, (7) can be solved efficiently, and the optimal solution can recover the true PCs.

#### 4. Are Global and Local PCs Identifiable?

Given the formulation (7), one may ask whether it is possible to identify the true local and global PCs by solving (7).

Apparently, global and local PCs cannot be decoupled in every case. As a simple counterexample, suppose all local PCs are the same. Then distinguishing local PCs from global ones becomes impossible, as they all can maximize the explained variance in (7). The edifying counterexample poses the fundamental question of model identifiability. Therefore we need to find out which data instances are identifiable. In the following, we will introduce an identifiability condition, then establish the relationship between the estimated and true PCs.

We restrict our analysis to recovering the subspace spanned by top PCs (Bhatia, 1997). Therefore we introduce the projection matrix notation  $\mathbf{P}_U$ : if  $\mathbf{U}$  is a matrix with orthonormal columns, i.e.  $\mathbf{U}^T \mathbf{U} = \mathbf{I}$ , then  $\mathbf{P}_U$  is defined as  $\mathbf{P}_U = \mathbf{U} \mathbf{U}^T$ . We use  $\mathbf{\Pi}_g$  to denote the projection matrix to the true global eigenspace, i.e.  $\mathbf{\Pi}_g = \mathbf{P}_{\mathbf{U}_{\text{true}}}$ , where  $\mathbf{U}_{\text{true}}$  are the true top global PCs. Also, we use  $\mathbf{\Pi}_{(i)}$  to denote the projection matrix to the local eigenspaces,  $\mathbf{\Pi}_{(i)} = \mathbf{P}_{\mathbf{V}_{(i),\text{true}}}$ , where  $\mathbf{V}_{(i),\text{true}}$  are the true top local PCs on client  $i$ .

Remember we model global and local PCs as mutually vertical features, such property can be formally characterised by the following assumption.

**Assumption 4.1** (*Orthogonality of global and local PCs*) Let  $\mathbf{\Pi}_g$  be the global projection matrix,  $\mathbf{\Pi}_{(i)}$ 's the local projection matrices. We assume the population covariance matrix on client  $i$ ,  $\mathbf{\Sigma}_{(i)}$ , has the following structure:

$$\mathbf{\Sigma}_{(i)} = \mathbf{\Sigma}_{(i),g} \oplus \mathbf{\Sigma}_{(i),l} \quad (10)$$

where  $\mathbf{\Sigma}_{(i),g}$  corresponds to variance contributed by global components:  $\text{col}(\mathbf{\Pi}_g) \subseteq \text{col}(\mathbf{\Sigma}_{(i),g})$ , and  $\mathbf{\Sigma}_{(i),l}$  corresponds to variance contributed by local components:  $\text{col}(\mathbf{\Pi}_{(i)}) \subseteq \text{col}(\mathbf{\Sigma}_{(i),l})$ .  $\oplus$  is the direct sum.

As the counterexample suggests, assumption 4.1 alone is insufficient to guarantee identifiability of global and local PCs. To distinguish them, we need another identifiability condition. To rule out the counterexample, local PCs should differ from each other. Thus  $\mathbf{\Pi}_{(i)}$  also should be different for them to be detectable. We resort to the maximum eigenvalue of average local projection matrices to characterize such difference. The assumption 4.2 is a formal statement of the identifiability condition.

**Assumption 4.2** (*Identifiability*) Let  $\mathbf{\Pi}_g$  be the global projection matrix,  $\mathbf{\Pi}_{(i)}$ 's the local projection matrices. We assume there exists a positive constant  $\theta \in (0, 1)$  such that:

$$\lambda_{\max} \left( \frac{1}{N} \sum_{i=1}^N \mathbf{\Pi}_{(i)} \right) \leq 1 - \theta \quad (11)$$

The constant  $\theta$  characterizes the difference between local principal spaces. When  $\theta$  is larger, the local eigenspaces are more heterogeneous. And when  $\theta$  is smaller, the local eigenspaces are more similar. As an extreme case, if all  $\mathbf{\Pi}_{(i)}$ 's are identical,  $\frac{1}{N} \sum_{i=1}^N \mathbf{\Pi}_{(i)}$  is still a projection, thus its maximum eigenvalue is 1 and  $\theta$  becomes zero.

It turns out that the identifiability assumption 4.2 is sufficient to ensure identifiability. The following perturbation bound shows that when the sample covariance matrix is close to the population covariance matrix, we can obtain relative accurate estimates of global and local eigenspaces through solving (7).

**Theorem 1** *Under assumption 4.1 and 4.2, and if there exists a constant  $\delta > 0$ , such that  $\min\{\lambda_{r_1}(\Sigma_{(i),g}), \lambda_{r_{2,(i)}}(\Sigma_{(i),l})\} - \max\{\lambda_{r_1+1}(\Sigma_{(i),g}), \lambda_{r_{2,(i)}+1}(\Sigma_{(i),l})\} \geq \delta$  for all  $i$ , we have:*

$$\|P_{\hat{U}} - \Pi_g\|_F^2 + \frac{1}{N} \sum_{i=1}^N \|P_{\hat{V}_{(i)}} - \Pi_{(i)}\|_F^2 \leq \frac{4}{\theta\delta^2} \frac{1}{N} \sum_{i=1}^N \|\Sigma_{(i)} - S_{(i)}\|_F^2 \quad (12)$$

where  $\hat{U}$ , and  $\hat{V}_{(i)}$ 's are the optimal solution to the objective in (7).

$\delta$  is usually called eigengap in literature (Vu et al., 2013; Huang and Pan, 2020). The  $\delta^{-2}$  factor on the right hand side of (12) is also standard for matrix perturbation analysis.

Theorem 1 confirms the intuition on identifiability. When  $\theta$  is larger, the right hand side of (12) is smaller, thus the estimation error is also smaller, which indicates that finding local and global PCs is easier. For the counter example,  $\theta \rightarrow 0$ , the right hand side approaches infinity. Hence one cannot accurately recover PCs.

In addition, Theorem 1 highlights the benefits of collaborative learning across multiple related clients. The right hand side of (12) is the average difference between the sample and population covariance matrix on all clients. For clients with a larger dataset, the distance is lower, and for clients with a smaller dataset, the distance can be higher. Through jointly optimizing objective (7), clients learn from each other and obtain principal components estimate with statistical error depending on the average distance.

#### 4.1 Proof of Theorem 1 and main lemmas

In this section, we will show the proof of Theorem 1. We first use the standard perturbation analysis on the eigenspaces of  $\Sigma_{(i)}$  (Vu et al., 2013). By assumption,  $\Pi_g$  and  $\Pi_{(i)}$  are the projections onto top eigenspaces of  $\Sigma_{(i)}$ , therefore for any orthogonal projection matrix  $P_{\hat{U}}$  and  $P_{\hat{V}_{(i)}}$ , we have:

$$\begin{aligned} & \left\langle \Sigma_{(i)}, \Pi_g + \Pi_{(i)} - P_{\hat{U}} - P_{\hat{V}_{(i)}} \right\rangle \\ &= \left\langle (\Pi_g + \Pi_{(i)}) \Sigma_{(i)}, I - P_{\hat{U}} - P_{\hat{V}_{(i)}} \right\rangle - \left\langle (I - \Pi_g - \Pi_{(i)}) \Sigma_{(i)}, P_{\hat{U}} + P_{\hat{V}_{(i)}} \right\rangle \\ &\geq \min\{\lambda_{r_1}(\Sigma_{(i),g}), \lambda_{r_{2,(i)}}(\Sigma_{(i),l})\} \left\langle \Pi_g + \Pi_{(i)}, I - P_{\hat{U}} - P_{\hat{V}_{(i)}} \right\rangle \\ &\quad - \max\{\lambda_{r_1+1}(\Sigma_{(i),g}), \lambda_{r_{2,(i)}+1}(\Sigma_{(i),l})\} \left\langle I - \Pi_g - \Pi_{(i)}, P_{\hat{U}} + P_{\hat{V}_{(i)}} \right\rangle \\ &\geq \delta \left( r_1 + r_{2,(i)} - \left\langle \Pi_g + \Pi_{(i)}, P_{\hat{U}} + P_{\hat{V}_{(i)}} \right\rangle \right) \end{aligned}$$

Summing both sides for  $i$  from 1 to  $N$ , we have:

$$\sum_{i=1}^N \left\langle \Sigma_{(i)}, \Pi_g + \Pi_{(i)} - P_{\hat{U}} - P_{\hat{V}_{(i)}} \right\rangle \geq \delta \sum_{i=1}^N \left( r_1 + r_{2,(i)} - \left\langle \Pi_g + \Pi_{(i)}, P_{\hat{U}} + P_{\hat{V}_{(i)}} \right\rangle \right) \quad (13)$$

Since  $\mathbf{P}_{\hat{\mathbf{U}}}$  and  $\{\mathbf{P}_{\hat{\mathbf{V}}(i)}\}$ 's are the optimal solution to (7), and  $\mathbf{\Pi}_g$  and  $\{\mathbf{\Pi}_{(i)}\}$ 's are feasible, we know that:

$$\sum_{i=1}^N \langle \mathbf{S}_{(i)}, \mathbf{P}_{\hat{\mathbf{U}}} + \mathbf{P}_{\hat{\mathbf{V}}(i)} \rangle \geq \sum_{i=1}^N \langle \mathbf{S}_{(i)}, \mathbf{\Pi}_g + \mathbf{\Pi}_{(i)} \rangle \quad (14)$$

Combining (13) and (14), we can obtain:

$$\sum_{i=1}^N \langle \mathbf{S}_{(i)} - \mathbf{\Sigma}_{(i)}, \mathbf{P}_{\hat{\mathbf{U}}} + \mathbf{P}_{\hat{\mathbf{V}}(i)} - \mathbf{\Pi}_g - \mathbf{\Pi}_{(i)} \rangle \geq \delta \sum_{i=1}^N \left( r_1 + r_{2,(i)} - \langle \mathbf{\Pi}_g + \mathbf{\Pi}_{(i)}, \mathbf{P}_{\hat{\mathbf{U}}} + \mathbf{P}_{\hat{\mathbf{V}}(i)} \rangle \right)$$

We can use the Cauchy-Schwartz inequality to further bound the left hand side as:

$$\langle \mathbf{S}_{(i)} - \mathbf{\Sigma}_{(i)}, \mathbf{P}_{\hat{\mathbf{U}}} + \mathbf{P}_{\hat{\mathbf{V}}(i)} - \mathbf{\Pi}_g - \mathbf{\Pi}_{(i)} \rangle \leq \|\mathbf{S}_{(i)} - \mathbf{\Sigma}_{(i)}\|_F \left\| \mathbf{P}_{\hat{\mathbf{U}}} + \mathbf{P}_{\hat{\mathbf{V}}(i)} - \mathbf{\Pi}_g - \mathbf{\Pi}_{(i)} \right\|_F$$

Notice that

$$\begin{aligned} & \left\| \mathbf{P}_{\hat{\mathbf{U}}} + \mathbf{P}_{\hat{\mathbf{V}}(i)} - \mathbf{\Pi}_g - \mathbf{\Pi}_{(i)} \right\|_F \\ &= \sqrt{\left\| \mathbf{P}_{\hat{\mathbf{U}}} + \mathbf{P}_{\hat{\mathbf{V}}(i)} \right\|_F^2 + \left\| \mathbf{\Pi}_g + \mathbf{\Pi}_{(i)} \right\|_F^2 - 2 \langle \mathbf{P}_{\hat{\mathbf{U}}} + \mathbf{P}_{\hat{\mathbf{V}}(i)}, \mathbf{\Pi}_g + \mathbf{\Pi}_{(i)} \rangle} \\ &= \sqrt{2} \sqrt{r_1 + r_{2,(i)} - \langle \mathbf{P}_{\hat{\mathbf{U}}} + \mathbf{P}_{\hat{\mathbf{V}}(i)}, \mathbf{\Pi}_g + \mathbf{\Pi}_{(i)} \rangle} \end{aligned}$$

We thus have:

$$\begin{aligned} & \sum_{i=1}^N \langle \mathbf{S}_{(i)} - \mathbf{\Sigma}_{(i)}, \mathbf{P}_{\hat{\mathbf{U}}} + \mathbf{P}_{\hat{\mathbf{V}}(i)} - \mathbf{\Pi}_g - \mathbf{\Pi}_{(i)} \rangle \\ & \leq \sqrt{2} \sqrt{\sum_{i=1}^N \|\mathbf{S}_{(i)} - \mathbf{\Sigma}_{(i)}\|_F^2} \sqrt{\sum_{i=1}^N \left[ r_1 + r_{2,(i)} - \langle \mathbf{P}_{\hat{\mathbf{U}}} + \mathbf{P}_{\hat{\mathbf{V}}(i)}, \mathbf{\Pi}_g + \mathbf{\Pi}_{(i)} \rangle \right]} \end{aligned}$$

by another application of Cauchy-Schwartz inequality.

And finally:

$$\frac{1}{N} \sum_{i=1}^N \left[ r_1 + r_{2,(i)} - \langle \mathbf{P}_{\hat{\mathbf{U}}} + \mathbf{P}_{\hat{\mathbf{V}}(i)}, \mathbf{\Pi}_g + \mathbf{\Pi}_{(i)} \rangle \right] \leq \frac{2}{N\delta^2} \sum_{i=1}^N \|\mathbf{S}_{(i)} - \mathbf{\Sigma}_{(i)}\|_F^2 \quad (15)$$

The relation (15) slightly extends the standard result from matrix perturbation theory. However, it only shows the summation of  $\mathbf{P}_{\hat{\mathbf{U}}}$  and  $\mathbf{P}_{\hat{\mathbf{V}}(i)}$  is close to the summation of  $\mathbf{\Pi}_g$  and  $\mathbf{\Pi}_{(i)}$ . One cannot infer additional information about the closeness of  $\mathbf{P}_{\hat{\mathbf{U}}}$  to  $\mathbf{\Pi}_g$ , or  $\mathbf{P}_{\hat{\mathbf{V}}(i)}$  to  $\mathbf{\Pi}_{(i)}$ . In other words, (15) alone does not ensure that the recovered global and local principal components correspond to true principal components.

Such guarantee is too weak in practice when we want to know if the solved  $\mathbf{U}$  and  $\mathbf{V}_{(i)}$ 's are close to the ground truth. Fortunately, we can show that this is indeed the case, if the problem satisfies the identifiability assumption 4.2. An important finding is the following lemma, which indicates that the closeness in direct sum space can lead to closeness in each global and local subspaces.

**Lemma 2** Suppose for  $i = 1, \dots, N$ ,  $\mathbf{P}_U$ ,  $\mathbf{P}_{V(i)}$  and  $\mathbf{P}_U^*$ ,  $\mathbf{P}_{V(i)}^*$  are projection matrices satisfying  $\mathbf{P}_U \mathbf{P}_{V(i)} = 0$  and  $\mathbf{P}_U^* \mathbf{P}_{V(i)}^* = 0$  for each  $i$ . Among them,  $\mathbf{P}_U$  and  $\mathbf{P}_U^*$  have rank  $r_1$ ,  $\mathbf{P}_{V(i)}$  and  $\mathbf{P}_{V(i)}^*$  have rank  $r_{2,(i)}$ . If there exists a positive constant  $\theta > 0$  such that

$$\lambda_{\max}\left(\frac{1}{N} \sum_{i=1}^N \mathbf{P}_{V(i)}^*\right) \leq 1 - \theta$$

we have the following bound:

$$\sum_{i=1}^N r_1 + r_{2,(i)} - \left\langle \mathbf{P}_U + \mathbf{P}_{V(i)}, \mathbf{P}_U^* + \mathbf{P}_{V(i)}^* \right\rangle \leq N(r_1 - \langle \mathbf{P}_U^*, \mathbf{P}_U \rangle) + \sum_{i=1}^N r_{2,(i)} - \left\langle \mathbf{P}_{V(i)}^*, \mathbf{P}_{V(i)} \right\rangle \quad (16)$$

And also:

$$\sum_{i=1}^N r_1 + r_{2,(i)} - \left\langle \mathbf{P}_U + \mathbf{P}_{V(i)}, \mathbf{P}_U^* + \mathbf{P}_{V(i)}^* \right\rangle \geq \frac{\theta}{2} \left( N(r_1 - \langle \mathbf{P}_U^*, \mathbf{P}_U \rangle) + \sum_{i=1}^N r_{2,(i)} - \left\langle \mathbf{P}_{V(i)}^*, \mathbf{P}_{V(i)} \right\rangle \right) \quad (17)$$

The proof of Lemma 2 is in the appendix. By applying inequality (17) to (15), we can prove the desired error bound in Theorem 1.

## 4.2 Sample complexity

In this section we estimate the statistical error when data are generated by a sub-Gaussian distribution. A random vector  $\mathbf{y} \in \mathbb{R}^d$  admits a sub-Gaussian distribution with parameter  $\sigma$  if for each fixed vector  $\mathbf{v} \in \mathbb{S}^{d-1}$ ,  $\mathbb{E}[e^{\langle \mathbf{v}, \mathbf{y} \rangle}] \leq e^{\frac{\lambda^2 \sigma^2}{2}}$  for all  $\lambda \in \mathbb{R}$ .  $\sigma$  is a parameter that denotes the variance level: when  $\sigma$  is larger the data are noisier. As a special case, if  $\mathbf{y}$  admits a Gaussian distribution with mean zero and covariance  $\Sigma_y$ , then  $\sigma^2 = \|\Sigma_y\|_{op}$  (Wainwright, 2019). The following corollary gives an upper bound of the estimation error.

**Corollary 3** If the dataset on each client  $i \{\mathbf{Y}_{(i)}\}_{i=1}^N$  admits i.i.d. sub-Gaussian distribution with parameter  $\sigma$ , and the assumptions in Theorem 1 are satisfied, then with probability at least  $1 - \tilde{\delta}$  (over the randomness of data generation process), we have:

$$\|\mathbf{P}_{\hat{U}} - \Pi_g\|_F^2 + \frac{1}{N} \sum_{i=1}^N \|\mathbf{P}_{\hat{V}(i)} - \Pi_{(i)}\|_F^2 \leq \frac{4}{\theta \delta^2} \sigma^4 C^2 \frac{d}{N} \sum_{i=1}^N \max \left\{ \left( \frac{d + \log \frac{2N}{\tilde{\delta}}}{n_i} \right)^2, \frac{d + \log \frac{2N}{\tilde{\delta}}}{n_i} \right\} \quad (18)$$

where  $C$  is a constant.

The inequality (18) essentially shows the consistency of the solution  $\hat{U}$  and  $\hat{V}$ . When the data dimension  $d$  is fixed and sample size  $n_i$  is relatively large, the right hand side of (18) decreases with  $\mathcal{O}\left(\sum_{i=1}^N \frac{1}{N \theta \delta^2 n_i}\right)$ . As  $n_i$ 's approach infinity, the subspace error also decreases to 0, and the estimated eigenspaces approach the true values accordingly.

Equation (18) also highlights the benefits of knowledge sharing. If each client only uses their own data to estimate the principal components, the estimation error would be  $\mathcal{O}\left(\frac{1}{n_i}\right)$ .

The error can be high for clients with few observations, or small  $n_i$ . However, if  $N$  clients collaborate in learning global and local principal components, the estimation error becomes the average of individual statistical errors  $\mathcal{O}\left(\sum_{i=1}^N \frac{1}{N\theta\delta^2 n_i}\right)$ . Data poor clients can thus borrow strength from other clients to improve the estimates of their principal components.

The statistical consistency and knowledge sharing effect will also be examined by numerical experiments in Sec 7.

Here we note that statistical consistency can not be achieved by existing estimates without personalized modeling. For example, the statistical error of **distPCA** (Fan et al., 2019) depends on  $\mathcal{O}\left(\frac{1}{N} \sum_{i=1}^N \|\Sigma_{(i),l}\|_{op}\right)$ , which does not decrease with number of observations  $n_i$  as long as  $\|\Sigma_{(i),l}\|_{op} > 0$ . The comparison highlights the advantages of formulation (7).

Now we present the proof of Corollary 3.

**Proof** We will adopt the covariance concentration bound in Wainwright (2019) and Rinaldo (2019). Since data on client  $i$  admits an independent sub-Gaussian distribution, theorem 13.3 in Rinaldo (2019) states that, with probability at least  $1 - \delta_1$ , there exists a constant  $C$  such that:

$$\|\Sigma_{(i)} - \mathbf{S}_{(i)}\|_{op} \leq \sigma^2 C \max \left\{ \sqrt{\frac{d + \log \frac{2}{\delta_1}}{n_i}}, \frac{d + \log \frac{2}{\delta_1}}{n_i} \right\}$$

We can choose  $\delta_1 = \frac{\tilde{\delta}}{N}$ . Then by a union bound, we know that with probability at least  $1 - \tilde{\delta}$ :

$$\|\Sigma_{(i)} - \mathbf{S}_{(i)}\|_{op} \leq \sigma^2 C \max \left\{ \sqrt{\frac{d + \log \frac{2N}{\tilde{\delta}}}{n_i}}, \frac{d + \log \frac{2N}{\tilde{\delta}}}{n_i} \right\}$$

holds for all  $i$ .

Combining this and Theorem 1, we can prove the bound in (18). ■

Equation (18) also gives a simple estimate of the sample complexity.

**Corollary 4** *Under the assumptions of Theorem 1, and assuming that data on client  $i$  admits an i.i.d sub-Gaussian with parameter  $\sigma$ , if each client has at least  $\mathcal{O}\left(\frac{1}{\epsilon} \frac{\sigma^4 d^2}{\theta \delta^2}\right)$  observations, then with high probability, the estimation error is smaller than  $\epsilon$ .*

**Proof** The proof is quite straightforward. Notice that when  $n_i \geq d$ , the right hand side of (18) is dominated by  $\frac{d}{n_i}$ . Thus if we and neglect the logarithm factors on the right hand side of (18) and set  $\frac{4}{\theta \delta^2} \sigma^4 C^2 d \frac{1}{N} \sum_{i=1}^N \frac{d}{n_i} \leq \epsilon$ , the statistical error will also be upper bounded by  $\epsilon$ .

It is natural to see that the inequality holds when each client has observations no less than  $\mathcal{O}\left(\frac{1}{\epsilon} \frac{\sigma^4 d^2}{\theta \delta^2}\right)$ . ■

## 5. Recovering Local and Global PCs

The statistical consistency proved in Sec. 4 dwells on the premise that the objective in (7) can be solved to optimality. This is not straightforward as (7) is nonconvex. In this section,

we develop an algorithm to solve (7). Our algorithm is naturally federated as inference is distributed over clients and only updates of the global PCs needs to be shared.

The major difficulty lies in the nonconvex constraints: in addition to the orthonormal constraints on  $\mathbf{U}$  and  $\mathbf{V}_{(i)}$ 's, we further require global and local PCs to be mutually orthogonal. The later constraints introduce interaction between local and global variables, which deems simple distributed Stiefel manifold descent (Chen et al., 2021b) incompetent.

To handle the orthogonality constraints, we propose an algorithm that adopts Stiefel manifold gradient descent. Before delving into the details of the algorithm, we review a few concepts from manifold optimization and provide our define for the an operation we call '*generalized retraction*'.

### 5.1 Generalized retractions

We begin by introducing the Stiefel manifold commonly used in matrix analysis (Edelman et al., 1998).

The Stiefel manifold  $St(d, r)$  is the set of all orthonormal matrices in a  $d$ -dimensional space:

$$St(d, r) = \{\mathbf{U} \in \mathbb{R}^{d \times r} | \mathbf{U}^T \mathbf{U} = \mathbf{I}\} \quad (19)$$

It is embedded in a  $d \times r$  dimensional Euclidean space. One can verify that  $St(d, r)$  is not convex in general (Edelman et al., 1998).

For  $\mathbf{U} \in St(d, r)$ , the tangent space of  $St(d, r)$  at  $\mathbf{U}$  is defined as:

$$\mathcal{T}_{\mathbf{U}} = \{\boldsymbol{\xi} \in \mathbb{R}^{d \times r} | \boldsymbol{\xi}^T \mathbf{U} + \mathbf{U}^T \boldsymbol{\xi} = 0\}$$

It can be derived by differentiating  $\mathbf{U}^T \mathbf{U} = \mathbf{I}$ . The normal space  $\mathcal{N}_{\mathbf{U}}$  is defined as the orthogonal space of the tangent space at  $\mathbf{U}$ .

Both  $\mathcal{T}_{\mathbf{U}}$  and  $\mathcal{N}_{\mathbf{U}}$  are linear subspaces of  $\mathbb{R}^{d \times r}$ . Therefore, we can define the projection onto them.  $\mathcal{P}_{\mathcal{N}_{\mathbf{U}}}$  denotes the projection onto the normal space:

$$\mathcal{P}_{\mathcal{N}_{\mathbf{U}}}(\mathbf{V}) = \frac{1}{2} \mathbf{U} (\mathbf{U}^T \mathbf{V} + \mathbf{V}^T \mathbf{U})$$

Similarly,  $\mathcal{P}_{\mathcal{T}_{\mathbf{U}}}$  denotes the projection onto the tangent space:

$$\mathcal{P}_{\mathcal{T}_{\mathbf{U}}}(\mathbf{V}) = \mathbf{V} - \mathcal{P}_{\mathcal{N}_{\mathbf{U}}}(\mathbf{V})$$

One can verify that  $\mathcal{P}_{\mathcal{T}_{\mathbf{U}}}(\mathbf{V})^T \mathbf{U} + \mathbf{U}^T \mathcal{P}_{\mathcal{T}_{\mathbf{U}}}(\mathbf{V}) = 0$

Next, we introduce the notion of a generalized retraction. The motivation of a generalized retraction is rather straightforward. For an orthogonal matrix  $\mathbf{U}$  and a general update matrix  $\boldsymbol{\xi}$ , the matrix  $\mathbf{U} + \boldsymbol{\xi}$  can probably violate the orthonormal constraint:  $(\mathbf{U} + \boldsymbol{\xi})^T (\mathbf{U} + \boldsymbol{\xi}) \neq \mathbf{I}$ . The generalized retraction finds an approximation  $\mathbf{U} + \boldsymbol{\xi}$  that strictly satisfies the orthonormal constraint. Ideally, the best approximation can be found via projection. However, the projection onto a nonlinear manifold  $St(d, r)$  is hard to analyze analytically. Therefore, one can relax this projection to a generalized retraction. More formally, a generalized retraction can be defined as:

**Definition 5** We call a mapping

$$\mathcal{GR}_{\mathbf{U}}(\cdot) : \mathbb{R}^{d \times r} \rightarrow St(d, r)$$

a generalized retraction if

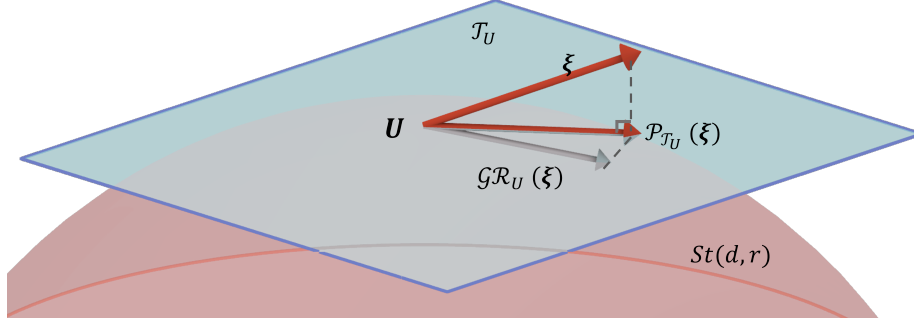


Figure 2: An illustration for Stiefel manifold, tangent space, and generalized retraction. The red surface represents the Stiefel manifold. The blue plane represents the tangent space at point  $\mathbf{U} \in St(d, r)$ .  $\xi$  is a general  $d$  by  $r$  matrix that represents the update direction.  $\mathcal{P}_{\mathcal{T}_U}(\xi)$  projects  $\xi$  to the tangent space on  $\mathbf{U}$ . Generalized retraction  $\mathcal{GR}_U(\xi)$  maps  $\mathbf{U} + \xi$  back to the Stiefel manifold.

1. (Property 1):  $col(\mathcal{GR}_U(\xi)) = col(\mathbf{U} + \xi)$ ,  $\forall \mathbf{U} \in St(d, r)$ ,  $\forall \xi \in \mathbb{R}^{d \times r}$
2. (Property 2): There exist constants  $M_1, M_2 \geq 0$  and  $M_3 > 0$  such that:

$$\|\mathcal{GR}_U(\xi) - (\mathbf{U} + \mathcal{P}_{\mathcal{T}_U}(\xi))\|_F \leq M_1 \|\mathcal{P}_{\mathcal{T}_U}(\xi)\|_F^2 + M_2 \|\xi - \mathcal{P}_{\mathcal{T}_U}(\xi)\|_F,$$

$$\forall \mathbf{U} \in St(d, r), \forall \xi \in \mathbb{R}^{d \times r}, \|\xi\|_F \leq M_3$$

Fig. 2 is an illustration of the Stiefel manifold, tangent space, and generalized retraction.

Notice that the definition of a generalized retraction extends the definition of retraction in literature (Absil et al., 2008). Retraction is usually defined as a mapping from the tangent bundle  $\mathcal{T}_U$  to the Stiefel manifold  $St(d, r)$  (Edelman et al., 1998). However, a generalized retraction is a mapping from a general  $\mathbb{R}^{d \times r}$  to the Stiefel manifold  $St(d, r)$ . We make the extension in definition so that we can apply generalized retraction to an arbitrary matrix without having to project it to the tangent space at first.

Property 1 requires that a generalized retraction preserves column spaces. This property is indispensable in our algorithm development as we use it to ensure the orthogonality of global and local PCs. The second property requires that  $\mathcal{GR}_U(\xi)$  be close to the projection to the tangent space  $\mathbf{U} + \mathcal{P}_{\mathcal{T}_U}(\xi)$ . In the special case of  $\xi \in \mathcal{T}_U$ , property 2 reduces to  $\|\mathcal{GR}_U(\xi) - (\mathbf{U} + \xi)\|_F \leq M_1 \|\xi\|_F^2$ , which coincides with the definition of retraction in literature (Chen et al., 2021a). When the norm of  $\xi$  is small, the requirement essentially implies that the difference between a generalized retraction and the projection to a tangent space is a higher order term.

Though Definition 5 looks demanding, we can show that there are several available choices for a generalized retraction.

**Proposition 6** *Polar projection defined as:*

$$\mathcal{GR}_U^{polar}(\xi) = (\mathbf{U} + \xi) (\mathbf{I} + \xi^T \mathbf{U} + \mathbf{U}^T \xi + \xi^T \xi)^{-\frac{1}{2}} \quad (20)$$

is a generalized retraction. The computation complexity is  $O(dr^2 + r^3)$ .

Notice that (20) can be equivalently calculated by the SVD of  $\mathbf{U} + \boldsymbol{\xi}$  (Breloy et al., 2021). We relegate the proof and the implementation details to Appendix A.1. An interesting property of the polar projection is that it is equivalent to the projection of  $\mathbf{U} + \boldsymbol{\xi}$  onto the Stiefel manifold:

$$\mathcal{GR}_U^{\text{polar}}(\boldsymbol{\xi}) = \arg \min_{\mathbf{V} \in St(d,r)} \|\mathbf{U} + \boldsymbol{\xi} - \mathbf{V}\|_F \quad (21)$$

The proof of (21) can be found in Kahan (2011).

QR decomposition is another influential algorithm in numerical linear algebra. It also satisfies the requirements of a generalized retraction.

**Proposition 7** *For a matrix  $\mathbf{U} + \boldsymbol{\xi} \in \mathbb{R}^{d \times r}$ , QR decomposition finds an orthogonal matrix  $\mathbf{Q} \in St(d,r)$  and a upper triangular matrix  $\mathbf{R} \in \mathbb{R}^{r \times r}$ , such that  $\mathbf{QR} = \mathbf{U} + \boldsymbol{\xi}$ . As such, a QR retraction defined as:*

$$\mathcal{GR}_U^{QR}(\boldsymbol{\xi}) = \mathbf{Q}$$

*is a generalized retraction. The computation complexity is  $O(dr^2)$ .*

We relegate the proof to Appendix A.2.

In all of our experiments, we choose the generalized retraction as a polar decomposition.

## 5.2 PerPCA: The algorithm

Now we are ready to introduce the personalized PCA algorithm, denoted as **PerPCA**. Recall our algorithm is naturally federated and requires multiple communication rounds between a client and some central server/entity that orchestrates the collaborative learning process. Suppose at communication round  $\tau$ , each client has feasible global components  $\mathbf{U}_\tau$  and local components  $\mathbf{V}_{(i),\tau}$ , i.e.,  $[\mathbf{U}_\tau, \mathbf{V}_{(i),\tau}] \in St(d, r_1 + r_{2,(i)})$ . Then client  $i$  calculates the gradient of objective  $f_i$  defined in (8):

$$\begin{cases} \nabla_{\mathbf{U}} f_i(\mathbf{U}_\tau, \mathbf{V}_{(i),\tau}) = \mathbf{S}_{(i)} \mathbf{U}_\tau \\ \nabla_{\mathbf{V}_{(i)}} f_i(\mathbf{U}_\tau, \mathbf{V}_{(i),\tau}) = \mathbf{S}_{(i)} \mathbf{V}_{(i),\tau} \end{cases}$$

Since the gradient direction generally does not align with the tangent space of  $\mathcal{T}_{[\mathbf{U}_\tau, \mathbf{V}_{(i),\tau}]}$ , simple gradient ascent will move  $[\mathbf{U}_\tau, \mathbf{V}_{(i),\tau}]$  out of  $St(d, r_1 + r_{2,(i)})$ . To ensure the iterates move along the manifold, Stiefel optimization firstly projects the gradient to the tangent space:

$$g_{(i),\tau} = \mathcal{P}_{\mathcal{T}_{[\mathbf{U}_\tau, \mathbf{V}_{(i),\tau}]}}(\mathbf{S}_{(i)} [\mathbf{U}_\tau, \mathbf{V}_{(i),\tau}]) \quad (22)$$

In literature,  $g_{(i),\tau}$  is usually referred to as the parallel gradient on the manifold (Edelman et al., 1998).

Clients then update global and local principal components by  $g_{(i),\tau}$ . As there is a small error between the Stiefel manifold and the tangent space, the updates are still not orthonormalized. Therefore we use a generalized retraction to retract the updated local components to the Stiefel manifold. We use  $\mathbf{V}_{(i),\tau+\frac{1}{2}}$  to denote the retracted matrix. For the global components, clients first send them to a server. The server then takes the average and uses generalized retraction to map the average to  $St(d, r)$ . The updated global principal component matrix is denoted as  $\mathbf{U}_{\tau+1}$ .

A major challenge then arises: after the server averages the global PCs,  $\mathbf{U}_{\tau+1}$  is not orthogonal to  $\mathbf{V}_{(i),\tau+\frac{1}{2}}$  anymore, i.e.  $\mathbf{U}_{\tau+1}^T \mathbf{V}_{(i),\tau+\frac{1}{2}} \neq 0$  in general. Thus  $\mathbf{U}_{\tau+1}$  and  $\mathbf{V}_{(i),\tau+\frac{1}{2}}$ 's become infeasible and the algorithm based on St-GD cannot proceed. One can verify that  $\mathbf{U}_{\tau}^T \mathbf{V}_{(i),\tau+\frac{1}{2}} = O(\eta_{\tau})$ , which has the same order as the parallel gradient update. Thus we cannot resolve the infeasibility issue by a decreasing stepsize. This is a fundamental limitation of a simple route that uses distributed St-GD.

Can we resolve the challenge by enforcing the orthogonality between global and local PC estimates? Inspired by Gram-Schmit orthonormalization we introduce a correction step on the local PCs. We calculate the projection of  $\mathbf{V}_{(i),\tau+\frac{1}{2}}$  onto the column space of  $\mathbf{U}_{\tau+1}$ , and subtract the projected matrix from  $\mathbf{V}_{(i),\tau+\frac{1}{2}}$ . The resulting (deflated) matrix is orthogonal to  $\mathbf{U}_{\tau+1}$ . Then, we use a generalized retraction to map the subtracted matrix to the Stiefel manifold. Remember that one key property of a generalized retraction is that it preserves the column space; the retracted matrix is still orthogonal to  $\mathbf{U}_{\tau+1}$ . We use  $\mathbf{V}_{(i),\tau+1}$  to denote the retracted matrix. Now  $\mathbf{U}_{\tau+1}$  and  $\mathbf{V}_{(i),\tau+1}$  are feasible and the updates can repeat over multiple communication rounds until convergence.

The pseudo code is summarized in Algorithm 1. The first line in the client loop

---

**Algorithm 1** PerPCA by St-GD

---

Input client covariance matrices  $\{\mathbf{S}_{(i)}\}_{i=1}^N$ , stepsize  $\eta_{\tau}$   
Initialize  $\mathbf{U}_1$ , and  $\mathbf{V}_{(1),\frac{1}{2}}, \dots, \mathbf{V}_{(N),\frac{1}{2}}$ .  
**for** Communication rounds  $\tau = 1, \dots, R$  **do**  
  **for** Client  $i = 1, \dots, N$  **do**  
     $\mathbf{V}_{(i),\tau} = \mathcal{GR}_{\mathbf{V}_{(i),\tau-\frac{1}{2}}} \left( -\mathbf{U}_{\tau} \mathbf{U}_{\tau}^T \mathbf{V}_{(i),\tau-\frac{1}{2}} \right)$   
    Choice 1:  
      Calculate  $g_{(i),\tau} = \mathcal{P}_{\mathcal{T}_{[\mathbf{U}_{\tau}, \mathbf{V}_{(i),\tau}]}} (\mathbf{S}_{(i)} [\mathbf{U}_{\tau}, \mathbf{V}_{(i),\tau}])$   
      Update  $\mathbf{U}_{(i),\tau+1} = \mathbf{U}_{\tau} + \eta_{\tau} (g_{(i),\tau})_{1:d,1:r_1}$   
      Update  $\mathbf{V}_{(i),\tau+\frac{1}{2}} = \mathcal{GR}_{\mathbf{V}_{(i),\tau}} \left( \eta_{\tau} (g_{(i),\tau})_{1:d,(r_1+1):(r_1+r_{2,(i)})} \right)$   
    Choice 2:  
      Update  $[\mathbf{U}_{(i),\tau+1}, \mathbf{V}_{(i),\tau+\frac{1}{2}}] = \mathcal{GR}_{[\mathbf{U}_{\tau}, \mathbf{V}_{(i),\tau}]}^{\text{polar}} (\eta_{\tau} \mathbf{S}_{(i)} [\mathbf{U}_{\tau}, \mathbf{V}_{(i),\tau}])$   
    Send  $\mathbf{U}_{(i),\tau+1}$  to the server.  
  **end for**  
  Server calculates  $\mathbf{U}_{\tau+1} = \mathcal{GR}_{\mathbf{U}_{\tau}} \left( \frac{1}{N} \sum_{i=1}^N \mathbf{U}_{(i),\tau+1} - \mathbf{U}_{\tau} \right)$   
  Server broadcasts  $\mathbf{U}_{\tau+1}$   
**end for**  
Return principal components  $\mathbf{U}_R$  and  $\mathbf{V}_{(i),R}$ 's.

---

$\mathbf{V}_{(i),\tau} = \mathcal{GR}_{\mathbf{V}_{(i),\tau-\frac{1}{2}}} \left( -\mathbf{U}_{\tau} \mathbf{U}_{\tau}^T \mathbf{V}_{(i),\tau-\frac{1}{2}} \right)$  represents the correction on the local PC matrix. Regardless of whether  $\mathbf{U}_{\tau}$  and  $\mathbf{V}_{(i),\tau-\frac{1}{2}}$  are orthogonal,  $\mathbf{U}_{\tau}$  and  $\mathbf{V}_{(i),\tau}$  are always feasible:  $[\mathbf{U}_{\tau}, \mathbf{V}_{(i),\tau}] \in St(d, r_1 + r_{2,(i)})$ . Then each client applies standard St-GD (choice 1) or a variant of St-GD (choice 2) to update  $\mathbf{U}_{(i),\tau+1}$  and  $\mathbf{V}_{(i),\tau+\frac{1}{2}}$  simultaneously. The updated global PCs are sent to the server. The server takes the simple average of all received global PCs and retracts the average to  $St(d, r_1)$ . The obtained  $\mathbf{U}_{\tau+1}$  is then broadcasted back to

the clients and become the starting point of the next iteration. The algorithm repeats for a certain number of communication rounds.

In Algorithm 1, we introduce two algorithmic choices on the client-side. For choice 1, clients perform standard St-GD: first project the updates to the tangent space, then retract them to the Stiefel manifold. For choice 2, clients use polar projection to replace the St-GD. This update rule is inspired by Minorization-Maximization algorithm (Breloy et al., 2021). Remember that by (21), polar projection acts as a projection into the nonlinear Stiefel manifold. Hence it is close to the composition of the projection onto the tangent space and the retraction from the tangent space onto the nonlinear manifold. We propose two choices to enrich practitioners' toolkits as they have similar performances in most of our numerical simulations. We focus on choice 1 in our theoretical analysis. However, it is observed in the video segmentation task that choice 2 allows us to use larger stepsizes, thus converging faster. Hence, we leave it to practitioners' discretion to make specific algorithmic choices.

## 6. Does Algorithm 1 Recover the Local and Global Truth?

Though the development of Algorithm 1 is intuitive and lucid, it is important to understand whether it converges and if so, what kind of solution it can recover. In this section, we will analyze the convergence of Algorithm 1 and show that, in general, Algorithm 1 converges into stationary points of the objective. In addition, when the local and global components are initialized properly, Algorithm 1 will converge into the global optimal solutions linearly and the result exactly recovers the true local and principal components.

### 6.1 Global convergence

To analyze the convergence, we make an additional assumption that the largest eigenvalues of the sample covariance matrices  $\mathbf{S}_{(i)}$ 's are upper bounded:

**Assumption 6.1** *We assume that the operator norms of  $\mathbf{S}_{(i)}$ 's are upper bounded by constants  $G_{(i),op}$ :*

$$\|\mathbf{S}_{(i)}\|_{op} \leq G_{(i),op} \quad (23)$$

*and the Frobenius norms of  $\mathbf{S}_{(i)}$ 's are upper bounded by constants  $G_{(i),F}$ :*

$$\|\mathbf{S}_{(i)}\|_F \leq G_{(i),F} \quad (24)$$

*We use  $G_{max,op}$  to denote  $\max_i G_{(i),op}$ , and  $G_{max,F}$  to denote  $\max_i G_{(i),F}$ .*

Assumption 6.1 is a common assumption in optimization literature, as it essentially assumes the objective is Lipschitz continuous. Also, if we assume the data are independently generated and follow a sub-Gaussian distribution, Assumption 6.1 will hold with high probability (Wainwright, 2019).

The first order condition (KKT condition) to problem (1) is that for the parallel gradients defined in (22), the local parts are zero on each client, and the average of the global parts is zero:

$$\begin{cases} (g_{(i)})_{1:d, (r_1+1):(r_1+r_{2,(i)}}) = 0, & \forall i \in \{1, 2, \dots, N\} \\ \frac{1}{N} \sum_{i=1}^N (g_{(i)})_{1:d, 1:(r_1+1)} = 0 \end{cases} \quad (25)$$

The proof of KKT conditions (25) is in Appendix C. Also, it is clear from Algorithm 1 that when (25) is satisfied, the global and local PC updates will be stationary. Thus (25) essentially describes the stationary points of (7).

On non-stationary points, (25) generally does not hold. The below theorem provides an upper bound on the magnitude of the violations to conditions (25). As the violations decrease to zero when the number of communication approaches infinity, the theorem shows that Algorithm 1 will converge into the KKT points. We use  $r$  to denote maximum rank  $r = \max\{r_1, r_{2,(1)}, \dots, r_{2,(N)}\}$ .

**Theorem 8** *Under Assumption 6.1, if we choose a constant stepsize  $\eta_\tau = \eta_1 \leq O(\frac{1}{G_{max,op}\sqrt{r}})$ , then Algorithm 1 with choice 1 will converge into stationary points:*

$$\min_{\tau \in \{1, \dots, R\}} \left[ \left\| \sum_{i=1}^N \left( \mathbf{I} - \mathbf{P}_{\mathbf{U}_\tau} - \mathbf{P}_{\mathbf{V}_{(i),\tau}} \right) \mathbf{S}_{(i)} \mathbf{U}_\tau \right\|^2 + \sum_{i=1}^N \left\| \left( \mathbf{I} - \mathbf{P}_{\mathbf{U}_\tau} - \mathbf{P}_{\mathbf{V}_{(i),\tau}} \right) \sum_{i=1}^N \mathbf{S}_{(i)} \mathbf{V}_{(i),\tau} \right\|^2 \right] \leq O\left(\frac{1}{R}\right)$$

Despite the nonconvex constraints in (7), Algorithm 1 provably converges to stationary points, regardless of initial conditions. The  $\frac{1}{R}$  convergence rate is comparable to the result in literature (Chen et al., 2021a).

Our algorithm handles global and local principal components at the same time, and attains the stationary points of both principal components. In the following section, we will show the proof sketch of Theorem 8. The complete proof is relegated to Appendix D.

### 6.1.1 PROOF SKETCH FOR THEOREM 8 AND KEY LEMMAS

As discussed before, one major difficulty to analyze Algorithm 1 lies in the correction step. The correction step changes local PCs by  $O(\eta_\tau)$ , which is comparable to that in the descent step. Therefore, a naïve treatment to the correction step will generate a large error term that cannot be bounded.

To bypass the issue, we exploit one nice structure in objective (8):  $f_i(\mathbf{U}, \mathbf{V}_{(i)})$  is dependent only on the subspace spanned by the concatenated matrix  $[\mathbf{U}, \mathbf{V}_{(i)}]$ . Therefore one can make adjustments on  $\text{col}(\mathbf{U})$  and  $\text{col}(\mathbf{V}_{(i)})$  without changing the objective value, as long as  $\text{col}([\mathbf{U}, \mathbf{V}_{(i)}])$  are the same.

One major technical novelty of our work is to introduce Lyapunov functions that take this key property into consideration. We define the two following Lyapunov functions:

$$\mathcal{L}_{(i),1}(\mathbf{U}, \mathbf{V}) = -\frac{1}{2} \text{Tr}(\mathbf{U}^T (\mathbf{I} - \mathbf{P}_\mathbf{V}) \mathbf{S}_{(i)} (\mathbf{I} - \mathbf{P}_\mathbf{V}) \mathbf{U}) \quad (26)$$

And:

$$\mathcal{L}_{(i),2}(\mathbf{U}, \mathbf{V}) = -\frac{1}{2} \text{Tr}(\mathbf{V}^T \mathbf{S}_{(i)} \mathbf{V}) \quad (27)$$

It's easy to see that when  $\mathbf{V}^T \mathbf{U} = 0$ , we have:

$$\mathcal{L}_{(i),1}(\mathbf{U}, \mathbf{V}) + \mathcal{L}_{(i),2}(\mathbf{U}, \mathbf{V}) = -\frac{1}{2} \text{Tr}(\mathbf{U}^T \mathbf{S}_{(i)} \mathbf{U}) - \frac{1}{2} \text{Tr}(\mathbf{V}^T \mathbf{S}_{(i)} \mathbf{V}) = -f_n(\mathbf{U}, \mathbf{V})$$

At each communication step  $\tau$ , global and local components are indeed orthogonal  $\mathbf{U}_\tau^T \mathbf{V}_{(i),\tau} = 0$ , thus  $\mathcal{L}_{(i),1}(\mathbf{U}_\tau, \mathbf{V}_{(i),\tau}) + \mathcal{L}_{(i),2}(\mathbf{U}_\tau, \mathbf{V}_{(i),\tau}) = -f_n(\mathbf{U}_\tau, \mathbf{V}_{(i),\tau})$ .

$\mathcal{L}_{(i),1}$  explicitly encodes the orthogonality constraint into the objective. Such design enables convenient handling of the correction step: we can prove that the correction step on  $\mathbf{V}$  changes  $\mathcal{L}_{(i),1} + \mathcal{L}_{(i),2}$  only by  $O(\eta_\tau^2)$ . Therefore only the descent step can change  $\mathcal{L}_{(i),1} + \mathcal{L}_{(i),2}$  by  $O(\eta_\tau)$ . Thus the change of Lyapunov functions is dominated by the update from the parallel gradient. By calculating the update of  $\mathbf{U}$  and  $\{\mathbf{V}_{(i)}\}$ 's in each communication round, we can have the following informal version of sufficient descent lemma:

**Lemma 9** (Informal) *When we choose the stepsize  $\eta \leq O\left(\frac{1}{G_{max,op}\sqrt{r}}\right)$ , and  $\mathbf{U}_\tau$  and  $\mathbf{V}_{(i),\tau}$  satisfy the orthogonality condition  $\mathbf{U}_\tau^T \mathbf{V}_{(i),\tau} = 0$ , we have:*

$$\begin{aligned} & \left\langle \sum_{i=1}^N \nabla_{\mathbf{U}} \mathcal{L}_{(i),1}(\mathbf{U}_\tau, \mathbf{V}_{(i),\tau}), \mathbf{U}_{\tau+1} - \mathbf{U}_\tau \right\rangle \\ & + \sum_{i=1}^N \left\langle \nabla_{\mathbf{V}_{(i)}} \mathcal{L}_{(i),1}(\mathbf{U}_\tau, \mathbf{V}_{(i),\tau}) + \nabla_{\mathbf{V}_{(i)}} \mathcal{L}_{(i),2}(\mathbf{U}_\tau, \mathbf{V}_{(i),\tau}), \mathbf{V}_{(i),\tau+1} - \mathbf{V}_{(i),\tau} \right\rangle \\ & \leq -\eta \left( \left\| \sum_{i=1}^N (\mathbf{I} - \mathbf{P}_{\mathbf{U}_\tau} - \mathbf{P}_{\mathbf{V}_{(i),\tau}}) \mathbf{S}_{(i)} \mathbf{U}_\tau \right\|^2 + \sum_{i=1}^N \left\| (\mathbf{I} - \mathbf{P}_{\mathbf{U}_\tau} - \mathbf{P}_{\mathbf{V}_{(i),\tau}}) \sum_{i=1}^N \mathbf{S}_{(i)} \mathbf{V}_{(i),\tau} \right\|^2 \right) \\ & + O(\eta^2) \end{aligned} \tag{28}$$

When  $\eta$  is small, the  $O(\eta)$  terms will dominate  $O(\eta^2)$  terms. Thus Lemma 9 essentially shows that in Algorithm 1, the change of Lyapunov functions is negative semidefinite in one communication round. With the sufficient decrease property, standard analysis on first order optimization yields a  $O\left(\frac{1}{R}\right)$  convergence rate.

Formal proofs of Theorem 8 and Lemma 9 can be found in Appendix C.

## 6.2 Local convergence

Theorem 8 only shows that Algorithm 1 converges into stationary points, but does not provide further information about the property of the final solution. In problems like feature extraction or dimension reduction, we want to know whether the stationary point is a globally optimal solution, or whether it corresponds to the ground truth principal components.

In this section, we will answer the problems by analyzing the convergence of global and local PCs. The convergence depends on a Polyak-Lojasiewicz style condition. Similar to Sec. 6.1, we will introduce another assumption about the eigenvalue distribution of the sample covariance matrix. Without loss of generality, in this section, we assume  $r_1 = r_{2,(1)} = \dots = r_{2,(N)} = r$ .

**Assumption 6.2** (Sample covariance matrix eigenvalue lower bound) *We further assume the minimum nonzero eigenvalues of  $\mathbf{S}_{(i)}$  is lower bounded by a constant  $\mu > 0$ :*

$$\mu (\mathbf{\Pi}_g \oplus \mathbf{\Pi}_{(i)}) \preceq \mathbf{S}_{(i)} \tag{29}$$

where  $\mathbf{\Pi}_g$  and  $\mathbf{\Pi}_{(i)}$  are rank- $r$  projection matrices.

Assumption 6.2 assumes that data covariance can be decomposed as noiseless global and local parts with rank  $r$ . This is the standard assumption in the local convergence analysis of many PCA algorithm (Tang, 2019). Also, if we assume the data on each dataset admits noiseless independent sub-Gaussian distributions, Assumption 6.2 follows with high probability.

The following theorem shows that if Algorithm 1 is initialized within the attractive basin of the global optimum, the iterates will converge to the global optimal solution linearly.

**Theorem 10** *Exact recovery: Under assumptions 4.2, 6.1, and 6.2, when we initialize close to the global optimum, and choose a constant stepsize  $\eta_t = \eta \leq O\left(\frac{1}{G_{op,max}\sqrt{r}}\right)$ , then Algorithm 1 with choice 1 will converge into the global optimum:*

$$f^* - f(\mathbf{U}_R, \{\mathbf{V}_{(i),R}\}) \leq O\left(\left(1 - \eta \frac{\mu^2 \ell(\theta)}{4G_{max,op}}\right)^R\right)$$

where  $f^*$  is the optimal value to problem (7), and  $\ell(\theta)$  is defined in (34).

Furthermore, we can recover the exact principal components:

$$\|\mathbf{P}_{\mathbf{U}_\tau} - \mathbf{\Pi}_g\|_2^2 + \frac{1}{N} \sum_{i=1}^N \|\mathbf{P}_{\mathbf{V}_{(i),\tau}} - \mathbf{\Pi}_{(i)}\|_2^2 \leq O\left(\left(1 - \eta \frac{\mu^2 \ell(\theta)}{4G_{max,op}}\right)^R\right)$$

It is worthwhile to point out that in Theorem 10, the convergence is faster for a larger  $\theta$ . This is intuitively understandable since when local eigenspaces are more heterogeneous, it is easier to identify different eigenspaces. On the other hand, if all the local eigenspaces are similar, it is difficult to distinguish local PCs from global PCs, thus the convergence is slower. *This result is in striking contrast to conventional federated learning (Li et al., 2020, 2018a), where data heterogeneity leads to slower convergence.* We will verify this finding in Sec. 7.

### 6.2.1 PROOF SKETCH OF THEOREM 10 AND KEY LEMMAS

To prove the exponential convergence in Theorem 10, we need a stronger version of the sufficient decrease inequality than Lemma 9. We should show that, in each communication round, the change in the Lyapunov functions is negative definite. This requires a careful analysis of the geometry of objective (7) around the global optimum  $\mathbf{\Pi}_g$  and  $\{\mathbf{\Pi}_{(i)}\}$ 's.

As discussed in Sec. 6.1.1, the solutions  $\mathbf{U}$  and  $\mathbf{V}_{(i)}$ 's to objective (7) are not unique: different  $\mathbf{U}$  and  $\mathbf{V}_{(i)}$ 's may have the same objective value, as long as they span the same column space. The degeneracy of solutions can cause issues when we analyze the local geometry of the objective, as some eigenvalues of the local Hessian are zero. Therefore, we first alleviate the degeneracy of solutions by introducing a new set of variables. We introduce a variable  $\zeta$  to denote the subspace distance between the estimate and ground truth:

$$\zeta_{(i),\tau} = r - \langle \mathbf{P}_{\mathbf{V}_{(i),\tau}}, \mathbf{\Pi}_{(i)} \rangle \quad (30)$$

for each  $i = 1, \dots, N$ , and,

$$\zeta_{(0),\tau} = r - \langle \mathbf{P}_{\mathbf{U}_\tau}, \mathbf{\Pi}_g \rangle \quad (31)$$

We use  $\zeta_\tau$  to denote:

$$\zeta_\tau = \zeta_{(0),\tau} + \frac{1}{N} \sum_{i=1}^N \zeta_{(i),\tau} \quad (32)$$

The  $\zeta_{(0),\tau}$  and  $\zeta_{(i),\tau}$ 's defined represent how far away the iterates are from the ground truth, measured by subspace distance. We will show that the local geometry of objective (7) has some nice properties, in terms of  $\zeta_{(0),\tau}$  and  $\zeta_{(i),\tau}$ 's.

**Lemma 11** *(Informal) (Personalized gradient dominance property) Under the same assumptions of Theorem 10, there exists  $\mathbf{U}_\tau^*$  and  $\mathbf{V}_{(i),\tau}^*$ 's such that  $\text{col}(\mathbf{U}_\tau^*) = \text{col}(\mathbf{\Pi}_g)$  and  $\text{col}(\mathbf{V}_{(i),\tau}^*) = \text{col}(\mathbf{\Pi}_{(i)})$ , and the following inequality holds:*

$$\left\| \left( \mathbf{I} - \mathbf{P}_{\mathbf{U}_\tau} - \sum_{j=1}^N \frac{1}{N} \mathbf{P}_{\mathbf{V}_{(j),\tau}} \right) \mathbf{U}_\tau^* \right\|_F^2 + \frac{1}{N} \sum_{i=1}^N \left\| \left( \mathbf{I} - \mathbf{P}_{\mathbf{U}_\tau} - \mathbf{P}_{\mathbf{V}_{(i),\tau}} \right) \mathbf{V}_{(i),\tau}^* \right\|_F^2 \geq \ell(\theta) \zeta_\tau - O(\zeta_\tau^{1.5}) \quad (33)$$

where  $\ell(\theta)$  is a function of  $\theta$ .

The left hand side of inequality (33) approximately represents the norm of the Stiefel gradient of  $\sum_{i=1}^N [\mathcal{L}_{(i),1} + \mathcal{L}_{(i),2}]$ , while the right hand side is the subspace distance. Therefore, the inequality (33) indicates that the Lyapunov function satisfies the Polyak-Lojasiewicz style inequality, when  $\zeta_\tau$  is small. Equation (33) can also be regarded as the personalized counterpart of the so-called gradient dominance property in Huang and Pan (2020) and Alimisis et al. (2021).

The major technical difficulty in proving Lemma 11 is to find a proper lower bound of the parallel gradient norm. We use Taylor expansions to analyze the Stiefel gradient norm. When  $\mathbf{P}_{\mathbf{U}_\tau}$  and  $\mathbf{P}_{\mathbf{V}_{(i),\tau}}$ 's are close to the optimal  $\mathbf{\Pi}_g$  and  $\mathbf{\Pi}_{(i)}$ 's, we can show that the leading term on the left hand side of (33) is a quadratic form of  $\|\mathbf{U}_\tau - \mathbf{U}_\tau^*\|_F$  and  $\|\mathbf{V}_{(i),\tau} - \mathbf{V}_{(i),\tau}^*\|_F$ . Therefore, we need to show that the quadratic form is positive definite. Fortunately, when  $\theta$  is positive, the positive definiteness of such quadratic form can be established. Lemma 12 is a formal statement of the result.

**Lemma 12** *We consider the following general form of a square matrix  $A \in \mathbb{R}^{(N+1)rd \times (N+1)rd}$ .*

$$A = \begin{pmatrix} \mathbf{I}_{rd} & B \\ N\mathbf{B}^T & \mathbf{I}_{Nrd} \end{pmatrix}$$

where  $B \in \mathbb{R}^{rd \times Nrd}$  is a block satisfying

$$0 \preceq N\mathbf{B}\mathbf{B}^T \preceq (1 - \theta) \mathbf{I}$$

for some  $\theta \in [0, 1]$ .

We call such matrix  $A$   $\theta$ -block-arrowhead matrix. For a  $\theta$ -block-arrowhead matrix  $A$ , we can define:

$$\mathcal{Q}(A) = \mathcal{D}_{\frac{1}{\sqrt{N}}, rd, Nrd} A^T \mathcal{D}_{N, rd, Nrd} A \mathcal{D}_{\frac{1}{\sqrt{N}}, rd, Nrd} = \begin{pmatrix} \mathbf{I} + N\mathbf{B}\mathbf{B}^T & 2\sqrt{N}B \\ 2\sqrt{N}\mathbf{B}^T & \mathbf{I} + N\mathbf{B}^T B \end{pmatrix}$$

where  $\mathbf{D}_{a,b,c}$  denotes a  $(b+c) \times (b+c)$  diagonal matrix, whose first  $b$  diagonal entries are  $a$  and whose remaining  $c$  diagonal entries are 1. Then the minimum eigenvalue of  $\mathcal{Q}(A)$  is lower bounded by:

$$\lambda_{\min}(\mathcal{Q}(A)) \geq \ell(\theta) = \frac{\theta^2}{2 - \theta + \sqrt{(2 - \theta)^2 - \theta^2}} \quad (34)$$

Interestingly, we noticed that Lemma 12 is novel and cannot be directly inferred from any previous results in matrix analysis. The most relevant result is the Gershgorin circle theorem (Feingold and Varga, 1962). Therefore, Lemma 12 has a stand-alone value as it gives a new lower bound of the eigenvalues of a specific form of structured matrices. The full proof of Lemma 12 is in Appendix E.

Lemma 12 is pivotal in characterizing the local geometry of objective (7). The positive definiteness of the quadratic form is equivalent to the positive definiteness of the defined  $\mathcal{Q}(A)$ . Thus with Lemma 12, we can prove the personalized gradient dominance property in Lemma 11. Combining Lemma 11 and Lipschitz continuity, we can derive a sufficient descent inequality:

$$-f(\mathbf{U}_{\tau+1}, \{\mathbf{V}_{(i),\tau+1}\}) \leq -f(\mathbf{U}_{\tau}, \{\mathbf{V}_{(i),\tau}\}) - \frac{\eta\mu^2\ell(\theta)}{4NG_{\max,op}} (f^* - f(\mathbf{U}_{\tau}, \{\mathbf{V}_{(i),\tau}\})).$$

Then, by applying standard analysis on convex optimization, we can show the exponential convergence of  $f(\mathbf{U}_{\tau}, \{\mathbf{V}_{(i),\tau}\})$ .

For global and local principal components, we can show that:

$$f^* - f(\mathbf{U}, \{\mathbf{V}_{(i)}\}) \geq \sum_{i=1}^N \mu \langle \mathbf{\Pi}_g + \mathbf{\Pi}_{(i)}, \mathbf{P}_U + \mathbf{P}_V \rangle$$

Combining this with Lemma 2, we have:

$$\|\mathbf{P}_{U_{\tau}} - \mathbf{\Pi}_g\|_2^2 + \frac{1}{N} \sum_{i=1}^N \|\mathbf{P}_{V_{(i),\tau}} - \mathbf{\Pi}_{(i)}\|_2^2 \leq \frac{1}{\mu\theta} (f^* - f(\mathbf{U}_{\tau}, \{\mathbf{V}_{(i),\tau}\}))$$

Thus the global and local subspaces also converge into the true subspaces.

The full proof of Lemma 11 and Theorem 10 is relegated to Appendix D.

## 7. Numerical Experiments

This section tests our model on a set of datasets across different applications. We start in Sec. 7.1 with a proof of concept study using a synthetic dataset to verify theoretical findings in Sec. 4 and Sec. 6. We also provide an approach for an interesting application of **PerPCA** in federated client clustering using local PCs. Then in Sec.7.2 we provide an illustrative example in comparison with **Robust PCA** to shed light on the end-goal of our model. Next, we apply **PerPCA** to a real-life heterogeneous distributed dataset FEMNIST and show **PerPCA**'s advantages in finding better features in Sec. 7.3. Finally, we demonstrate how **PerPCA** can separate shared and unique features in video and language data in Sec. 7.4.

We note that from Theorem 10, a suitable initialization is needed for the best performance of **PerPCA**. We thus employ the standard one-communication round distributed PCA algorithm proposed in Qu et al. (2002) as the initialization of global PCs in Algorithm 1, unless specified otherwise. Local PCs are always randomly initialized. In this section we assume  $r_{2,(1)} = r_{2,(2)} = \dots = r_{2,(N)} = r_2$ .

## 7.1 Proof of concept on synthetic datasets

To examine the empirical performance of **PerPCA** and compare it with theoretical results, we first test Algorithm 1 on a synthetic data example. We generate data from model (1). The  $\mathbf{u}_q$ 's and  $\mathbf{v}_q$ 's are set to be orthogonal components. After obtaining  $\mathbf{u}_q$ 's and  $\mathbf{v}_q$ 's, we sample the score coefficients  $\phi_{(i),q}$ 's and  $\varphi_{(i),q}$ 's from i.i.d. Gaussian distributions. Noise  $\epsilon_{(i)}$  are sampled from i.i.d. Gaussian distributions.

We will discuss a few issues in this section: in Sec. 7.1.1, we revisit the example in Fig. 1 and examine the convergence behavior of **PerPCA** numerically. In Sec. 7.1.2, 7.1.3, and 7.1.4, we demonstrate how the statistical errors change with the (i) number of observations  $n$ , (ii) data dimension  $d$ , and (iii) number of clients  $N$ , and compare the results with our theory. In Sec. 7.1.5 we show that in **PerPCA**, clients benefit from knowledge sharing to improve their PC estimates. Finally, in Sec. 7.1.6, we describe a method that exploits the estimated local PCs for client clustering.

### 7.1.1 CONVERGENCE OF **PERPCA**

We firstly analyze the convergence of **PerPCA**. Theorem 10 predicts that (i) **PerPCA** has local linear convergence, and a larger  $\theta$  can expedite convergence. To verify the two theoretical results, we run **PerPCA** on a group of synthetic data. We set  $d = 3$  and  $N = 2$ . Each client has exactly one global  $\mathbf{u}_1$  and one local component  $\mathbf{v}_{(i),1}$ . By changing the direction of  $\mathbf{v}_{(1),1}$  and  $\mathbf{v}_{(2),1}$ , we can modify  $\theta$ :

$$\theta = 1 - \cos \left( \frac{1}{2} \arccos(\mathbf{v}_{(1),1}^T \mathbf{v}_{(2),1}) \right)$$

We plot the raw data and learned PCs for  $\theta = 0.127$  in Fig. 1 (shown in the introduction). It is clear that the learned PCs accurately characterize global and local features.

To see the  $\theta$ 's effect on convergence, we generate the data with  $\theta$  ranging from 0 to 0.3. In this experiment, we initialize global and local PCs to be random Gaussian vectors. We run each experiment from 10 different random initializations and collect the reconstruction error in each communication round. The reconstruction error is defined as the objective in (5):

$$\text{Reconstruction error} = \frac{1}{n_i} \left\| \mathbf{Y}_{(i)} - \left( \mathbf{P}_U + \mathbf{P}_{\mathbf{V}_{(i)}} \right) \mathbf{Y}_{(i)} \right\|_F^2 \quad (35)$$

where  $n_i$  is the number of data points on client  $i$ . Results are shown in Fig. 3. From the left figure of Fig. 3, we can see that **PerPCA** indeed enjoys linear convergence. Furthermore, bluer curves have a larger slope, which indicates that a larger  $\theta$  leads to faster convergence. Such finding is corroborated by the right figure of Fig. 3, which plots the log error at the 100-th communication round with respect to  $\theta$ . It is clear that when  $\theta$  is larger, the final error is smaller. These results thus confirm insights from Theorem 10.

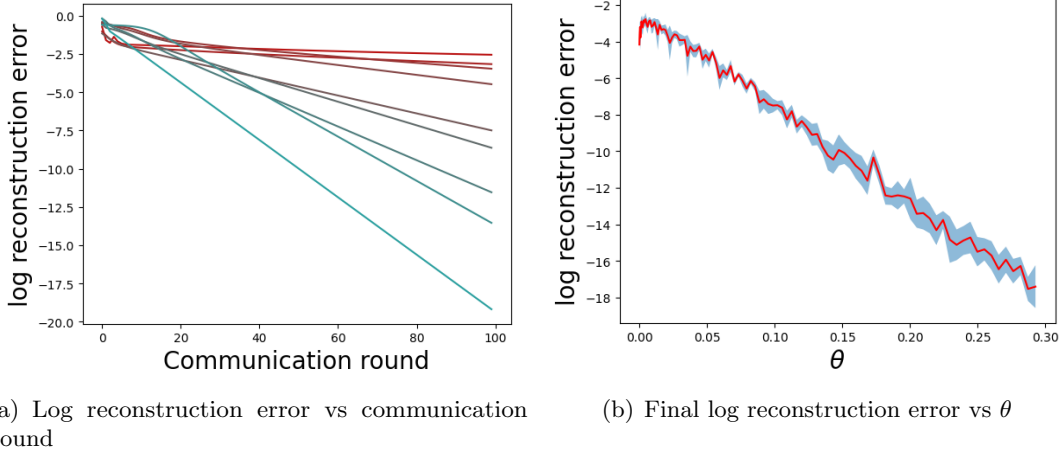


Figure 3: Left: the learning curve of the reconstruction error. Each curve represents one set of experiments with one  $\theta$ . The bluer the curve is, the larger  $\theta$  is. Right: log reconstruction error after 100 communication rounds for datasets with different heterogeneity  $\theta$ . We run each experiment 10 times, each with a different random initialization. The red line represents the mean log final error for the ten experiments, and the blue shaded region shows the confidence interval.

### 7.1.2 DEPENDENCE OF STATISTICAL ERROR ON $n$

Knowing that **PerPCA** converges rather quickly, we can use the final iterates of Algorithm 1 as an estimate of the optimal solution to problem (7). To show that the estimate can indeed recover the true local and global PCs, we calculate the subspace error between eigenspace estimates and true values:

$$\text{Subspace error} = \|\mathbf{P}_{U_\tau} - \mathbf{\Pi}_g\|_F^2 + \frac{1}{N} \sum_{i=1}^N \left\| \mathbf{P}_{V_{(i),\tau}} - \mathbf{\Pi}_{(i)} \right\|_F^2 \quad (36)$$

Remember that Theorem 1 shows that such error should decrease to 0 as the number of observations on each client approaches infinity. Additionally, Corollary 3 gives a finite-sample error bound of the subspace error.

Here we benchmark with a one-shot approach **distPCA** (Fan et al., 2019). However, we provide a simple variant of **distPCA** to make it amenable for personalization. For standard **distPCA**, each client firstly calculates the top  $r_1 + r_2$  principal components, and sends them to the server. The server then concatenates all the received principal components into a  $d \times N(r_1 + r_2)$  matrix, and calculates the top  $r_1$  principal components of the matrix. To enable personalization in **distPCA**, we take the following route: we use the obtained top  $r_1$  principal components  $\mathbf{U}_{\text{distPCA}}$  as estimates of the global principal components. Then we estimate local PCs with the help of the global ones. Specifically, the global PCs  $\mathbf{U}_{\text{distPCA}}$  are sent back to clients. Each client then deflates the sample covariance matrix  $\mathbf{S}_{(i),\text{deflate}} = (\mathbf{I} - \mathbf{P}_{\mathbf{U}_{\text{distPCA}}}) \mathbf{S}_{(i)} (\mathbf{I} - \mathbf{P}_{\mathbf{U}_{\text{distPCA}}})$ , and calculates the top  $r_2$  principal components of  $\mathbf{S}_{(i),\text{deflate}}$  as local principal components.

To analyze the statistical consistency, we run **PerPCA** on datasets with varying numbers of observations  $n$ , and compare with the benchmark algorithm **distPCA**. We fix data dimension  $d = 15$ , and generate data from 2 global principal components and 10 local principal components. On each client, the variances contributed by local PCs are set to be 100 times larger than those contributed by global PCs to simulate large heterogeneity. We use 100 clients. Among them 50 clients have  $n$  observations, and the rest 50 clients only have  $\frac{1}{10}n$  observations. We run both algorithms and estimate the subspace error (36) from 5 different random seeds.

Results in Fig. 4 show that **PerPCA** achieves smaller statistical error for almost all  $n$ , and more importantly, the error decreases with  $n$ , which indicates that **PerPCA** gives consistent estimates of global and local PCs. The slope of the curve is approximately  $-1$ , which matches the theoretical error upper bound  $O(\frac{1}{n})$  in Corollary 3.

In comparison, the statistical error of **distPCA** does not decrease even when  $n$  is very large, implying that the method is not consistent for heterogeneous datasets. This result also sheds light on an important insight. Simply learning global components and using them for personalization in a train-then-personalize philosophy is not optimal as global components from aggregated data may not contain useful information required for personalization.

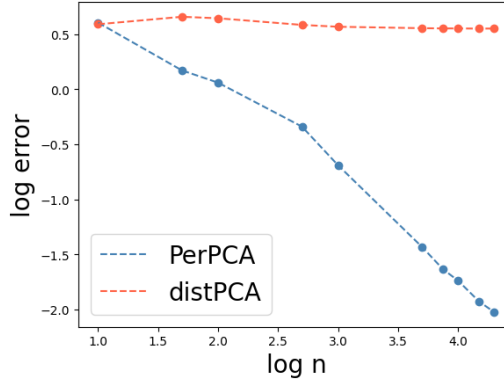
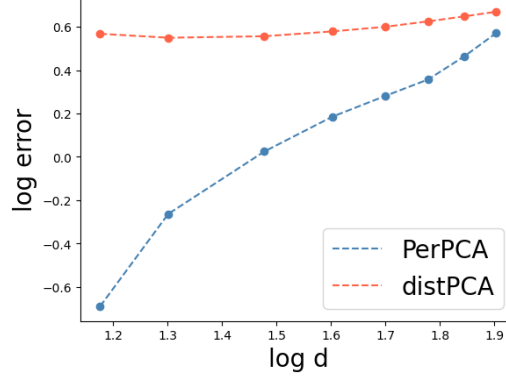


Figure 4: The relation between log error and number of observations on each client  $n$ . **PerPCA** is consistent while **distPCA** is not.

### 7.1.3 DEPENDENCE OF STATISTICAL ERROR ON $d$

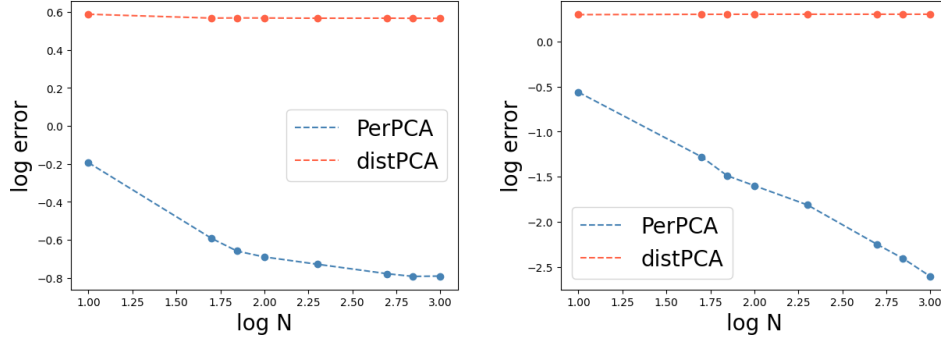
We also examine the performance of **PerPCA** on data with different dimensions  $d$ . We fix  $n = 10000$ , and generate data with different  $d$ . Other settings are the same as Sec. 7.1.2. We calculate the subspace error of estimates given by **PerPCA** and **distPCA**. Results are plotted in Fig. 5.

From Fig. 5, **PerPCA** still achieves smaller statistical error for all  $d$ . Also, the error grows almost quadratically with  $d$ , which again matches the upper bound given by Corollary 3.

Figure 5: The relation between log error and data dimension  $d$ .

#### 7.1.4 DEPENDENCE OF STATISTICAL ERROR ON $N$

In this section, we explore whether the number of clients  $N$  effects the statistical error. We fix  $d = 15$ ,  $n = 10000$ , and change  $N$  from 10 to 1000. The other settings are also the same as in Sec. 7.1.2. After obtaining global and local PCs, we calculate the average subspace error of both global and local PCs (36) and the subspace error of only global PCs  $\|\mathbf{P}_U - \mathbf{\Pi}_g\|_F^2$ . Results are plotted in Fig. 6.



(a) Average of subspace error of global and local PC estimates      (b) Subspace error of global PC estimates

Figure 6: Left: the average of local and global PCs' subspace error. Right: Global PCs' subspace error.

Fig. 6(a) shows that when  $N$  increases, the average subspace error decreases slowly. The decreasing trend is more conspicuous for the subspace error of global PCs shown in Fig. 6(b). This is understandable as when more clients participate in PerPCA, more observations are available. Thus global PCs can be better estimated.

### 7.1.5 SHARED KNOWLEDGE

When the PCs on different clients are extremely heterogeneous, it is natural to ask whether clients are sharing knowledge and learning from each other in **PerPCA**. Corollary 3 indicates that clients can benefit from participating in the collaborative learning process from a theoretical perspective. In this section, we show numerical results on how the learned global components improve client-level predictions.

The dataset on client  $i$  is split into a training set  $\mathbf{Y}_{(i),train}$  and testing set  $\mathbf{Y}_{(i),test}$ . We use the training set  $\mathbf{Y}_{(i),train}$  to find estimates for global and local components and testing set to calculate the testing error. We focus on the reconstruction error defined in (35). As in Sec. 7.1.2, we simulate two groups of clients with highly unbalanced dataset sizes. One group of clients has  $n$  observations, we call them data rich clients. The other group of clients have only  $\frac{1}{10}n$  observations. We call them data-sparse clients. We set  $N = 100$  and  $n = 100$ .

In this experiment, we compare **PerPCA** with 3 benchmarks: **indivPCA**, **CPCA**, and **distPCA**. For **indivPCA**, each client uses their own data to calculate principal components independently without any knowledge sharing. **CPCA** represents PCA on the pooled data from all clients, i.e. all data is uploaded to a central server PCA is learned on the aggregated dataset. The algorithmic procedure of **distPCA** is introduced in Sec. 7.1.2. For fair comparison, we allow **indivPCA** and **CPCA** to retain  $r_1 + r_2$  principal components. The results of testing reconstruction error averaged on each group are shown in Table. 2. **Ground Truth** corresponds to the testing loss by the true principal components.

Client Group	<b>indivPCA</b>	<b>CPCA</b>	<b>disPCA</b>	<b>PerPCA</b>	<b>Ground Truth</b>
Data sparse	$1.87 \pm 0.01$	$2.07 \pm 0.01$	$1.91 \pm 0.01$	<b><math>1.68 \pm 0.02</math></b>	$1.50 \pm 0.01$
Data rich	$1.80 \pm 0.01$	$2.10 \pm 0.01$	$1.88 \pm 0.01$	<b><math>1.52 \pm 0.01</math></b>	$1.50 \pm 0.01$

Table 2: Testing reconstruction error averaged on each group

From Table 2, it is clear that **PerPCA** achieves the smallest testing error in both the data-sparse and the data-rich group, thus having the best predictive performance. As **PerPCA** outperforms **indivPCA**, we can conclude that **PerPCA** learns useful shared knowledge. The results highlight **PerPCA**’s ability to extract common features from heterogeneous datasets. Also, **CPCA** exhibits the worst performance. This again highlights the need for personalized learning when data comes from heterogeneous sources.

### 7.1.6 CLUSTERING BASED ON LOCAL PRINCIPAL COMPONENTS

Apart from capturing the variance structure in the data, the learned local and global components can reveal high-level information about the clients inter-relatedness. Below we highlight an interesting application of **PerPCA** in client clustering.

An important question in federated and distributed learning is how to cluster clients based on some summary statistics from their data. This is usually done by exploiting some distance metrics over the estimated parameters or gradients (Sattler et al., 2019) from each client. **PerPCA** can pose as an alternative approach for client clustering based on local PCs. More specifically, when  $r_{2,(1)} = \dots = r_{2,(N)} = r_2$ , one can calculate the subspace distance

between client  $i$  and  $j$   $\rho_{i,j}$  defined as:

$$\rho_{i,j} = \frac{1}{r_2} \left\| \mathbf{P}_{V(i)} - \mathbf{P}_{V(j)} \right\|_F^2 \quad (37)$$

If the column space of  $V(i)$  and  $V(j)$  are more similar,  $\rho_{i,j}$  will be smaller.

The  $\rho_{i,j}$ 's measure the closeness of local subspaces, thus revealing a similarity structure among clients. They form an  $N \times N$  matrix  $\boldsymbol{\rho}$ . As such, a simple spectral clustering algorithm (Hastie et al., 2009) on  $\boldsymbol{\rho}$  can be used to analyze the relations among different clients.

As an example, we generate clients from 10 different client groups. Clients in one group have the same local PCs. Different groups have different local PCs. The data on clients within one group thus have a similar variance structure. We set  $r_1 = 2$ ,  $r_2 = 3$ , and  $d = 15$  in this experiment. We apply **PerPCA** on the dataset and calculate matrix  $\boldsymbol{\rho}$  with each communication round. Then we use multidimensional scaling (MDS) (Hastie et al., 2009) and spectral clustering on  $\boldsymbol{\rho}$ . Results are shown in Fig. 7.

As local PCs are randomly initialized, it is hard to find meaningful structures from initialization in Fig. 7(a). However, after only one communication round, the clustering structure emerges in Fig. 7(b). After 30 communication rounds, clients can be effectively clustered based on their learned local PCs.

## 7.2 An illustrative example in comparison to Robust PCA

The philosophy of finding common and unique features can be applied to other tasks beyond explaining data variance. In this section, we use a simple example to demonstrate how **PerPCA** can separate shared and unique features from image data.

We compare **PerPCA** with **Robust PCA**. Though **Robust PCA** is proposed to learn low rank and sparse parts of the observation matrix, it is also potentially useful in finding irregular and common patterns from a dataset. When data come from different sources  $\{\mathbf{Y}_{(i)}\}$ , one can stack them into one matrix  $\mathbf{Y}_{\text{stack}} = [\text{vec}(\mathbf{Y}_{(1)}), \dots, \text{vec}(\mathbf{Y}_{(N)})]$ . Then **Robust PCA** can be applied on the stacked matrix  $\mathbf{Y}_{\text{stack}} \in \mathbb{R}^{nd \times N}$  to distinguish low rank and sparse parts. The common wisdom is to use a low-rank part to represent shared patterns and a sparse part to represent irregular trends (Candes et al., 2011).

The underlying assumption of such an approach is that unique features are somewhat sparse among all datasets. However, there are cases where a sparse matrix cannot model unique features. An example is shown in Table 3. We create 4 images of different icons (triangle, disk, cross, and cloud) on similar background textures using PowerPoint, and distinguish the icons from the background. As a grey-scale image can naturally be represented by an observation matrix with dimensions of its height and width, we can construct 4 datasets representing 4 images. Then we apply **PerPCA** and **Robust PCA** to identify the icons.

From Table 3, it is apparent that **Robust PCA** does not perform well as it cannot recover the icons and always leaves shadows of icons on other images, probably because icons occupy a large space in the image and thus cannot be modeled by sparse noise. **PerPCA** recovers the icons by projecting the images to the subspace spanned by local PCs. The third row in Table. 3 shows that **PerPCA** has decent performance as the icons recovered have clear edges and shapes.

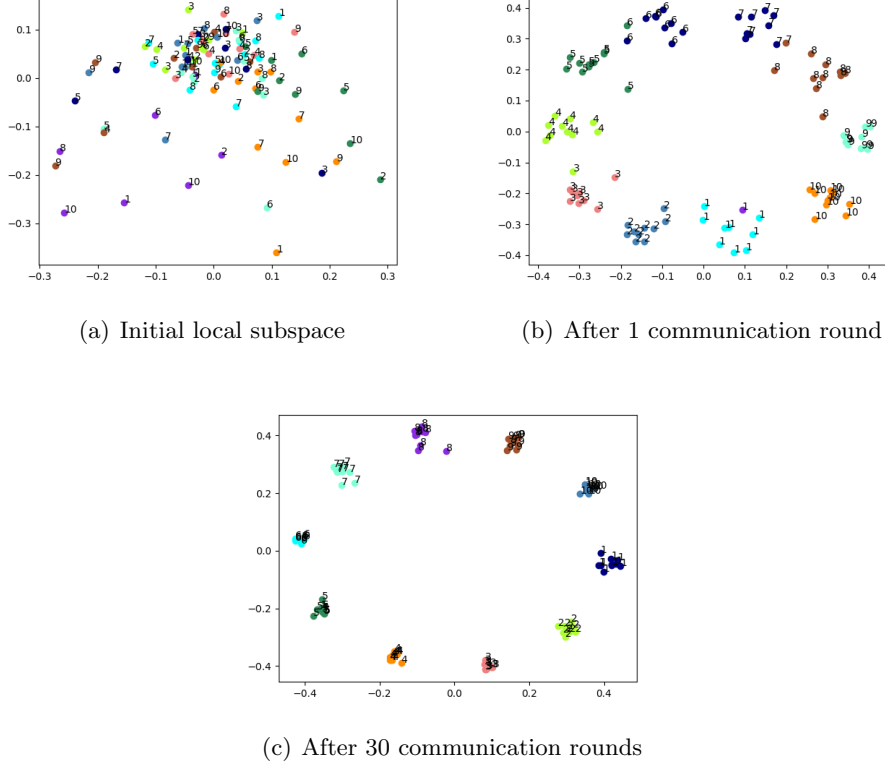


Figure 7: MDS of the distance matrix  $\mathbf{g}$ . Color denotes the output of the spectral clustering algorithm. Numbers denote the true cluster label.

This highlights the need for personalized inference in many applications where PCA is utilized.

### 7.3 Real life federated dataset

We also apply our algorithm on FEMNIST (Caldas et al., 2019). FEMNIST is a popular dataset in federated analytics. It consists of images of handwritten digits and English letters contributed by 3550 different writers. Each image has  $28 \times 28 = 784$  pixels. Different writers have different writing styles. Thus the datasets are inherently heterogeneous. Our task is to learn a few PCs that can represent the dataset. On average, each client has 89 images. We represent an image by a vector in  $\mathbb{R}^{784}$ . For these vectors, we randomly choose 80% of them to form the training set and take the rest as the test set. We use **PerPCA**, **indivPCA**, **CPCA**, and **distPCA** to fit PCs on training sets. Then we evaluate the reconstruction loss (35) on both training and test sets. The average reconstruction loss is shown in Table 4.

As the reconstruction loss represents the difference between the original and reconstructed image, it represents how well the learned PCs can characterize the features in the image. In Table. 4, **indivPCA** achieves the lowest training error but incurs high testing error, suggesting

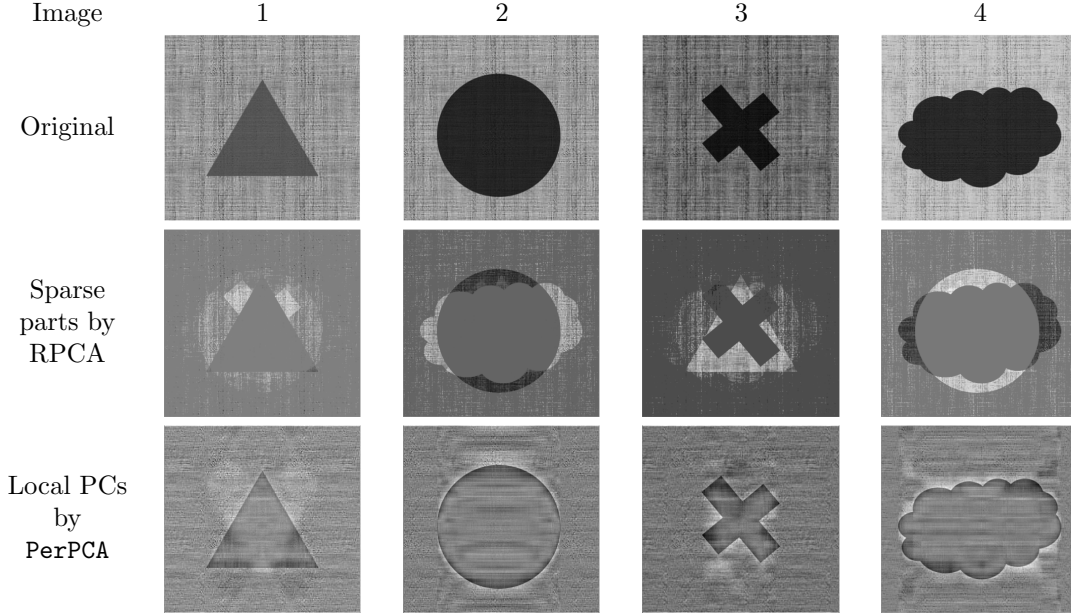


Table 3: A comparison of **PerPCA** and **Robust PCA** on images of icons on background textures.

Reconstruction error	<b>indivPCA</b>	CPCA	disPCA	<b>PerPCA</b>
Training	<b><math>0.49 \pm 0.01</math></b>	$1.72 \pm 0.01$	$1.43 \pm 0.01$	$1.44 \pm 0.02$
Testing	$1.97 \pm 0.03$	$1.73 \pm 0.01$	$1.73 \pm 0.01$	<b><math>1.70 \pm 0.01</math></b>

Table 4: Averaging training and testing reconstruction loss on FEMNIST

that learned PCs overfit the training sets. **PerPCA** has the lowest testing loss, highlighting **PerPCA**'s ability to leverage common knowledge with unique trends to find better features from data.

## 7.4 Applications beyond maximizing explained variance

Besides the experiments in the previous sections, **PerPCA** can excel in various tasks that require separating shared and unique features. In this section, we will use video segmentation and topic extraction as two examples to show the applicability of **PerPCA**.

### 7.4.1 VIDEO SEGMENTATION

The task of video segmentation is to separate moving parts (foreground) from stationary backgrounds in a video. For a video with  $F$  frames, where each frame is an image with width  $W$  and height  $H$ , we can model it as  $F$  separated datasets. Each dataset has the data of one image frame or  $H$  observations from  $\mathbb{R}^W$ . Therefore we can naturally apply **PerPCA** to recover local and global PCs from the constructed datasets of all frames. Intuitively, the global PCs should capture shared features across all frames, which correspond to the

stationary background. Local PCs learn the unique features in each frame, which corresponds to the moving parts. Hence, after obtaining global and local PCs, we project the original picture into the space spanned by global and local PCs to extract the background and foreground.

We use a surveillance video example from Cuevas et al. (2016). We use 50 global PCs and 50 local PCs and apply Algorithm 1 with choice 2. Some segmentation results are shown in Table. 5. From Table. 5, we can see that backgrounds and moving parts are well separated by global and local PCs, validating PerPCA’s ability to find common and unique features in image datasets.

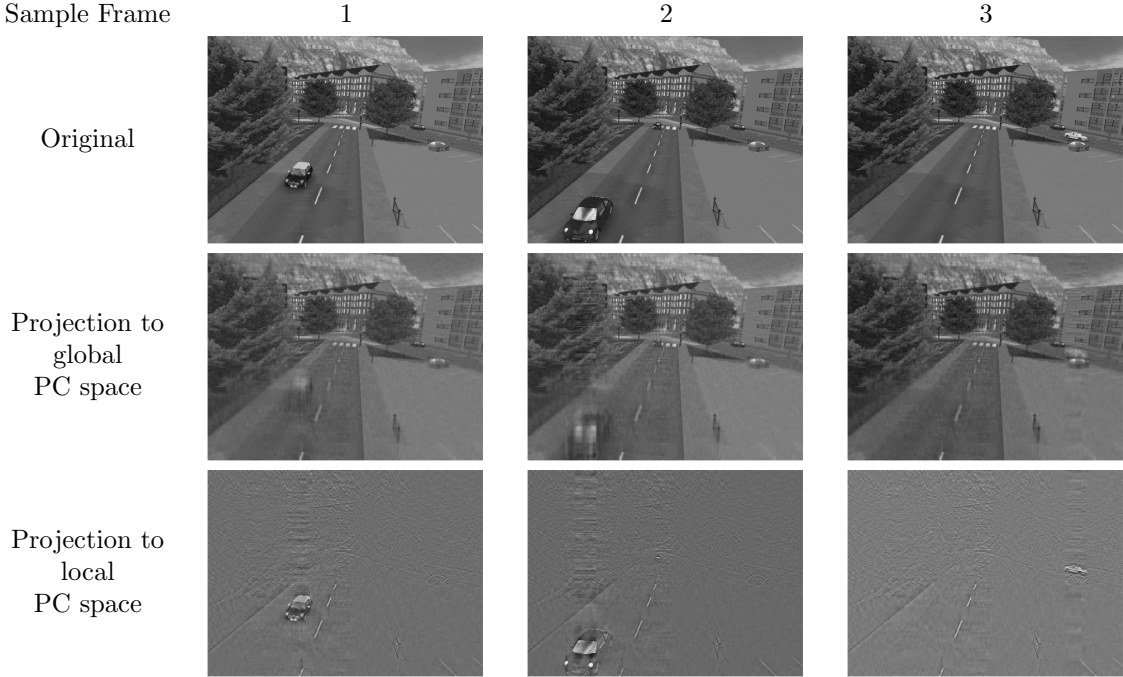


Table 5: Video segmentation. We separate moving cars from the background in a video from (Cuevas et al., 2016).

#### 7.4.2 TOPIC EXTRACTION

PerPCA is also useful in modeling changing topics in language datasets. As a demonstration, we analyze the presidential debate transcriptions from 1960 to 2020 (Kaggle, 2022). The goal is to extract key debating topics for each specific election year.

The dataset contains 9135 dialogues in 46 debates from 13 election years, where one dialogue is the speech the speaker makes in the debate before another person speaks. After we remove common English words such as “you”, “I”, “and”, “at”, “that”, from the text corpus, there are 5464 different words used in the dataset. We also model the dataset as a collection of 13 separate datasets, each of which has all the dialogues in one election year.

Table 6: U.S. presidential debate key topics represented by local PCs.

Year	Top local principal components words
1960	peace, Castro, Africa, Kennedy, now, world, ...
1976	billion, Carter, Governor, Africa, Ford, people, world, ...
1980	coal, oil, money, energy, Social, Security, Reagan, ...
1984	Union, tax, Soviet, arms, leadership, proposal, ...
1988	drug, young, strong, build, future, enforcement, good, ...
1992	Bill, school, children, care, health, taxes, reform, plan, control, ...
1996	Clinton, Security, Medicare, budget, tax, Dole, Bob, ...
2000	school, public, plan, children, money, Social, Security, health, tax, ...
2004	wrong, plan, cost, free, Saddam, troops, Iraq, war, health, tax, ...
2008	nuclear, oil, troops, Iraq, Afghanistan, Pakistan, health, Iran, energy, ...
2012	million, small, business, China, Medicare, Romney, jobs, tax, ...
2016	Russia, Trump, Hillary, companies, taxes, Mosul, Iran, deal, ...
2020	Harris, Pence, Trump, down, Joe, Biden, jobs, Donald, health, ...

To construct the observation matrix  $\mathbf{Y}_{(i)}$ , we first use one-hot encoding to map an English word into a vector in  $\mathbb{R}^{5464}$ . Then we add all vectors corresponding to words that appear in one dialogue. The added vector is one observation in  $\mathbb{R}^{5464}$ .  $\mathbf{Y}_{(i)}$  is formed by concatenating observations corresponding to dialogues in the election year.

With the datasets constructed, we run **PerPCA** for 20 communication rounds to extract local PCs. We use 2 global PCs and 2 local PCs for each client. To show the key topics represented by the two local PCs, we find the words corresponding to the dimensions in each local PC that have the top 20 largest absolute values. Table 6 contains most informative key words from the top 20 key words obtained.

From Table 6, one can find different debating key topics for different years. For some years, the key topics are about public finance and the domestic economic reform. For others, the key topics are more about international relations. These topics represent the central issues in a specific time in history. The results demonstrate **PerPCA**'s capability in finding unique features from high-dimensional language data.

## 8. Conclusion

This work proposes **PerPCA**, a systematic approach to decouple shared and unique features from heterogeneous datasets. We show that the problem is well formulated, and the consistency can be guaranteed under mild conditions. A fully federated algorithm with a convergence guarantee is designed to efficiently obtain global and local PCs from noisy observations. Extensive simulations highlight **PerPCA**'s ability to separate shared and unique features in various applications.

As **PerPCA** is the first work to analyze shared and unique features quantitatively, many areas remain unexplored. On the optimization side, it is promising to design algorithms that can converge faster or require lower computation resources, including Grassmannian gradient descent, conjugate Stiefel gradient descent, and adaptive Stiefel gradient descent.

Also, extensions of **PerPCA** to consider missing data, large noise, sparse factors, or malicious intruders are important directions for future work.

## References

- P.-A. Absil, R. Mahony, and R. Sepulchre. *Optimization algorithms on matrix manifolds*. Princeton University Press, 2008.
- A. M. Aguilera, F. A. Ocaña, and M. J. Valderrama. Forecasting time series by functional pca. discussion of several weighted approaches. *Computational Statistics*, 14(3):443–467, 1999.
- F. Alimisis, P. Davies, B. Vandereycken, and D. Alistarh. Distributed principal component analysis with limited communication. In A. Beygelzimer, Y. Dauphin, P. Liang, and J. W. Vaughan, editors, *Advances in Neural Information Processing Systems*, 2021. URL <https://openreview.net/forum?id=edCFRv1WqV>.
- R. Bhatia. *Matrix Analysis*. Springer, New York, NY, 1997.
- N. Boumal. An introduction to optimization on smooth manifolds. To appear with Cambridge University Press, Apr 2022. URL <http://www.nicolasboumal.net/book>.
- T. Bouwmans, S. Javed, H. Zhang, Z. Lin, and R. Otazo. On the applications of robust pca in image and video processing. *Proceedings of the IEEE*, 106(8):1427–1457, 2018. doi: 10.1109/JPROC.2018.2853589.
- A. Breloy, S. Kumar, Y. Sun, and D. P. Palomar. Majorization-minimization on the stiefel manifold with application to robust sparse pca. *IEEE Transactions on Signal Processing*, 69:1507–1520, 2021. doi: 10.1109/TSP.2021.3058442.
- S. Caldas, S. M. K. Duddu, P. Wu, T. Li, J. Konecny, H. B. McMahan, V. Smith, and A. Talwalkar. Leaf: A benchmark for federated settings. In *NeurIPS*, 2019.
- E. J. Candes, X. Li, Y. Ma, and J. Wright. Robust principal component analysis? *Journal of the ACM (JACM)*, 2011.
- S. Chen, A. Garcia, M. Hong, and S. Shahrampour. On the local linear rate of consensus on the stiefel manifold. In *Arxiv*, 2021a. URL <https://arxiv.org/pdf/2101.09346.pdf>.
- S. Chen, A. Garcia, M. Hong, and S. Shahrampour. Decentralized riemannian gradient descent on the stiefel manifold. In M. Meila and T. Zhang, editors, *Proceedings of the 38th International Conference on Machine Learning*, volume 139 of *Proceedings of Machine Learning Research*, pages 1594–1605. PMLR, 18–24 Jul 2021b. URL <https://proceedings.mlr.press/v139/chen21g.html>.
- X. Chen, J. D. Lee, H. Li, and Y. Yang. Distributed estimation for principal component analysis: a gap-free approach. *CoRR*, abs/2004.02336, 2020. URL <https://arxiv.org/abs/2004.02336>.
- C. Cuevas, E. M. Yáñez, , and N. García. Labeled dataset for integral evaluation of moving object detection algorithms: Lasiesta. In *Computer Vision and Image Understanding*, volume 152. PMLR, 2016. doi: doi:10.1016/j.cviu.2016.08.005. URL [https://www.gti.ssr.upm.es/data/lasiesta\\_database.html](https://www.gti.ssr.upm.es/data/lasiesta_database.html).

- C.-A. Deledalle, J. Salmon, and A. Dalalyan. Image denoising with patch-based pca: local versus global. In *The 22nd British Machine Vision Conference*, 2011.
- A. Edelman, T. A. Arias, and S. T. Smith. The geometry of algorithms with orthogonality constraints. *SIAM Journal on Matrix Analysis and Applications*, 20(2):303–353, 1998. doi: 10.1137/S0895479895290954.
- J. Fan, D. Wang, K. Wang, and Z. Zhu. Distributed estimation of principal eigenspaces. *Annals of statistics*, 47,6:3009–3031, 2019. doi: 10.1214/18-AOS1713.
- D. G. Feingold and R. S. Varga. Block diagonally dominant matrices and generalizations of the gerschgorin circle theorem. In *Pacific journal of mathematics*, volume 12, 1962.
- D. Feldman, M. Schmidt, and C. Sohler. Turning big data into tiny data: Constant-size coresets for k-means, pca and projective clustering. In *Proceedings of the Twenty-Fourth Annual ACM-SIAM Symposium on Discrete Algorithms*, SODA '13, page 1434–1453, USA, 2013. Society for Industrial and Applied Mathematics. ISBN 9781611972511.
- K. P. F.R.S. Liii. on lines and planes of closest fit to systems of points in space. *Philosophical Magazine Series 1*, 2:559–572, 1901.
- D. Garber and E. Hazan. Fast and simple pca via convex optimization. *ArXiv*, abs/1509.05647, 2015. URL <https://arxiv.org/abs/1509.05647>.
- D. Garber, O. Shamir, and N. Srebro. Communication-efficient algorithms for distributed stochastic principal component analysis. In *ICML*, pages 1203–1212, 2017. URL <http://proceedings.mlr.press/v70/garber17a.html>.
- A. Grammenos, R. Mendoza Smith, J. Crowcroft, and C. Mascolo. Federated principal component analysis. In H. Larochelle, M. Ranzato, R. Hadsell, M. Balcan, and H. Lin, editors, *Advances in Neural Information Processing Systems*, volume 33, pages 6453–6464. Curran Associates, Inc., 2020. URL <https://proceedings.neurips.cc/paper/2020/file/47a658229eb2368a99f1d032c8848542-Paper.pdf>.
- T. Hastie, R. Tibshirani, and J. Friedman. *The Elements of Statistical Learning*. Springer Series in Statistics, 2009.
- D. Hong, F. Yang, J. A. Fessler, and L. Balzano. Optimally weighted pca for high-dimensional heteroscedastic data. In *Arxiv*, 2021. URL <https://arxiv.org/pdf/1810.12862.pdf>.
- H. Hotelling. Analysis of a complex of statistical variables into principal components. *Journal of Educational Psychology*, 24:417–441, 1933. doi: <http://dx.doi.org/10.1037/h0071325>.
- L.-K. Huang and S. Pan. Communication-efficient distributed PCA by Riemannian optimization. In H. D. III and A. Singh, editors, *Proceedings of the 37th International Conference on Machine Learning*, volume 119 of *Proceedings of Machine Learning Research*, pages 4465–4474. PMLR, 13–18 Jul 2020. URL <https://proceedings.mlr.press/v119/huang20e.html>.

- H. Jégou and O. Chum. Negative evidences and co-occurrences in image retrieval: The benefit of pca and whitening. In A. Fitzgibbon, S. Lazebnik, P. Perona, Y. Sato, and C. Schmid, editors, *Computer Vision – ECCV 2012*, pages 774–787, Berlin, Heidelberg, 2012. Springer Berlin Heidelberg. ISBN 978-3-642-33709-3.
- Kaggle. Us presidential debate transcripts 1960-2020. 2022. URL <https://www.kaggle.com/datasets/arenagrenade/us-presidential-debate-transcripts-19602020>.
- W. Kahan. The nearest orthogonal or unitary matrix. 2011.
- R. Kontar, S. Zhou, C. Sankavaram, X. Du, and Y. Zhang. Nonparametric-condition-based remaining useful life prediction incorporating external factors. *IEEE Transactions on Reliability*, 67(1):41–52, 2017.
- R. Kontar, S. Zhou, C. Sankavaram, X. Du, and Y. Zhang. Nonparametric modeling and prognosis of condition monitoring signals using multivariate gaussian convolution processes. *Technometrics*, 60(4):484–496, 2018.
- R. Kontar, N. Shi, X. Yue, S. Chung, E. Byon, M. Chowdhury, J. Jin, W. Kontar, N. Masoud, M. Nouiehed, et al. The internet of federated things (ioft). *IEEE Access*, 9:156071–156113, 2021.
- V. Kulkarni, M. Kulkarni, and A. Pant. Survey of personalization techniques for federated learning. In *2020 Fourth World Conference on Smart Trends in Systems, Security and Sustainability (WorldS4)*, pages 794–797, 2020. doi: 10.1109/WorldS450073.2020.9210355.
- T. Li, A. K. Sahu, M. Zaheer, M. Sanjabi, and V. S. Ameet Talwalkar. Federated optimization in heterogeneous networks. *Proceedings of the 3rd MLSys Conference*, 2018a.
- W. Li, M. Peng, and Q. Wang. Fault detectability analysis in pca method during condition monitoring of sensors in a nuclear power plant. *Annals of Nuclear Energy*, 119:342–351, 2018b.
- X. Li, K. Huang, W. Yang, S. Wang, and Z. Zhang. On the convergence of fedavg on non-iid data. In *International Conference on Learning Representations*, 2020. URL <https://openreview.net/forum?id=HJxNANvtDS>.
- Y. Liang, M.-F. F. Balcan, V. Kanchanapally, and D. Woodruff. Improved distributed principal component analysis. In Z. Ghahramani, M. Welling, C. Cortes, N. Lawrence, and K. Weinberger, editors, *Advances in Neural Information Processing Systems*, volume 27. Curran Associates, Inc., 2014. URL <https://proceedings.neurips.cc/paper/2014/file/52947e0ade57a09e4a1386d08f17b656-Paper.pdf>.
- H. Liu, A. M.-C. So, and W. Wu. Quadratic optimization with orthogonality constraint: Explicit lojasiewicz exponent and linear convergence of retraction-based line-search and stochastic variance-reduced gradient methods. In *Proceedings of the 33rd International Conference on Machine Learning*, 2019.
- J. Novembre and M. Stephens. Interpreting principal component analyses of spatial population genetic variation. *Nature genetics*, 40(5):646–649, 2008.

- S. Oba, M. Kawanabe, K.-R. Müller, and S. Ishii. Heterogeneous component analysis. In J. Platt, D. Koller, Y. Singer, and S. Roweis, editors, *Advances in Neural Information Processing Systems*, volume 20. Curran Associates, Inc., 2007. URL <https://proceedings.neurips.cc/paper/2007/file/a8abb4bb284b5b27aa7cb790dc20f80b-Paper.pdf>.
- F. Pozo, Y. Vidal, and Ó. Salgado. Wind turbine condition monitoring strategy through multiway pca and multivariate inference. *Energies*, 11(4):749, 2018.
- Y. Qu, G. Ostrouchov, N. Samatova, and A. Geist. Principal component analysis for dimension reduction in massive distributed data sets. 04 2002.
- D. Reich, A. L. Price, and N. Patterson. Principal component analysis of genetic data. *Nature genetics*, 40(5):491–492, 2008.
- A. Rinaldo. Lecture notes in advanced statistical theory, Fall 2019.
- F. Sattler, K.-R. Müller, and W. Samek. Clustered federated learning: Model-agnostic distributed multi-task optimization under privacy constraints. *arXiv preprint arXiv:1910.01991*, 2019.
- R. Sun and Z. Luo. Guaranteed matrix completion via non-convex factorization. *FOCS*, 2015.
- C. Tang. Exponentially convergent stochastic k-pca without variance reduction. In *Advances in Neural Information Processing Systems*, volume 32. Curran Associates, Inc., 2019.
- V. Q. Vu, J. Cho, J. Lei, and K. Rohe. Fantope projection and selection: A near-optimal convex relaxation of sparse pca. In *Advances in Neural Information Processing Systems*, volume 26. Curran Associates, Inc., 2013. URL <https://proceedings.neurips.cc/paper/2013/file/81e5f81db77c596492e6f1a5a792ed53-Paper.pdf>.
- M. J. Wainwright. *High-Dimensional Statistics: A Non-Asymptotic Viewpoint*. Cambridge University Press, 2019. doi: 10.1017/9781108627771.
- H. Xu, C. Caramanis, and S. Sanghavi. Robust pca via outlier pursuit. *IEEE Transactions on Information Theory*, 58(5):3047–3064, 2012. doi: 10.1109/TIT.2011.2173156.
- K. Yang and C. Shahabi. A pca-based similarity measure for multivariate time series. In *Proceedings of the 2nd ACM international workshop on Multimedia databases*, pages 65–74, 2004.
- H. Zou, T. Hastie, and R. Tibshirani. Sparse principal component analysis. *Journal of Computational and Graphical Statistics*, 15(2):265–286, 2006. doi: 10.1198/106186006X113430.

## A. Some examples of generalized retraction

In this section, we discuss two popular normalization schemes: polar projection and QR decomposition. We prove that both fit the definition 5 of a generalized retraction. The analysis in this section is inspired by Liu et al. (2019). However Liu et al. (2019) only consider conventional retraction operations, while we consider generalized retractions.

### A.1 Polar projection

Polar projection is defined as:

$$\mathcal{GR}_U^{\text{polar}}(\xi) = (U + \xi) (I + U^T \xi + \xi^T U + \xi^T \xi)^{-\frac{1}{2}}$$

Then obviously,

$$\text{col}(\mathcal{GR}_U(\xi)) = \text{col}(U + \xi)$$

To verify the second property, we can calculate the difference between  $\mathcal{GR}_U(\xi)$  and  $U + \mathcal{P}_{\mathcal{T}_U}(\xi)$ .

Notice that

$$\begin{aligned} & (I + U^T \xi + \xi^T U + \xi^T \xi)^{-\frac{1}{2}} \\ &= I - \frac{1}{2} U^T \xi - \frac{1}{2} \xi^T U - \frac{1}{2} \xi^T \xi + \sum_{n=2}^{\infty} (U^T \xi + \xi^T U + \xi^T \xi)^n \frac{(2n-1)!!(-1)^n}{2^n n!} \end{aligned}$$

We have

$$\begin{aligned} & \mathcal{GR}_U(\xi) - (U + \mathcal{P}_{\mathcal{T}_U}(\xi)) \\ &= (U + \xi) \left( I - \frac{1}{2} U^T \xi - \frac{1}{2} \xi^T U - \frac{1}{2} \xi^T \xi + \sum_{n=2}^{\infty} (U^T \xi + \xi^T U + \xi^T \xi)^n \frac{(2n-1)!!(-1)^n}{2^n n!} \right) \\ & \quad - \left( U - \xi + \frac{1}{2} U^T \xi + \frac{1}{2} \xi^T U \right) \\ &= \left( -\frac{1}{2} \xi^T U^T \xi - \frac{1}{2} \xi^T \xi^T U - \frac{1}{2} \xi^T \xi^T \xi + (U + \xi) \sum_{n=2}^{\infty} (U^T \xi + \xi^T U + \xi^T \xi)^n \frac{(2n-1)!!(-1)^n}{2^n n!} \right) \end{aligned} \tag{38}$$

By property of Frobinus norm:

$$\begin{aligned} & \|U^T \xi + \xi^T U + \xi^T \xi\|_F \\ & \leq 2 \|\xi\|_F \|U^T\|_{op} + \|\xi\|_F^2 \\ & = 2 \|\xi\|_F + \|\xi\|_F^2 \\ & \leq 3 \|\xi\|_F \end{aligned}$$

Therefore,

$$\begin{aligned}
 & \|\mathcal{GR}_U(\boldsymbol{\xi}) - (\mathbf{U} + \mathcal{P}_{\mathcal{T}_U}(\boldsymbol{\xi}))\|_F \\
 & \leq \frac{1}{2} \|\boldsymbol{\xi}^T \mathbf{U}^T \boldsymbol{\xi}\|_F + \frac{1}{2} \|\boldsymbol{\xi}^T \boldsymbol{\xi}^T \mathbf{U}\|_F + \frac{1}{2} \|\boldsymbol{\xi}^T \boldsymbol{\xi}^T \boldsymbol{\xi}\|_F + \|\mathbf{U} + \boldsymbol{\xi}\|_F \sum_{n=2}^{\infty} \|\mathbf{U}^T \boldsymbol{\xi} + \boldsymbol{\xi}^T \mathbf{U} + \boldsymbol{\xi}^T \boldsymbol{\xi}\|_F^n \frac{(2n-1)!!}{2^n n!} \\
 & \leq \|\boldsymbol{\xi}\|_F^2 + \frac{1}{2} \|\boldsymbol{\xi}\|_F^3 + (1 + \|\boldsymbol{\xi}\|_F) \sum_{n=2}^{\infty} (3 \|\boldsymbol{\xi}\|_F)^n \frac{(2n-1)!!}{2^n n!} \\
 & = \|\boldsymbol{\xi}\|_F^2 + \frac{1}{2} \|\boldsymbol{\xi}\|_F^3 + (1 + \|\boldsymbol{\xi}\|_F) \frac{3(3 \|\boldsymbol{\xi}\|_F)^2 + (3 \|\boldsymbol{\xi}\|_F)^3}{2} \\
 & \leq M_{polar} \|\boldsymbol{\xi}\|_F^2
 \end{aligned}$$

where  $M_{polar} = \frac{253}{8}$ . We applied the following summation in the derivation:

$$\begin{aligned}
 & \sum_{n=2}^{\infty} x^n \frac{(2n-1)!!}{2^n n!} \\
 & = (1-x)^{-1/2} - (1 + \frac{x}{2}) \\
 & = \frac{3x^2 + x^3}{\sqrt{1-x} + (1-x)(1 + \frac{x}{2})}
 \end{aligned}$$

and the fact that  $x \leq \frac{1}{2}$  in the third inequality.

Since

$$\begin{aligned}
 & \|\boldsymbol{\xi}\|_F^2 \\
 & = \|\mathcal{P}_{\mathcal{T}_U}(\boldsymbol{\xi}) + \mathcal{P}_{\mathcal{N}_U}(\boldsymbol{\xi})\|_F^2 \\
 & \leq 2 \|\mathcal{P}_{\mathcal{T}_U}(\boldsymbol{\xi})\|_F^2 + 2 \|\mathcal{P}_{\mathcal{N}_U}(\boldsymbol{\xi})\|_F^2 \\
 & \leq 2 \|\mathcal{P}_{\mathcal{T}_U}(\boldsymbol{\xi})\|_F^2 + \|\mathcal{P}_{\mathcal{N}_U}(\boldsymbol{\xi})\|_F
 \end{aligned}$$

We prove that polar projection is a generalized retraction with  $M_1 = \frac{253}{4}$  and  $M_2 = \frac{253}{8}$ .

Polar projection can be implemented via singular value decomposition of  $\mathbf{U} + \boldsymbol{\xi}$ , whose computational complexity is  $O(dr^2 + r^3)$  (Breloy et al., 2021).

## A.2 QR decomposition

QR decomposition is an extension of Gram-Schmidt orthonormalization. For a matrix  $\mathbf{U} + \boldsymbol{\xi} \in \mathbb{R}^{d \times r}$ , the method finds a orthogonal matrix  $\mathbf{Q} \in \mathbb{R}^{d \times r}$  and an upper triangular matrix  $\mathbf{R} \in \mathbb{R}^{r \times r}$ , such that  $\mathbf{QR} = \mathbf{U} + \boldsymbol{\xi}$ . Then  $\mathcal{GR}_U^{\text{QR}}(\boldsymbol{\xi}) = \mathbf{Q}$ .

In this section, we will prove that QR decomposition is a generalized retraction for  $\|\boldsymbol{\xi}\| \leq \frac{1}{4}$ . Our proof in this section extends that in Liu et al. (2019).

Notice that  $\text{col}(\mathbf{U} + \boldsymbol{\xi}) = \text{col}(\mathbf{Q})$ , thus the first property of generalized retraction in Definition 5 is satisfied. We will prove the second in the case  $M_3 = \frac{1}{4}$

Similar to Liu et al. (2019), we define  $\mathbf{U}(t) = \mathbf{U} + t\boldsymbol{\xi}$ , for  $t \in [0, 1]$ , and use  $\mathbf{Q}(t)\mathbf{R}(t)$  to denote the QR decomposition of  $\mathbf{U}(t)$ . Then:

$$\begin{aligned} & \left\| \mathcal{GR}_U^{\text{QR}}(\boldsymbol{\xi}) - (\mathbf{U} + \boldsymbol{\xi}) \right\|_F \\ &= \left\| \mathbf{Q}(1) - \mathbf{Q}(1)\mathbf{R}(1) \right\|_F = \left\| \mathbf{Q}(1)(\mathbf{I} - \mathbf{R}(1)) \right\|_F \\ &\leq \left\| \mathbf{R}(1) - \mathbf{R}(0) \right\|_F \\ &= \left\| \int_0^1 \mathbf{R}'(t) dt \right\|_F \\ &\leq \int_0^1 \left\| \mathbf{R}'(t) \right\|_F dt \end{aligned}$$

Since  $\mathbf{Q}(t)\mathbf{R}(t)$  is the QR decomposition of  $\mathbf{U}(t)$ , we have:

$$\mathbf{R}^T(t)\mathbf{R}(t) = \mathbf{U}^T(t)\mathbf{U}(t) = \mathbf{U}^T\mathbf{U} + t\boldsymbol{\xi}^T\mathbf{U} + t\mathbf{U}^T\boldsymbol{\xi} + t^2\boldsymbol{\xi}^T\boldsymbol{\xi} \quad (39)$$

Taking the derivative with respect to  $t$  on both sides, we have:

$$\begin{aligned} & \left( \mathbf{R}' \right)^T(t)\mathbf{R}(t) + \mathbf{R}^T(t)\mathbf{R}'(t) \\ &= \boldsymbol{\xi}^T\mathbf{U} + \mathbf{U}^T\boldsymbol{\xi} + 2t\boldsymbol{\xi}^T\boldsymbol{\xi} \end{aligned}$$

We can left multiply both sides by  $(\mathbf{R}^{-1})^T(t)$ , and right multiply both sides by  $\mathbf{R}^{-1}(t)$ , to obtain:

$$(\mathbf{R}^{-1})^T(t) \left( \mathbf{R}' \right)^T(t) + \mathbf{R}'(t)\mathbf{R}^{-1}(t) = (\mathbf{R}^{-1})^T(t) (\boldsymbol{\xi}^T\mathbf{U} + \mathbf{U}^T\boldsymbol{\xi} + 2t\boldsymbol{\xi}^T\boldsymbol{\xi}) \mathbf{R}^{-1}(t)$$

Since on the left hand side,  $\mathbf{R}'(t)\mathbf{R}^{-1}(t)$  is an upper triangular matrix, its transpose  $(\mathbf{R}^{-1})^T(t) \left( \mathbf{R}' \right)^T(t)$  is a lower triangular matrix, we have:

$$\mathbf{R}'(t)\mathbf{R}^{-1}(t) = \text{up} \left[ (\mathbf{R}^{-1})^T(t) (\boldsymbol{\xi}^T\mathbf{U} + \mathbf{U}^T\boldsymbol{\xi} + 2t\boldsymbol{\xi}^T\boldsymbol{\xi}) \mathbf{R}^{-1}(t) \right]$$

where for  $\mathbf{C} \in \mathbb{R}^{d \times d}$ ,  $\text{up}[\cdot]$  is defined as:

$$\text{up}[\mathbf{C}]_{ij} = \begin{cases} C_{ij}, & \text{if } j > i \\ \frac{1}{2}C_{ii}, & \text{if } j = i \\ 0, & \text{if } j < i \end{cases}$$

Therefore,

$$\mathbf{R}'(t) = \text{up} \left[ (\mathbf{R}^{-1})^T(t) (\boldsymbol{\xi}^T\mathbf{U} + \mathbf{U}^T\boldsymbol{\xi} + 2t\boldsymbol{\xi}^T\boldsymbol{\xi}) \mathbf{R}^{-1}(t) \right] \mathbf{R}(t)$$

and accordingly:

$$\begin{aligned} \left\| \mathbf{R}'(t) \right\|_F &= \left\| \text{up} \left[ (\mathbf{R}^{-1})^T(t) (\boldsymbol{\xi}^T\mathbf{U} + \mathbf{U}^T\boldsymbol{\xi} + 2t\boldsymbol{\xi}^T\boldsymbol{\xi}) \mathbf{R}^{-1}(t) \right] \mathbf{R}(t) \right\|_F \\ &\leq \left\| \text{up} \left[ (\mathbf{R}^{-1})^T(t) (\boldsymbol{\xi}^T\mathbf{U} + \mathbf{U}^T\boldsymbol{\xi} + 2t\boldsymbol{\xi}^T\boldsymbol{\xi}) \mathbf{R}^{-1}(t) \right] \right\|_F \left\| \mathbf{R}(t) \right\|_{op} \\ &\leq \left\| (\mathbf{R}^{-1})^T(t) (\boldsymbol{\xi}^T\mathbf{U} + \mathbf{U}^T\boldsymbol{\xi} + 2t\boldsymbol{\xi}^T\boldsymbol{\xi}) \mathbf{R}^{-1}(t) \right\|_F \left\| \mathbf{R}(t) \right\|_{op} \end{aligned}$$

where we used Lemma 14 for the first inequality.

From (39), we know that:

$$\begin{aligned}
 \|\mathbf{R}(t)\|_{op}^2 &= \|\mathbf{R}(t)^T \mathbf{R}(t)\|_{op} \\
 &= \|\mathbf{I} + t(\boldsymbol{\xi}^T \mathbf{U} + \mathbf{U}^T \boldsymbol{\xi}) + t^2 \boldsymbol{\xi}^T \boldsymbol{\xi}\|_{op} \\
 &\geq 1 - t \|\boldsymbol{\xi}^T \mathbf{U} + \mathbf{U}^T \boldsymbol{\xi}\|_{op} - t^2 \|\boldsymbol{\xi}^T \boldsymbol{\xi}\|_{op} \\
 &\geq 1 - 2 \|\boldsymbol{\xi}\|_F - \|\boldsymbol{\xi}^T \boldsymbol{\xi}\|_F \\
 &\geq \frac{7}{16}
 \end{aligned}$$

where the first inequality comes from the triangle inequality, the second comes from the fact that  $\|\cdot\|_F \geq \|\cdot\|_{op}$ , and the third comes from the requirement  $\|\boldsymbol{\xi}\|_F \leq \frac{1}{4}$ .

Similarly, we can derive:

$$\|\mathbf{R}(t)\|_{op}^2 = \|\mathbf{R}(t)^T \mathbf{R}(t)\|_{op} \leq 1 + 2 \|\boldsymbol{\xi}\|_F + \|\boldsymbol{\xi}^T \boldsymbol{\xi}\|_F \leq \frac{25}{16}$$

As a result,

$$\begin{aligned}
 \|\mathbf{R}'(t)\|_F &\leq \|(\mathbf{R}^{-1})^T(t) (\boldsymbol{\xi}^T \mathbf{U} + \mathbf{U}^T \boldsymbol{\xi} + 2t \boldsymbol{\xi}^T \boldsymbol{\xi}) \mathbf{R}^{-1}(t)\|_F \|\mathbf{R}(t)\|_{op} \\
 &\leq \left( \|(\mathbf{R}^{-1})^T(t) (\boldsymbol{\xi}^T \mathbf{U} + \mathbf{U}^T \boldsymbol{\xi}) \mathbf{R}^{-1}(t)\|_F + \|(\mathbf{R}^{-1})^T(t) (2t \boldsymbol{\xi}^T \boldsymbol{\xi}) \mathbf{R}^{-1}(t)\|_F \right) \frac{5}{4} \\
 &\leq \frac{5}{4} \left( \|\boldsymbol{\xi}^T \mathbf{U} + \mathbf{U}^T \boldsymbol{\xi}\|_F \|(\mathbf{R}^{-1})^T(t) \mathbf{R}^{-1}(t)\|_{op} + 2t \|\boldsymbol{\xi}^T \boldsymbol{\xi}\|_F \|(\mathbf{R}^{-1})^T(t) \mathbf{R}^{-1}(t)\|_{op} \right) \\
 &\leq \frac{20}{7} (\|\boldsymbol{\xi}^T \mathbf{U} + \mathbf{U}^T \boldsymbol{\xi}\|_F + 2t \|\boldsymbol{\xi}^T \boldsymbol{\xi}\|_F)
 \end{aligned}$$

Hence,

$$\begin{aligned}
 &\left\| \mathcal{GR}_U^{\text{QR}}(\boldsymbol{\xi}) - (\mathbf{U} + \boldsymbol{\xi}) \right\|_F \\
 &\leq \frac{20}{7} (\|\boldsymbol{\xi}^T \mathbf{U} + \mathbf{U}^T \boldsymbol{\xi}\|_F + \|\boldsymbol{\xi}^T \boldsymbol{\xi}\|_F)
 \end{aligned}$$

Since  $\mathbf{U}$  is an orthogonal matrix,  $\|\mathcal{P}_{\mathcal{N}_U}(\boldsymbol{\xi})\|_F = \frac{1}{2} \|\mathbf{U}(\boldsymbol{\xi}^T \mathbf{U} + \mathbf{U}^T \boldsymbol{\xi})\|_F = \frac{1}{2} \|\boldsymbol{\xi}^T \mathbf{U} + \mathbf{U}^T \boldsymbol{\xi}\|_F$ . By Cauchy-Schwartz inequality,  $\|\boldsymbol{\xi}^T \boldsymbol{\xi}\|_F = \|(\mathcal{P}_{\mathcal{N}_U}(\boldsymbol{\xi}) + \mathcal{P}_{\mathcal{T}_U}(\boldsymbol{\xi}))^T (\mathcal{P}_{\mathcal{N}_U}(\boldsymbol{\xi}) + \mathcal{P}_{\mathcal{T}_U}(\boldsymbol{\xi}))\|_F \leq 2 \|\mathcal{P}_{\mathcal{N}_U}(\boldsymbol{\xi})\|_F^2 + 2 \|\mathcal{P}_{\mathcal{T}_U}(\boldsymbol{\xi})\|_F^2$ .

Thus we have:

$$\begin{aligned}
 &\left\| \mathcal{GR}_U^{\text{QR}}(\boldsymbol{\xi}) - (\mathbf{U} + \boldsymbol{\xi}) \right\|_F \\
 &\leq \frac{20}{7} \left( 2 \|\mathcal{P}_{\mathcal{N}_U}(\boldsymbol{\xi})\|_F + 2 \|\mathcal{P}_{\mathcal{N}_U}(\boldsymbol{\xi})\|_F^2 + 2 \|\mathcal{P}_{\mathcal{T}_U}(\boldsymbol{\xi})\|_F^2 \right) \\
 &\leq \frac{80}{7} \|\mathcal{P}_{\mathcal{N}_U}(\boldsymbol{\xi})\|_F + \frac{40}{7} \|\mathcal{P}_{\mathcal{T}_U}(\boldsymbol{\xi})\|_F^2
 \end{aligned}$$

Hence the second property of definition holds with  $M_1 = \frac{40}{7}$  and  $M_2 = \frac{80}{7}$ .

QR decomposition can be implemented by Gram-Schmidt or Householder algorithm with computation complexity of  $O(dr^2)$

## B. Some lemmas

In this section, we show some lemma useful for later derivations.

We begin with some general inequalities related to matrix trace norm.

**Lemma 13** *For two matrices  $A, B \in \mathbb{R}^{d \times d}$ , if both  $A, B$  are symmetric positive definite, then:*

$$\text{Tr}(AB) \geq 0$$

A simple corollary is that if  $A_1, A_2, B \in \mathbb{R}^{d \times d}$  are symmetric and  $B$  is positive semi-definite, and  $A_1 \succeq A_2$ , then

$$\text{Tr}(A_1 B) \geq \text{Tr}(A_2 B)$$

**Proof** Since both  $A$  and  $B$  are positive symmetric, there exists  $X, Y \in \mathbb{R}^{d \times d}$ , such that  $A = X^T X$  and  $B = Y^T Y$ , therefore:

$$\begin{aligned} \text{Tr}(AB) &= \text{Tr}(X^T X Y^T Y) \\ &= \text{Tr}((Y X^T)^T Y X^T) \\ &\geq 0 \end{aligned}$$

■

The following lemma presents an upper bound of the Frobenius norm of the product of two matrices.

**Lemma 14** *For two matrices  $A \in \mathbb{R}^{m \times n}$ , and  $B \in \mathbb{R}^{n \times k}$ , we have:*

$$\|AB\|_F \leq \|A\|_{op} \|B\|_F$$

and:

$$\|AB\|_F \leq \|A\|_F \|B\|_{op}$$

The proof of the lemma can be found in Sun and Luo (2015).

The following lemma introduces a simple upper bound on the Frobenius norm of  $\mathbf{I}_r - \mathbf{U}^T \mathbf{P} \mathbf{U}$ .

**Lemma 15** *For any rank- $r$  orthonormal matrix  $\mathbf{U} \in \mathbb{R}^{d \times r}$ , and rank- $r$  projection matrix  $\mathbf{P} \in \mathbb{R}^{d \times d}$ , we have:*

$$\|\mathbf{I}_r - \mathbf{U}^T \mathbf{P} \mathbf{U}\|_F \leq r - \text{Tr}(\mathbf{U}^T \mathbf{P} \mathbf{U}) \quad (40)$$

**Proof** It is easy to see that  $\mathbf{I}_r - \mathbf{U}^T \mathbf{P} \mathbf{U}$  is positive semidefinite. And for a positive semidefinite matrix, its Frobenius norm is upper bounded by its trace. Inequality (40) follows accordingly. ■

We can proceed to the following lemma that upper bounds the trace of the  $k$ -th power of  $\mathbf{I}_r - \mathbf{U}^T \mathbf{P} \mathbf{U}$ .

**Lemma 16** *For any rank- $r$  orthonormal matrix  $\mathbf{U} \in \mathbb{R}^{d \times r}$ , and rank- $r$  projection matrix  $\mathbf{P} \in \mathbb{R}^{d \times d}$ ,  $k = 1, 2, \dots$ ,  $(\mathbf{I}_r - \mathbf{U}^T \mathbf{P} \mathbf{U})^k$  is positive semi-definite and:*

$$0 \leq \text{Tr}((\mathbf{I}_r - \mathbf{U}^T \mathbf{P} \mathbf{U})^k) \leq (r - \text{Tr}(\mathbf{U}^T \mathbf{P} \mathbf{U}))^k \quad (41)$$

**Proof** Since  $\mathbf{I}_r - \mathbf{U}^T \mathbf{P} \mathbf{U}$  is symmetric positive semidefinite,  $(\mathbf{I}_r - \mathbf{U}^T \mathbf{P} \mathbf{U})^k$  is also symmetric positive semidefinite. Assume eigenvalues of  $\mathbf{I}_r - \mathbf{U}^T \mathbf{P} \mathbf{U}$  are  $\lambda_1, \lambda_2, \dots, \lambda_d$ , with  $\lambda_1 \geq \lambda_2 \geq \dots \geq \lambda_d$ , we know that  $\text{Tr}((\mathbf{I}_r - \mathbf{U}^T \mathbf{P} \mathbf{U})^k) = \sum_{i=1}^d \lambda_i^k \leq \lambda_1^{k-1} \sum_{i=1}^d \lambda_i$ .

By Lemma 15, we know that

$$\lambda_1^{k-1} \leq \|\mathbf{I}_r - \mathbf{U}^T \mathbf{P} \mathbf{U}\|_F^{k-1} \leq (r - \text{Tr}(\mathbf{U}^T \mathbf{P} \mathbf{U}))^{k-1}$$

This completes our proof. ■

Based on the above results, we can discuss some properties of the projection of a matrix onto a subspace. Suppose we know the column space of  $\mathbf{U} \in \mathbb{R}^{d \times r}$  is close to that of  $\mathbf{P} \in \mathbb{R}^{d \times d}$ , can we find a matrix  $\mathbf{U}^*$  close to  $\mathbf{U}$  with column vectors in  $\text{col}(\mathbf{P})$ ? The following two lemmas give affirmative answers.

**Lemma 17** *For any rank- $r$  orthonormal matrix  $\mathbf{U} \in \mathbb{R}^{d \times r}$ , and rank- $r$  projection matrix  $\mathbf{P} \in \mathbb{R}^{d \times d}$ , we define:*

$$\mathbf{U}^* = \mathbf{P} \mathbf{U} (\mathbf{U}^T \mathbf{P} \mathbf{U})^{-1/2}$$

If  $r - \text{Tr}(\mathbf{U}^T \mathbf{P} \mathbf{U}) \leq 1$ , we have:

$$\|\mathbf{U} - \mathbf{U}^*\|_F^2 \geq r - \text{Tr}(\mathbf{U}^T \mathbf{P} \mathbf{U}) \quad (42)$$

and:

$$\|\mathbf{U} - \mathbf{U}^*\|_F^2 \leq 2(r - \text{Tr}(\mathbf{U}^T \mathbf{P} \mathbf{U})) \quad (43)$$

**Proof** Since:

$$\begin{aligned} \|\mathbf{U} - \mathbf{U}^*\|_F^2 &= \langle \mathbf{U}, \mathbf{U} \rangle + \langle \mathbf{U}^*, \mathbf{U}^* \rangle - 2\langle \mathbf{U}, \mathbf{U}^* \rangle \\ &= 2r - 2\langle \mathbf{U}, \mathbf{U}^* \rangle \end{aligned}$$

We need to find an upper bound for  $\langle \mathbf{U}, \mathbf{U}^* \rangle$ .

Notice that:

$$\begin{aligned} &\langle \mathbf{U}, \mathbf{U}^* \rangle \\ &= \text{Tr}(\mathbf{U}^T \mathbf{U}^*) \\ &= \text{Tr}(\mathbf{U}^T \mathbf{P} \mathbf{U} (\mathbf{U}^T \mathbf{P} \mathbf{U})^{-1/2}) \\ &= \text{Tr}((\mathbf{U}^T \mathbf{P} \mathbf{U})^{1/2}) \\ &= \text{Tr}((\mathbf{I}_r - (\mathbf{I}_r - \mathbf{U}^T \mathbf{P} \mathbf{U}))^{1/2}) \\ &= \text{Tr}\left(\mathbf{I}_r - \frac{1}{2}(\mathbf{I}_r - \mathbf{U}^T \mathbf{P} \mathbf{U}) - \sum_{n=2}^{\infty} \frac{(2n-3)!!}{2^n n!} (\mathbf{I}_r - \mathbf{U}^T \mathbf{P} \mathbf{U})^n\right) \\ &= r - \frac{1}{2} \text{Tr}(\mathbf{I}_r - \mathbf{U}^T \mathbf{P} \mathbf{U}) - \sum_{n=2}^{\infty} \frac{(2n-3)!!}{2^n n!} \text{Tr}((\mathbf{I}_r - \mathbf{U}^T \mathbf{P} \mathbf{U})^n) \\ &\leq r - \frac{1}{2} \text{Tr}(\mathbf{I}_r - \mathbf{U}^T \mathbf{P} \mathbf{U}) \end{aligned}$$

We used the series  $(1-x)^{\frac{1}{2}} = 1 - \frac{1}{2}x - \sum_{n=2}^{\infty} \frac{(2n-3)!!}{2^n n!} x^n$ , and the result  $\text{Tr}((\mathbf{I}_r - \mathbf{U}^T \mathbf{P} \mathbf{U})^n) \geq 0$  from Lemma 16.

As a result:

$$\|\mathbf{U} - \mathbf{U}^*\|_F^2 \geq \text{Tr}(\mathbf{I}_r - \mathbf{U}^T \mathbf{P} \mathbf{U}) = r - \text{Tr}(\mathbf{U}^T \mathbf{P} \mathbf{U})$$

Similarly, from Lemma 16,  $\text{Tr}((\mathbf{I}_r - \mathbf{U}^T \mathbf{P} \mathbf{U})^n) \leq \text{Tr}(\mathbf{I}_r - \mathbf{U}^T \mathbf{P} \mathbf{U})^n$ , thus:

$$\begin{aligned} & \langle \mathbf{U}, \mathbf{U}^* \rangle \\ &= r - \frac{1}{2} \text{Tr}(\mathbf{I}_r - \mathbf{U}^T \mathbf{P} \mathbf{U}) - \sum_{n=2}^{\infty} \frac{(2n-3)!!}{2^n n!} \text{Tr}((\mathbf{I}_r - \mathbf{U}^T \mathbf{P} \mathbf{U})^n) \\ &\geq r - \frac{1}{2} \text{Tr}(\mathbf{I}_r - \mathbf{U}^T \mathbf{P} \mathbf{U}) - \sum_{n=2}^{\infty} \frac{(2n-3)!!}{2^n n!} \text{Tr}(\mathbf{I}_r - \mathbf{U}^T \mathbf{P} \mathbf{U})^n \\ &= r + (1 - \text{Tr}(\mathbf{I}_r - \mathbf{U}^T \mathbf{P} \mathbf{U}))^{\frac{1}{2}} - 1 \\ &\geq -\text{Tr}(\mathbf{I}_r - \mathbf{U}^T \mathbf{P} \mathbf{U}) \end{aligned}$$

where we used the relation  $\sqrt{1-x} - 1 \geq -x, \forall x \in [0, 1]$ , in the last inequality.

Thus

$$\|\mathbf{U} - \mathbf{U}^*\|_F^2 \leq 2 \text{Tr}(\mathbf{I}_r - \mathbf{U}^T \mathbf{P} \mathbf{U}) = 2(r - \text{Tr}(\mathbf{U}^T \mathbf{P} \mathbf{U}))$$

■

The following lemma corresponds to Lemma 2 in the main paper. It shows that we can identify global PCs from local PCs.

**Lemma 18** *Suppose for  $i = 1, \dots, N$ ,  $\mathbf{P}_U$ ,  $\mathbf{P}_{V(i)}$  and  $\mathbf{P}_U^*$ ,  $\mathbf{P}_{V(i)}^*$  are projection matrices satisfying  $\mathbf{P}_U \mathbf{P}_{V(i)} = 0$  and  $\mathbf{P}_U^* \mathbf{P}_{V(i)}^* = 0$  for each  $i$ . Among them,  $\mathbf{P}_U$  and  $\mathbf{P}_U^*$  have rank  $r_1$ ,  $\mathbf{P}_{V(i)}$  and  $\mathbf{P}_{V(i)}^*$  have rank  $r_{2,(i)}$ . If there exists a positive constant  $\theta > 0$  such that*

$$\lambda_{\max}\left(\frac{1}{N} \sum_{i=1}^N \mathbf{P}_{V(i)}^*\right) \leq 1 - \theta$$

*we have the following bound:*

$$\sum_{i=1}^N r_1 + r_{2,(i)} - \text{Tr}\left((\mathbf{P}_U + \mathbf{P}_{V(i)}) (\mathbf{P}_U^* + \mathbf{P}_{V(i)}^*)\right) \leq N(r_1 - \text{Tr}(\mathbf{P}_U^* \mathbf{P}_U)) + \sum_{i=1}^N r_{2,(i)} - \text{Tr}(\mathbf{P}_{V(i)}^* \mathbf{P}_{V(i)}) \quad (44)$$

And also:

$$\begin{aligned} & \sum_{i=1}^N r_1 + r_{2,(i)} - \text{Tr}\left((\mathbf{P}_U + \mathbf{P}_{V(i)}) (\mathbf{P}_U^* + \mathbf{P}_{V(i)}^*)\right) \\ & \geq \frac{\theta}{2} \left( N(r_1 - \text{Tr}(\mathbf{P}_U^* \mathbf{P}_U)) + \sum_{i=1}^N r_{2,(i)} - \text{Tr}(\mathbf{P}_{V(i)}^* \mathbf{P}_{V(i)}) \right) \end{aligned} \quad (45)$$

Notice that we can replace  $+$  by  $\oplus$  on the left hand side of (44) and (45)

**Proof** We first calculate the upper bound.

Since  $\mathbf{P}_U \mathbf{P}_{V(i)}^* \mathbf{P}_U$  is positive semidefinite, we know that:

$$\text{Tr} \left( \mathbf{P}_U \mathbf{P}_{V(i)}^* \mathbf{P}_U \right) \geq 0$$

Thus

$$\text{Tr} \left( \mathbf{P}_U \mathbf{P}_{V(i)}^* \mathbf{P}_U \right) = \text{Tr} \left( \mathbf{P}_U \mathbf{P}_{V(i)}^* \right) \geq 0$$

Similarly, we have:

$$\text{Tr} \left( \mathbf{P}_U^* \mathbf{P}_{V(i)} \right) \geq 0$$

Combining them, we have:

$$\begin{aligned} & \text{Tr} \left( \left( \mathbf{P}_U + \mathbf{P}_{V(i)} \right) \left( \mathbf{P}_U^* + \mathbf{P}_{V(i)}^* \right) \right) \\ &= \text{Tr} \left( \mathbf{P}_U \mathbf{P}_U^* \right) + \text{Tr} \left( \mathbf{P}_U \mathbf{P}_{V(i)}^* \right) + \text{Tr} \left( \mathbf{P}_{V(i)} \mathbf{P}_U^* \right) + \text{Tr} \left( \mathbf{P}_{V(i)} \mathbf{P}_{V(i)}^* \right) \\ &\geq \text{Tr} \left( \mathbf{P}_U \mathbf{P}_U^* \right) + \text{Tr} \left( \mathbf{P}_{V(i)} \mathbf{P}_{V(i)}^* \right) \end{aligned}$$

This proves inequality (44).

Next we calculate the lower bound.

$$\begin{aligned} & \sum_{i=1}^N \text{Tr} \left( \left( \mathbf{P}_U + \mathbf{P}_{V(i)} \right) \left( \mathbf{P}_U^* + \mathbf{P}_{V(i)}^* \right) \right) \\ &= \sum_{i=1}^N \text{Tr} \left( \mathbf{P}_U \mathbf{P}_U^* \right) + \text{Tr} \left( \mathbf{P}_U \mathbf{P}_{V(i)}^* \right) + \text{Tr} \left( \mathbf{P}_{V(i)} \mathbf{P}_U^* \right) + \text{Tr} \left( \mathbf{P}_{V(i)} \mathbf{P}_{V(i)}^* \right) \\ &= \sum_{i=1}^N \text{Tr} \left( \mathbf{P}_U \mathbf{P}_U^* \right) + \text{Tr} \left( \mathbf{P}_U \left( \mathbf{I} - \mathbf{P}_U^* \right) \mathbf{P}_{V(i)}^* \left( \mathbf{I} - \mathbf{P}_U^* \right) \right) + \text{Tr} \left( \mathbf{P}_{V(i)} \mathbf{P}_U^* \right) + \text{Tr} \left( \mathbf{P}_{V(i)} \mathbf{P}_{V(i)}^* \right) \\ &= \sum_{i=1}^N \text{Tr} \left( \mathbf{P}_U \mathbf{P}_U^* \right) + \text{Tr} \left( \left( \mathbf{I} - \mathbf{P}_U^* \right) \mathbf{P}_U \left( \mathbf{I} - \mathbf{P}_U^* \right) \mathbf{P}_{V(i)}^* \right) + \text{Tr} \left( \mathbf{P}_{V(i)} \mathbf{P}_U^* \right) + \text{Tr} \left( \mathbf{P}_{V(i)} \mathbf{P}_{V(i)}^* \right) \end{aligned}$$

Since  $\left( \mathbf{I} - \mathbf{P}_U^* \right) \mathbf{P}_U \left( \mathbf{I} - \mathbf{P}_U^* \right)$  and  $\mathbf{P}_{V(i)}^*$  are both symmetric positive semidefinite, we have:

$$\begin{aligned} & \text{Tr} \left( \left( \mathbf{I} - \mathbf{P}_U^* \right) \mathbf{P}_U \left( \mathbf{I} - \mathbf{P}_U^* \right) \frac{1}{N} \sum_{i=1}^N \mathbf{P}_{V(i)}^* \right) \\ &\leq \text{Tr} \left( \left( \mathbf{I} - \mathbf{P}_U^* \right) \mathbf{P}_U \left( \mathbf{I} - \mathbf{P}_U^* \right) \right) \lambda_{\max} \left( \frac{1}{N} \sum_{i=1}^N \mathbf{P}_{V(i)}^* \right) \\ &\leq \text{Tr} \left( \mathbf{P}_U - \mathbf{P}_U \mathbf{P}_U^* \right) (1 - \theta) \\ &= (r_1 - \text{Tr} \left( \mathbf{P}_U \mathbf{P}_U^* \right)) (1 - \theta) \end{aligned}$$

For notation simplicity, we define  $z_0 = r_1 - \text{Tr} \left( \mathbf{P}_U \mathbf{P}_U^* \right)$  and  $z_i = r_{2,(i)} - \text{Tr} \left( \mathbf{P}_{V(i)} \mathbf{P}_{V(i)}^* \right)$ .

From the orthogonality, we have:

$$\begin{aligned}
& \text{Tr} \left( P_{V(i)} P_U^* \right) \\
&= \text{Tr} \left( P_{V(i)} \left( I - P_{V(i)}^* \right) P_U^* \left( I - P_{V(i)}^* \right) \right) \\
&= \text{Tr} \left( \left( I - P_{V(i)}^* \right) P_{V(i)} \left( I - P_{V(i)}^* \right) P_U^* \right) \\
&\leq \text{Tr} \left( \left( I - P_{V(i)}^* \right) P_{V(i)} \left( I - P_{V(i)}^* \right) \right) \lambda_{\max} (P_U^*) \\
&\leq \text{Tr} \left( \left( I - P_{V(i)}^* \right) P_{V(i)} \left( I - P_{V(i)}^* \right) \right) \\
&= \text{Tr} \left( P_{V(i)} - P_{V(i)} P_{V(i)}^* \right) \\
&= z_i
\end{aligned}$$

Also, from the orthogonality, we have:

$$\begin{aligned}
& \text{Tr} \left( P_{V(i)} P_U^* \right) \\
&= \text{Tr} \left( (I - P_U) P_{V(i)} (I - P_U) P_U^* \right) \\
&= \text{Tr} \left( P_{V(i)} (I - P_U) P_U^* (I - P_U) \right) \\
&\leq \text{Tr} \left( (I - P_U) P_U^* (I - P_U) \right) \lambda_{\max} (P_{V(i)}) \\
&\leq \text{Tr} \left( (I - P_U) P_U^* (I - P_U) \right) \\
&= \text{Tr} (P_U^* - P_U P_U^*) \\
&= z_0
\end{aligned}$$

Combining the two:

$$\text{Tr} \left( P_{V(i)} P_U^* \right) \leq \min\{z_0, z_i\}$$

As a result:

$$\begin{aligned}
& \sum_{i=1}^N r_1 + r_{2,(i)} - \left[ \text{Tr} (P_U P_U^*) + \text{Tr} \left( (I - P_U^*) P_U (I - P_U^*) P_{V(i)}^* \right) + \text{Tr} \left( P_{V(i)} P_U^* \right) + \text{Tr} \left( P_{V(i)} P_{V(i)}^* \right) \right] \\
&\geq \sum_{i=1}^N z_0 - (1 - \theta) z_0 + z_i - \min\{z_0, z_i\}
\end{aligned}$$

Since for any number  $\nu \in (0, 1)$ , we know:

$$z_i - \min\{z_0, z_i\} \geq \nu (z_i - z_0)$$

We can set  $\nu = \frac{\theta}{2}$ , then

$$\begin{aligned} & \sum_{i=1}^N z_0 - (1 - \theta) z_0 + z_i - \min\{z_0, z_i\} \\ & \geq \sum_{i=1}^N \theta z_0 + \frac{\theta}{2} (z_i - z_0) \\ & = \frac{\theta}{2} \sum_{i=1}^N z_0 + z_i \end{aligned}$$

This proves inequality (45). ■

### C. KKT condition and proof of Theorem 8

We first show KKT conditions (25). The lagrangian to the objective (7) is:

$$\begin{aligned} \mathcal{L} = \sum_{i=1}^N & \left[ \frac{1}{2} \text{Tr}(\mathbf{U}^T \mathbf{S}_{(i)} \mathbf{U}) + \frac{1}{2} \text{Tr}(\mathbf{V}_{(i)}^T \mathbf{S}_{(i)} \mathbf{V}_{(i)}) + \langle \boldsymbol{\Lambda}_{2,(i)}, \mathbf{V}_{(i)}^T \mathbf{V}_{(i)} - \mathbf{I} \rangle + \langle \boldsymbol{\Lambda}_{3,(i)}, \mathbf{U}^T \mathbf{V}_{(i)} \rangle \right] \\ & + \langle \boldsymbol{\Lambda}_1, \mathbf{U}^T \mathbf{U} \rangle \end{aligned} \quad (46)$$

where  $\boldsymbol{\Lambda}_1 \in \mathbb{R}^{r_1 \times r_1}$ ,  $\boldsymbol{\Lambda}_{2,(i)} \in \mathbb{R}^{r_{2,(i)} \times r_{2,(i)}}$ , and  $\boldsymbol{\Lambda}_{3,(i)} \in \mathbb{R}^{r_1 \times r_{2,(i)}}$  are dual variables. The KKT conditions are:

$$\begin{cases} \mathbf{S}_{(i)} \mathbf{V}_{(i)} + \mathbf{V}_{(i)} (\boldsymbol{\Lambda}_{2,(i)} + \boldsymbol{\Lambda}_{2,(i)}^T) + \mathbf{U} \boldsymbol{\Lambda}_{3,(i)} = 0 \\ \sum_{i=1}^N [\mathbf{S}_{(i)} \mathbf{U} + \mathbf{V}_{(i)} \boldsymbol{\Lambda}_{3,(i)}^T] + \mathbf{U} (\boldsymbol{\Lambda}_1 + \boldsymbol{\Lambda}_1^T) = 0 \\ \mathbf{U}^T \mathbf{U} = \mathbf{I}_{r_1}, \mathbf{V}_{(i)}^T \mathbf{V}_{(i)} = \mathbf{I}_{r_{2,(i)}}, \mathbf{U}^T \mathbf{V}_i = 0 \end{cases} \quad (47)$$

By left multiplying the first equation in (47) with  $\mathbf{I} - \mathbf{P}_\mathbf{U} - \mathbf{P}_{\mathbf{V}_{(i)}}$ , we have  $(\mathbf{I} - \mathbf{P}_\mathbf{U} - \mathbf{P}_{\mathbf{V}_{(i)}}) \mathbf{S}_{(i)} \mathbf{V}_{(i)} = 0$ , which is the first equation in (25). By left multiplying the first equation in (47) with  $\mathbf{U}^T$ , we have  $\boldsymbol{\Lambda}_{3,(i)} = -\mathbf{U}^T \mathbf{S}_{(i)} \mathbf{V}_{(i)}$ . Plugging this into the second equation in (47), we have  $\sum_{i=1}^N [\mathbf{S}_{(i)} \mathbf{U} - \mathbf{P}_{\mathbf{V}_{(i)}} \mathbf{S}_{(i)} \mathbf{U}] + \mathbf{U} (\boldsymbol{\Lambda}_1 + \boldsymbol{\Lambda}_1^T) = 0$ . We then left multiply both sides again by  $\mathbf{I} - \mathbf{P}_\mathbf{U}$ . The second equation in (25) follows accordingly. One can also infer (47) from (25).

Then we consider the global convergence. We begin by calculate the derivative of  $\mathcal{L}_{(i),1}$  and  $\mathcal{L}_{(i),2}$ . The derivative of  $\mathcal{L}_{(i),1}$  over  $\mathbf{U}$  is:

$$\nabla_{\mathbf{U}} \mathcal{L}_{(i),1}(\mathbf{U}, \mathbf{V}) = -(\mathbf{I} - \mathbf{P}_\mathbf{V}) \mathbf{S}_{(i)} (\mathbf{I} - \mathbf{P}_\mathbf{V}) \mathbf{U} \quad (48)$$

When  $\mathbf{V}^T \mathbf{U} = 0$ , this reduces to:

$$\nabla_{\mathbf{U}} \mathcal{L}_{(i),1}(\mathbf{U}, \mathbf{V}) = -(\mathbf{I} - \mathbf{P}_\mathbf{V}) \mathbf{S}_{(i)} \mathbf{U}$$

And the derivative of  $\mathcal{L}_{(i),1}$  over  $\mathbf{V}$  is:

$$\nabla_{\mathbf{V}} \mathcal{L}_{(i),1}(\mathbf{U}, \mathbf{V}) = \mathbf{P}_{\mathbf{U}} \mathbf{S}_{(i)} \mathbf{V} + \mathbf{S}_{(i)} \mathbf{P}_{\mathbf{U}} \mathbf{V} - \mathbf{P}_{\mathbf{U}} \mathbf{P}_{\mathbf{V}} \mathbf{S}_{(i)} \mathbf{V} - \mathbf{S}_{(i)} \mathbf{P}_{\mathbf{V}} \mathbf{P}_{\mathbf{U}} \mathbf{V} \quad (49)$$

When  $\mathbf{V}^T \mathbf{U} = 0$ , this reduces to:

$$\nabla_{\mathbf{V}} \mathcal{L}_{(i),1}(\mathbf{U}, \mathbf{V}) = \mathbf{P}_{\mathbf{U}} \mathbf{S}_{(i)} \mathbf{V}$$

Similarly, the derivative of  $\mathcal{L}_{(i),2}$  over  $\mathbf{V}$  is:

$$\nabla_{\mathbf{V}} \mathcal{L}_{(i),2}(\mathbf{U}, \mathbf{V}) = -\mathbf{S}_{(i)} \mathbf{V} \quad (50)$$

The following lemma shows the function we introduced is Lipschitz continuous.

**Lemma 19** *When  $\|\mathbf{U}\|_{op}$  and  $\|\mathbf{V}\|_{op}$  are upper bounded by 1, the functions  $\mathcal{L}_{(i),1} + \mathcal{L}_{(i),2}$  are Lipschitz continuous with constant  $L$ . More formally, for any  $\mathbf{U}_1, \mathbf{U}_2, \mathbf{V}_1, \mathbf{V}_2 \in \mathbb{R}^{d \times r}$ , such that  $\|\mathbf{U}_1\|_{op}, \|\mathbf{U}_2\|_{op}, \|\mathbf{V}_1\|_{op}, \|\mathbf{V}_2\|_{op} \leq 1$ , we have:*

$$\begin{aligned} & \left\| \left[ \nabla_{\mathbf{U}} \mathcal{L}_{(i),1}(\mathbf{U}_2, \mathbf{V}_2) - \nabla_{\mathbf{U}} \mathcal{L}_{(i),1}(\mathbf{U}_1, \mathbf{V}_1), \right. \right. \\ & \left. \nabla_{\mathbf{V}} \mathcal{L}_{(i),1}(\mathbf{U}_2, \mathbf{V}_2) + \nabla_{\mathbf{V}} \mathcal{L}_{(i),2}(\mathbf{U}_2, \mathbf{V}_2) - \nabla_{\mathbf{V}} \mathcal{L}_{(i),1}(\mathbf{U}_1, \mathbf{V}_1) - \nabla_{\mathbf{V}} \mathcal{L}_{(i),2}(\mathbf{U}_1, \mathbf{V}_1) \right] \Big\|_F \\ & \leq L \sqrt{\|\mathbf{U}_1 - \mathbf{U}_2\|_F^2 + \|\mathbf{V}_1 - \mathbf{V}_2\|_F^2} \end{aligned} \quad (51)$$

where

$$L = 9\sqrt{2}G_{(i),op} \quad (52)$$

**Proof** First we calculate the difference in the gradient of  $\mathbf{U}$ :

$$\begin{aligned} & \left\| \nabla_{\mathbf{U}} \mathcal{L}_{(i),1}(\mathbf{U}_2, \mathbf{V}_2) - \nabla_{\mathbf{U}} \mathcal{L}_{(i),1}(\mathbf{U}_1, \mathbf{V}_1) \right\|_F \\ & = \left\| (\mathbf{I} - \mathbf{V}_1 \mathbf{V}_1^T) \mathbf{S}_{(i)} \mathbf{U}_1 - (\mathbf{I} - \mathbf{V}_2 \mathbf{V}_2^T) \mathbf{S}_{(i)} \mathbf{U}_2 \right\|_F \\ & \leq \left\| (\mathbf{I} - \mathbf{V}_1 \mathbf{V}_1^T) \mathbf{S}_{(i)} \mathbf{U}_1 - (\mathbf{I} - \mathbf{V}_2 \mathbf{V}_2^T) \mathbf{S}_{(i)} \mathbf{U}_1 \right\|_F + \left\| (\mathbf{I} - \mathbf{V}_2 \mathbf{V}_2^T) \mathbf{S}_{(i)} \mathbf{U}_1 - (\mathbf{I} - \mathbf{V}_2 \mathbf{V}_2^T) \mathbf{S}_{(i)} \mathbf{U}_2 \right\|_F \\ & \leq \left\| \mathbf{V}_1 \mathbf{V}_1^T - \mathbf{V}_2 \mathbf{V}_2^T \right\|_F G_{(i),op} + \|\mathbf{U}_1 - \mathbf{U}_2\|_F G_{(i),op} \\ & \leq 2 \|\mathbf{V}_1 - \mathbf{V}_2\|_F G_{(i),op} + \|\mathbf{U}_1 - \mathbf{U}_2\|_F G_{(i),op} \end{aligned}$$

where we used the triangle inequality for the Frobenius norm for the first inequality, and Lemma 14 for the second and third inequality. Next we calculate the difference in the gradient of  $\mathbf{V}$ :

$$\begin{aligned} & \left\| \nabla_{\mathbf{V}} \mathcal{L}_{(i),1}(\mathbf{U}_2, \mathbf{V}_2) + \nabla_{\mathbf{V}} \mathcal{L}_{(i),2}(\mathbf{U}_2, \mathbf{V}_2) - \nabla_{\mathbf{V}} \mathcal{L}_{(i),1}(\mathbf{U}_1, \mathbf{V}_1) - \nabla_{\mathbf{V}} \mathcal{L}_{(i),2}(\mathbf{U}_1, \mathbf{V}_1) \right\|_F \\ & \leq \left\| (\mathbf{P}_{\mathbf{U}_2} - \mathbf{I}) \mathbf{S}_{(i)} \mathbf{V}_2 - (\mathbf{P}_{\mathbf{U}_1} - \mathbf{I}) \mathbf{S}_{(i)} \mathbf{V}_1 \right\|_F + \left\| \mathbf{S}_{(i)} \mathbf{P}_{\mathbf{U}_2} \mathbf{V}_2 - \mathbf{S}_{(i)} \mathbf{P}_{\mathbf{U}_1} \mathbf{V}_1 \right\|_F \\ & + \left\| \mathbf{P}_{\mathbf{U}_2} \mathbf{P}_{\mathbf{V}_2} \mathbf{S}_{(i)} \mathbf{V}_2 - \mathbf{P}_{\mathbf{U}_1} \mathbf{P}_{\mathbf{V}_1} \mathbf{S}_{(i)} \mathbf{V}_1 \right\|_F + \left\| \mathbf{S}_{(i)} \mathbf{P}_{\mathbf{V}_2} \mathbf{P}_{\mathbf{U}_2} \mathbf{V}_2 - \mathbf{S}_{(i)} \mathbf{P}_{\mathbf{V}_1} \mathbf{P}_{\mathbf{U}_1} \mathbf{V}_1 \right\|_F \\ & \leq 7 \|\mathbf{V}_1 - \mathbf{V}_2\|_F G_{(i),op} + 6 \|\mathbf{U}_1 - \mathbf{U}_2\|_F G_{(i),op} \end{aligned}$$

Summing them up, we know:

$$\begin{aligned}
 & \left\| \left[ \nabla_{\mathbf{U}} \mathcal{L}_{(i),1}(\mathbf{U}_2, \mathbf{V}_2) - \nabla_{\mathbf{U}} \mathcal{L}_{(i),1}(\mathbf{U}_1, \mathbf{V}_1), \right. \right. \\
 & \left. \nabla_{\mathbf{V}} \mathcal{L}_{(i),1}(\mathbf{U}_2, \mathbf{V}_2) + \nabla_{\mathbf{V}} \mathcal{L}_{(i),2}(\mathbf{U}_2, \mathbf{V}_2) - \nabla_{\mathbf{V}} \mathcal{L}_{(i),1}(\mathbf{U}_1, \mathbf{V}_1) - \nabla_{\mathbf{V}} \mathcal{L}_{(i),2}(\mathbf{U}_1, \mathbf{V}_1) \right] \right\|_F \\
 & \leq \left\| \nabla_{\mathbf{U}} \mathcal{L}_{(i),1}(\mathbf{U}_2, \mathbf{V}_2) - \nabla_{\mathbf{U}} \mathcal{L}_{(i),1}(\mathbf{U}_1, \mathbf{V}_1) \right\|_F \\
 & + \left\| \nabla_{\mathbf{V}} \mathcal{L}_{(i),1}(\mathbf{U}_2, \mathbf{V}_2) + \nabla_{\mathbf{V}} \mathcal{L}_{(i),2}(\mathbf{U}_2, \mathbf{V}_2) - \nabla_{\mathbf{V}} \mathcal{L}_{(i),1}(\mathbf{U}_1, \mathbf{V}_1) - \nabla_{\mathbf{V}} \mathcal{L}_{(i),2}(\mathbf{U}_1, \mathbf{V}_1) \right\|_F \\
 & \leq 9 \|\mathbf{V}_1 - \mathbf{V}_2\|_F G_{(i),op} + 7 \|\mathbf{U}_1 - \mathbf{U}_2\|_F G_{(i),op} \\
 & \leq 9\sqrt{2} G_{max,op} \sqrt{\|\mathbf{U}_1 - \mathbf{U}_2\|_F^2 + \|\mathbf{V}_1 - \mathbf{V}_2\|_F^2}
 \end{aligned} \tag{53}$$

We thus complete the proof. ■

Now we introduce some notations:

$$\square \mathbf{U}_\tau = \frac{1}{N} \sum_{i=1}^N \left( \mathbf{I} - \mathbf{P}_{\mathbf{U}_\tau} - \mathbf{P}_{\mathbf{V}_{(i),\tau}} \right) \mathbf{S}_{(i)} \mathbf{U}_\tau \tag{54}$$

It is easy to verify  $\square \mathbf{U}_\tau \in \mathcal{T}_{\mathbf{U}_\tau}$  when  $\mathbf{U}^T \mathbf{V}_{(i),\tau} = 0$ :

$$\mathbf{U}_\tau^T \square \mathbf{U}_\tau = 0$$

The Frobenius norm of  $\square \mathbf{U}_\tau$  is upper bounded by:

$$\begin{aligned}
 & \|\square \mathbf{U}_\tau\|_F \\
 & = \left\| \frac{1}{N} \sum_{i=1}^N \left( \mathbf{I} - \mathbf{P}_{\mathbf{U}_\tau} - \mathbf{P}_{\mathbf{V}_{(i),\tau}} \right) \mathbf{S}_{(i)} \mathbf{U}_\tau \right\|_F \\
 & \leq \frac{1}{N} \sum_{i=1}^N \left\| \left( \mathbf{I} - \mathbf{P}_{\mathbf{U}_\tau} - \mathbf{P}_{\mathbf{V}_{(i),\tau}} \right) \right\|_{op} \|\mathbf{S}_{(i)}\|_{op} \|\mathbf{U}_\tau\|_F \\
 & \leq \frac{1}{N} \sum_{i=1}^N G_{max,op} \sqrt{r} \\
 & = G_{max,op} \sqrt{r}
 \end{aligned} \tag{55}$$

where we applied Lemma 14 for the first inequality.

By the client update rule, we know that:

$$\mathbf{U}_{(i),\tau+1} = \mathbf{U}_\tau + \eta_\tau \left( \mathbf{I} - \mathbf{P}_{\mathbf{U}_\tau} - \mathbf{P}_{\mathbf{V}_{(i),\tau}} \right) \mathbf{S}_{(i)} \mathbf{U}_\tau \tag{56}$$

Therefore, after the server takes the average of  $\mathbf{U}_{(i),\tau+1}$  and performs generalized retraction, the following holds:

$$\mathbf{U}_{\tau+1} = \mathbf{U}_\tau + \eta_\tau \square \mathbf{U}_\tau + \eta_\tau^2 \mathbf{e}_{1,\tau} \tag{57}$$

where  $\mathbf{e}_{1,\tau}$  is an error term defined as:

$$\mathbf{e}_{1,\tau} = \frac{1}{\eta_\tau^2} (\mathbf{U}_{\tau+1} - \mathbf{U}_\tau - \eta_\tau \square \mathbf{U}_\tau)$$

By definition of generalized retraction, since  $\square \mathbf{U}_\tau$  is in the tangent space of  $\mathbf{U}_\tau$ , we have:

$$\|\mathbf{e}_{1,\tau}\|_F \leq M_1 \|\square \mathbf{U}_\tau\|_F^2$$

where we applied the condition  $\eta_\tau \leq \frac{M_3}{\sqrt{r}G_{max,op}}$  thus  $\|\eta_\tau \square \mathbf{U}_\tau\|_F \leq M_3$ .

Similarly we define:

$$\square \mathbf{V}_{(i),\tau} = \left( \mathbf{I} - \mathbf{P}_{\mathbf{U}_\tau} - \mathbf{P}_{\mathbf{V}_{(i),\tau}} \right) \mathbf{S}_{(i)} \mathbf{V}_{(i),\tau} \quad (58)$$

Also by Lemma 14, the Frobenius norm of  $\square \mathbf{V}_{(i),\tau}$  is upper bounded by:

$$\begin{aligned} & \|\square \mathbf{V}_{(i),\tau}\|_F \\ &= \left\| \left( \mathbf{I} - \mathbf{P}_{\mathbf{U}_\tau} - \mathbf{P}_{\mathbf{V}_{(i),\tau}} \right) \mathbf{S}_{(i)} \mathbf{V}_{(i),\tau} \right\|_F \\ &\leq \left\| \left( \mathbf{I} - \mathbf{P}_{\mathbf{U}_\tau} - \mathbf{P}_{\mathbf{V}_{(i),\tau}} \right) \right\|_{op} \|\mathbf{S}_{(i)}\|_{op} \|\mathbf{V}_{(i),\tau}\|_F \\ &\leq G_{(i),op} \sqrt{r} \end{aligned} \quad (59)$$

Now we calculate the update of  $\mathbf{V}_{(i),\tau}$  in one communication round. We summarize the result in the following lemma.

**Lemma 20** *If we choose the stepsize  $\eta_\tau \leq \min \left\{ \frac{M_3}{2}, \frac{\sqrt{M_3}}{\sqrt{6+12M_1+M_1^2}} \right\} \frac{1}{G_{max,op}\sqrt{r}}$ , the update of  $\mathbf{V}_n$  is given by:*

$$\mathbf{V}_{(i),\tau+1} = \mathbf{V}_{(i),\tau} + \eta_\tau \square \mathbf{V}_{(i),\tau} - \eta_\tau \mathbf{U}_\tau \square \mathbf{U}_\tau^T \mathbf{V}_{(i),\tau} + \eta_\tau^2 \mathbf{e}_{5,(i),\tau}$$

where  $\mathbf{e}_{5,(i),\tau}$  is an error term that satisfies:

$$\|\mathbf{e}_{5,(i),\tau}\| \leq C_{5,0} \|\square \mathbf{U}_\tau\|^2 + C_{5,1} \|\square \mathbf{V}_{(i),\tau}\|^2$$

where  $C_{5,0}$  and  $C_{5,1}$  are two constants that only depend on  $M_1$  and  $M_2$  from the generalized retraction definition 5.

**Proof** We firstly calculate the projection:

$$\begin{aligned} & \mathbf{U}_{\tau+1} \mathbf{U}_{\tau+1}^T \\ &= (\mathbf{U}_\tau + \eta_\tau \square \mathbf{U}_\tau + \eta_\tau^2 \mathbf{e}_{1,\tau}) (\mathbf{U}_\tau + \eta_\tau \square \mathbf{U}_\tau + \eta_\tau^2 \mathbf{e}_{1,\tau})^T \\ &= \mathbf{U}_\tau \mathbf{U}_\tau^T + \eta_\tau (\mathbf{U}_\tau \square \mathbf{U}_\tau^T + \square \mathbf{U}_\tau \mathbf{U}_\tau^T) + \eta_\tau^2 \mathbf{e}_{2,(i),\tau} \end{aligned}$$

where  $\mathbf{e}_{2,(i),\tau}$  is defined as:

$$\mathbf{e}_{2,(i),\tau} = \square \mathbf{U}_\tau \square \mathbf{U}_\tau^T + \mathbf{U}_\tau \mathbf{e}_{1,(i),\tau}^T + \mathbf{e}_{1,(i),\tau} \mathbf{U}_\tau^T + \eta_\tau \square \mathbf{U}_\tau \mathbf{e}_{1,(i),\tau}^T + \eta \mathbf{e}_{1,(i),\tau} \square \mathbf{U}_\tau^T + \eta^2 \mathbf{e}_{1,(i),\tau} \mathbf{e}_{1,(i),\tau}^T$$

Its norm is upper bounded by:

$$\begin{aligned}
 & \|e_{2,(i),\tau}\|_F \\
 & \leq \|\square U_\tau\|_F^2 + 2\|U_\tau\|_{op} \|e_{1,(i),\tau}\|_F + 2\eta_\tau \|\square U_\tau\|_F \|e_{1,(i),\tau}\|_F + \eta_\tau^2 \|e_{1,(i),\tau}\|_F^2 \\
 & \leq \|\square U_\tau\|_F^2 + 2M_1 \|\square U_\tau\|_F^2 + 2\eta_\tau M_1 \|\square U_\tau\|_F^3 + \eta_\tau^2 M_1^2 \|\square U_\tau\|_F^4 \\
 & \leq (1 + 3M_1 + \frac{1}{4}M_1^2) \|\square U_\tau\|_F^2
 \end{aligned}$$

where the final inequality comes from upper bound (55) and the choice of stepsize  $\eta_\tau$ :

$$\eta_\tau \leq \frac{1}{G_{max,op}\sqrt{r}} \frac{1}{\sqrt{6+12M_1+M_1^2}} \leq \frac{1}{2G_{max,op}\sqrt{r}}.$$

Similarly, we define  $e_{3,(i),\tau}$  as:

$$\eta_\tau^2 e_{3,(i),\tau} = \frac{1}{\eta_\tau^2} \left( V_{(i),\tau+\frac{1}{2}} - V_{(i),\tau} - \eta_\tau \square V_{(i),\tau} \right)$$

By definition of a retraction, the norm of  $e_{3,(i),\tau}$  is upper bounded by:

$$\|e_{3,(i),\tau}\|_F \leq M_1 \|\square V_{(i),\tau}\|_F^2$$

Then

$$\begin{aligned}
 & U_{\tau+1} U_{\tau+1}^T V_{(i),\tau+\frac{1}{2}} \\
 & = U_\tau U_\tau^T V_{(i),\tau+\frac{1}{2}} + \eta_\tau (U_\tau \square U_\tau^T + \square U_\tau U_\tau^T) V_{(i),\tau+\frac{1}{2}} + \eta_\tau^2 e_{2,(i),\tau} V_{(i),\tau+\frac{1}{2}} \\
 & = U_\tau U_\tau^T (V_{(i),\tau} + \eta_\tau \square V_{(i),\tau} + \eta_\tau^2 e_{3,(i),\tau}) \\
 & + \eta_\tau (U_\tau \square U_\tau^T + \square U_\tau U_\tau^T) (V_{(i),\tau} + \eta_\tau \square V_{(i),\tau} + \eta_\tau^2 e_{3,(i),\tau}) + \eta_\tau^2 e_{2,(i),\tau} V_{(i),\tau+\frac{1}{2}} \\
 & = \eta_\tau U_\tau \square U_\tau^T V_{(i),\tau} + \eta_\tau^2 U_\tau U_\tau^T e_{3,(i),\tau} + \eta_\tau^2 e_{2,(i),\tau} V_{(i),\tau+\frac{1}{2}} + \eta_\tau^2 U_\tau \square U_\tau^T \square V_{(i),\tau} \\
 & + \eta_\tau^3 (U_\tau \square U_\tau^T + \square U_\tau U_\tau^T) e_{3,(i),\tau} \\
 & = \eta_\tau U_\tau \square U_\tau^T V_{(i),\tau} + \eta_\tau^2 e_{4,(i),\tau}
 \end{aligned}$$

where we use  $e_{4,(i),\tau}$  to denote:

$$e_{4,(i),\tau} = U_\tau U_\tau^T e_{3,(i),\tau} + e_{2,(i),\tau} V_{(i),\tau+\frac{1}{2}} + U_\tau \square U_\tau^T \square V_{(i),\tau} + \eta_\tau (U_\tau \square U_\tau^T + \square U_\tau U_\tau^T) e_{3,(i),\tau}$$

Its norm is upper bounded as:

$$\begin{aligned}
 & \|e_{4,(i),\tau}\|_F \\
 & \leq \|e_{3,(i),\tau}\|_F + \|e_{2,(i),\tau}\|_F + \|\square U_\tau\|_F \|\square V_{(i),\tau}\|_F + \eta_\tau (\|\square U_\tau\|_F + \|\square V_{(i),\tau}\|_F) \|e_{3,(i),\tau}\|_F \\
 & \leq C_{4,0} \|\square U_\tau\|_F^2 + C_{4,1} \|\square V_{(i),\tau}\|_F^2
 \end{aligned}$$

where

$$C_{4,0} = \frac{3}{2} + 3M_1 + \frac{1}{4}M_1^2$$

and

$$C_{4,1} = \frac{1}{2} + 2M_1$$

Thus we know when  $\eta_\tau \leq \min\{\frac{M_3}{2}, \sqrt{\frac{M_3}{4C_{4,0}}}\} \frac{1}{G_{max,op}\sqrt{r}}$ ,  $\|U_{\tau+1}U_{\tau+1}^T V_{(i),\tau+\frac{1}{2}}\|_F \leq M_3$

Next we calculate the projection  $\mathcal{P}_{\mathcal{N}_{V_{(i),\tau+\frac{1}{2}}}}(-U_{\tau+1}U_{\tau+1}^T V_{(i),\tau+\frac{1}{2}})$ :

$$\begin{aligned} \mathcal{P}_{\mathcal{N}_{V_{(i),\tau+\frac{1}{2}}}}(-U_{\tau+1}U_{\tau+1}^T V_{(i),\tau+\frac{1}{2}}) &= -V_{(i),\tau+\frac{1}{2}} \left( V_{(i),\tau+\frac{1}{2}}^T U_{\tau+1}U_{\tau+1}^T V_{(i),\tau+\frac{1}{2}} \right) \\ &= \eta_\tau^2 V_{(i),\tau+\frac{1}{2}} V_{(i),\tau+\frac{1}{2}}^T e_{4,(i),\tau} \end{aligned}$$

We use  $e_{5,(i),\tau}$  to denote the difference between  $\mathcal{GR}_{V_{(i),\tau+\frac{1}{2}}}(-U_{\tau+1}U_{\tau+1}^T V_{(i),\tau+\frac{1}{2}})$  and  $V_{(i),\tau} + \eta_\tau \square V_{(i),\tau} - \eta_\tau U_\tau \square U_\tau^T V_{(i),\tau}$ , then its norm is upper bounded by:

$$\begin{aligned} &\eta_\tau^2 \|e_{5,(i),\tau}\|_F \\ &= \left\| \mathcal{GR}_{V_{(i),\tau+\frac{1}{2}}}(-U_{\tau+1}U_{\tau+1}^T V_{(i),\tau+\frac{1}{2}}) - V_{(i),\tau} - \eta_\tau \square V_{(i),\tau} + \eta_\tau U_\tau \square U_\tau^T V_{(i),\tau} \right\|_F \\ &\leq \left\| \mathcal{GR}_{V_{(i),\tau+\frac{1}{2}}}(-U_{\tau+1}U_{\tau+1}^T V_{(i),\tau+\frac{1}{2}}) - V_{(i),\tau+\frac{1}{2}} + U_{\tau+1}U_{\tau+1}^T V_{(i),\tau+\frac{1}{2}} \right\|_F \\ &\quad + \left\| V_{(i),\tau+\frac{1}{2}} - U_{\tau+1}U_{\tau+1}^T V_{(i),\tau+\frac{1}{2}} - V_{(i),\tau} - \eta_\tau \square V_{(i),\tau} + \eta_\tau U_\tau \square U_\tau^T V_{(i),\tau} \right\|_F \end{aligned}$$

By property 2 of the generalized retraction in Definition 5, we have:

$$\begin{aligned} &\left\| \mathcal{GR}_{V_{(i),\tau+\frac{1}{2}}}(-U_{\tau+1}U_{\tau+1}^T V_{(i),\tau+\frac{1}{2}}) - \left( V_{(i),\tau+\frac{1}{2}} - U_{\tau+1}U_{\tau+1}^T V_{(i),\tau+\frac{1}{2}} \right) \right\|_F \\ &\leq M_1 \left\| \mathcal{P}_{\mathcal{T}_{V_{(i),\tau+\frac{1}{2}}}}(-U_{\tau+1}U_{\tau+1}^T V_{(i),\tau+\frac{1}{2}}) \right\|_F^2 + (M_2 + 1) \left\| \mathcal{P}_{\mathcal{N}_{V_{(i),\tau+\frac{1}{2}}}}(-U_{\tau+1}U_{\tau+1}^T V_{(i),\tau+\frac{1}{2}}) \right\|_F \\ &\leq M_1 \left\| -U_{\tau+1}U_{\tau+1}^T V_{(i),\tau+\frac{1}{2}} \right\|_F^2 + (M_2 + 1) \eta_\tau^2 \left\| V_{(i),\tau+\frac{1}{2}} V_{(i),\tau+\frac{1}{2}}^T e_{4,(i),\tau} \right\|_F \\ &= M_1 \left\| \eta_\tau U_\tau \square U_\tau^T V_{(i),\tau} + \eta_\tau^2 e_{4,(i),\tau} \right\|_F^2 + (M_2 + 1) \eta_\tau^2 \left\| V_{(i),\tau+\frac{1}{2}} V_{(i),\tau+\frac{1}{2}}^T e_{4,(i),\tau} \right\|_F \\ &\leq 2M_1 \eta_\tau^2 \left( \left\| U_\tau \square U_\tau^T V_{(i),\tau} \right\|_F^2 + \eta_\tau^4 \left\| e_{4,(i),\tau} \right\|_F^2 \right) + (M_2 + 1) \eta_\tau^2 \left\| V_{(i),\tau+\frac{1}{2}} V_{(i),\tau+\frac{1}{2}}^T e_{4,(i),\tau} \right\|_F \\ &\leq \eta_\tau^2 \left\| \square U_\tau \right\|_F^2 (2M_1(C_{4,0} + C_{4,1})C_{4,0} + 2M_1 + M_2 C_{4,0}) \\ &\quad + \eta_\tau^2 \left\| \square V_{(i),\tau} \right\|_F^2 (2M_1(C_{4,0} + C_{4,1})C_{4,1} + M_2 C_{4,1}) \end{aligned}$$

For the second part:

$$\begin{aligned} &\left\| V_{(i),\tau+\frac{1}{2}} - U_{\tau+1}U_{\tau+1}^T V_{(i),\tau+\frac{1}{2}} - V_{(i),\tau} - \eta_\tau \square V_{(i),\tau} + \eta_\tau U_\tau \square U_\tau^T V_{(i),\tau} \right\|_F \\ &= \eta_\tau^2 \|e_{3,(n),\tau} - e_{4,(n),\tau}\|_F \\ &\leq \eta_\tau^2 \|e_{3,(n),\tau}\|_F + \eta_\tau^2 \|e_{4,(n),\tau}\|_F \end{aligned}$$

Therefore, the norm of  $e_{5,(i),\tau}$  is upper bounded as:

$$\begin{aligned} &\|e_{5,(i),\tau}\|_F \\ &\leq \left\| \square U_\tau \right\|_F^2 (2M_1(C_{4,0} + C_{4,1})C_{4,0} + 2M_1 + M_2 C_{4,0} + C_{4,0}) \\ &\quad + \left\| \square V_{(i),\tau} \right\|_F^2 (2M_1(C_{4,0} + C_{4,1})C_{4,1} + M_2 C_{4,1} + M_1 + C_{4,1}) \end{aligned}$$

This completes our proof, with

$$C_{5,0} = \frac{1}{8} (12 (M_2 + 1) + M_1 (24M_2 + M_1 (M_1 (M_1 + 32) + 254) + 2 (M_2 + 109)) + 88))$$

and

$$C_{5,1} = M_1^4 + \frac{81M_1^3}{4} + 13M_1^2 + (2M_2 + 5) M_1 + \frac{1}{2} (M_2 + 1)$$

■

The following lemma shows the sufficient decrease property:

**Lemma 21** (*Formal version of Lemma 9*) *When we choose the stepsize  $\eta_\tau \leq \frac{1}{G_{max,op}\sqrt{r}} \min \left\{ \frac{M_3}{2}, \frac{\sqrt{M_3}}{\sqrt{6+12M_1+M_1^2}} \right\}$ , and  $\mathbf{U}_\tau$  and  $\mathbf{V}_{(i),\tau}$  satisfy the orthogonality condition  $\mathbf{U}_\tau^T \mathbf{V}_{(i),\tau} = 0$ , we have:*

$$\begin{aligned} & \left\langle \sum_{i=1}^N \nabla_{\mathbf{U}} \mathcal{L}_{(i),1}(\mathbf{U}_\tau, \mathbf{V}_{(i),\tau}), \mathbf{U}_{\tau+1} - \mathbf{U}_\tau \right\rangle \\ & + \sum_{i=1}^N \left\langle \nabla_{\mathbf{V}_{(i)}} \mathcal{L}_{(i),1}(\mathbf{U}_\tau, \mathbf{V}_{(i),\tau}) + \nabla_{\mathbf{V}_{(i)}} \mathcal{L}_{(i),2}(\mathbf{U}_\tau, \mathbf{V}_{(i),\tau}), \mathbf{V}_{(i),\tau+1} - \mathbf{V}_{(i),\tau} \right\rangle \\ & \leq -\eta_\tau N \|\square \mathbf{U}_\tau\|_F^2 - \eta_\tau \sum_{i=1}^N \|\square \mathbf{V}_{(i),\tau}\|_F^2 + \eta_\tau^2 \left( C_{6,0} N \|\square \mathbf{U}_\tau\|_F^2 + C_{6,1} \sum_{i=1}^N \|\square \mathbf{V}_{(i),\tau}\|_F^2 \right) \end{aligned} \quad (60)$$

where  $C_{6,0}$  and  $C_{6,1}$  are constants dependent only on  $M_1$ ,  $M_2$ ,  $r$ , and  $G_{max,op}$ .

$$C_{6,0} = G_{max,op}\sqrt{r}(M_1 + C_{5,0})$$

and

$$C_{6,1} = G_{max,op}\sqrt{r}C_{5,1}$$

**Proof** We firstly calculate the sufficient decrease of  $\mathbf{U}$ :

$$\begin{aligned}
& \left\langle \sum_{i=1}^N \nabla_{\mathbf{U}} \mathcal{L}_{(i),1}(\mathbf{U}_\tau, \mathbf{V}_{(i),\tau}), \mathbf{U}_{\tau+1} - \mathbf{U}_\tau \right\rangle \\
&= \left\langle - \sum_{i=1}^N (\mathbf{I} - \mathbf{P}_{\mathbf{V}_{(i),\tau}}) \mathbf{S}_{(i)} \mathbf{U}_\tau, \mathbf{U}_{\tau+1} - \mathbf{U}_\tau \right\rangle \\
&= - \left\langle \sum_{i=1}^N (\mathbf{I} - \mathbf{P}_{\mathbf{V}_{(i),\tau}}) \mathbf{S}_{(i)} \mathbf{U}_\tau, \frac{\eta_\tau}{N} \sum_{i=1}^N (\mathbf{I} - \mathbf{P}_{\mathbf{V}_{(i),\tau}} - \mathbf{P}_{\mathbf{U}_\tau}) \mathbf{S}_{(i)} \mathbf{U}_\tau + \eta_\tau^2 \mathbf{e}_{1,\tau} \right\rangle \\
&= - \left\langle \sum_{i=1}^N (\mathbf{I} - \mathbf{P}_{\mathbf{V}_{(i),\tau}}) \mathbf{S}_{(i)} \mathbf{U}_\tau, \frac{\eta_\tau}{N} \sum_{i=1}^N (\mathbf{I} - \mathbf{P}_{\mathbf{V}_{(i),\tau}} - \mathbf{P}_{\mathbf{U}_\tau}) \mathbf{S}_{(i)} \mathbf{U}_\tau \right\rangle \\
&\quad - \left\langle \sum_{i=1}^N (\mathbf{I} - \mathbf{P}_{\mathbf{V}_{(i),\tau}}) \mathbf{S}_{(i)} \mathbf{U}_\tau, \eta_\tau^2 \mathbf{e}_{1,\tau} \right\rangle \\
&= - \left\langle \sum_{i=1}^N (\mathbf{I} - \mathbf{P}_{\mathbf{V}_{(i),\tau}} - \mathbf{P}_{\mathbf{U}_\tau}) \mathbf{S}_{(i)} \mathbf{U}_\tau, \frac{\eta_\tau}{N} \sum_{i=1}^N (\mathbf{I} - \mathbf{P}_{\mathbf{V}_{(i),\tau}} - \mathbf{P}_{\mathbf{U}_\tau}) \mathbf{S}_{(i)} \mathbf{U}_\tau \right\rangle \\
&\quad - \left\langle \sum_{i=1}^N (\mathbf{I} - \mathbf{P}_{\mathbf{V}_{(i),\tau}}) \mathbf{S}_{(i)} \mathbf{U}_\tau, \eta_\tau^2 \mathbf{e}_{1,\tau} \right\rangle \\
&\leq -\eta_\tau N \|\square \mathbf{U}_\tau\|_F^2 + \eta_\tau^2 \|\mathbf{e}_{1,\tau}\|_F \sum_{i=1}^N \left\| (\mathbf{I} - \mathbf{P}_{\mathbf{V}_{(i),\tau}}) \mathbf{S}_{(i)} \mathbf{U}_\tau \right\|_F \\
&\leq -\eta_\tau N \|\square \mathbf{U}_\tau\|_F^2 + M_1 \eta_\tau^2 \|\square \mathbf{U}_\tau\|_F^2 \sum_{i=1}^N G_{(i),op} \sqrt{r}
\end{aligned}$$

Next, we calculate:

$$\begin{aligned}
& \left\langle \nabla_{\mathbf{V}_{(i)}} \mathcal{L}_{(i),1}(\mathbf{U}_\tau, \mathbf{V}_{(i),\tau}) + \nabla_{\mathbf{V}_{(i)}} \mathcal{L}_{(i),2}(\mathbf{U}_\tau, \mathbf{V}_{(i),\tau}), \mathbf{V}_{(i),\tau+1} - \mathbf{V}_{(i),\tau} \right\rangle \\
&= \left\langle -(\mathbf{I} - \mathbf{P}_{\mathbf{U}_\tau}) \mathbf{S}_{(i)} \mathbf{V}_{(i),\tau}, \eta_\tau \square \mathbf{V}_{(i),\tau} + \eta_\tau \mathbf{U}_\tau \square \mathbf{U}_\tau^T \mathbf{V}_{(i),\tau} + \eta_\tau^2 \mathbf{e}_{5,(i),\tau} \right\rangle \\
&= \left\langle -(\mathbf{I} - \mathbf{P}_{\mathbf{U}_\tau}) \mathbf{S}_{(i)} \mathbf{V}_{(i),\tau}, \eta_\tau \square \mathbf{V}_{(i),\tau} \right\rangle + \left\langle -(\mathbf{I} - \mathbf{P}_{\mathbf{U}_\tau}) \mathbf{S}_{(i)} \mathbf{V}_{(i),\tau}, \eta_\tau \mathbf{U}_\tau \square \mathbf{U}_\tau^T \mathbf{V}_{(i),\tau} \right\rangle \\
&\quad + \left\langle -(\mathbf{I} - \mathbf{P}_{\mathbf{U}_\tau}) \mathbf{S}_{(i)} \mathbf{V}_{(i),\tau}, \eta_\tau^2 \mathbf{e}_{5,(i),\tau} \right\rangle \\
&= \left\langle -(\mathbf{I} - \mathbf{P}_{\mathbf{U}_\tau} - \mathbf{P}_{\mathbf{V}_{(i),\tau}}) \mathbf{S}_{(i)} \mathbf{V}_{(i),\tau}, \eta_\tau \square \mathbf{V}_{(i),\tau} \right\rangle + \left\langle -(\mathbf{I} - \mathbf{P}_{\mathbf{U}_\tau}) \mathbf{S}_{(i)} \mathbf{V}_{(i),\tau}, \eta_\tau^2 \mathbf{e}_{5,(i),\tau} \right\rangle \\
&\leq -\eta_\tau \|\square \mathbf{V}_{(i),\tau}\|_F^2 + \eta_\tau^2 \|(\mathbf{I} - \mathbf{P}_{\mathbf{U}_\tau}) \mathbf{S}_{(i)} \mathbf{V}_{(i),\tau}\|_F \|\mathbf{e}_{5,(i),\tau}\|_F \\
&\leq -\eta_\tau \|\square \mathbf{V}_{(i),\tau}\|_F^2 + \eta_\tau^2 G_{(i),op} \sqrt{r} \left( C_{5,0} \|\square \mathbf{U}_\tau\|_F^2 + C_{5,1} \|\square \mathbf{V}_{(i),\tau}\|^2 \right)
\end{aligned}$$

Adding them, we have:

$$\begin{aligned}
 & \left\langle \sum_{i=1}^N \nabla_U \mathcal{L}_{(i),1}(\mathbf{U}_\tau, \mathbf{V}_{(i),\tau}), \mathbf{U}_{\tau+1} - \mathbf{U}_\tau \right\rangle \\
 & + \left\langle \nabla_{\mathbf{V}_{(i)}} \mathcal{L}_{(i),1}(\mathbf{U}_\tau, \mathbf{V}_{(i),\tau}) + \nabla_{\mathbf{V}_{(i)}} \mathcal{L}_{(i),2}(\mathbf{U}_\tau, \mathbf{V}_{(i),\tau}), \mathbf{V}_{(i),\tau+1} - \mathbf{V}_{(i),\tau} \right\rangle \\
 & \leq -\eta_\tau N \|\square \mathbf{U}_\tau\|_F^2 - \sum_{i=1}^N \eta_\tau \|\square \mathbf{V}_{(i),\tau}\|_F^2 + \eta_\tau^2 \left( NC_{6,0} \|\square \mathbf{U}_\tau\|_F^2 + C_{6,1} \sum_{i=1}^N \|\square \mathbf{V}_{(i),\tau}\|_F^2 \right)
 \end{aligned}$$

where the constants are:

$$C_{6,0} = G_{max,op} \sqrt{r} (M_1 + C_{5,0})$$

and

$$C_{6,1} = G_{max,op} \sqrt{r} C_{5,1}$$

■

Finally we come to the proof of Theorem 8.

**Proof** We choose constant stepsize  $\eta_\tau = \eta_1$  small enough:

$$\begin{aligned}
 \eta_1 \leq \eta_c = \min & \left\{ \frac{1}{2C_{6,0} + L \left( \left( \left( 1 + \frac{M_2}{2} \right)^2 + 2 \left( 1 + \frac{C_{5,0}}{2} \right)^2 \right) \right)}, \frac{1}{2C_{6,1} + 2L \left( 1 + \frac{C_{5,1}}{2} \right)^2}, \right. \\
 & \left. \frac{1}{G_{max,op} \sqrt{r}} \frac{M_3}{2}, \frac{1}{G_{max,op} \sqrt{r}} \frac{\sqrt{M_3}}{\sqrt{6 + 12M_1 + M_1^2}} \right\}
 \end{aligned} \tag{61}$$

Obviously,  $\eta_\tau$  satisfies the requirement in Lemma 20 and 21.

By the property of Lipschitz continuity, we have:

$$\begin{aligned}
 \mathcal{L}_{(i)}(\mathbf{U}_{\tau+1}, \mathbf{V}_{(i),\tau+1}) & \leq \mathcal{L}_{(i)}(\mathbf{U}_\tau, \mathbf{V}_{(i),\tau}) \\
 & + \langle \nabla_U \mathcal{L}_{(i)}(\mathbf{U}_\tau, \mathbf{V}_{(i),\tau}), \mathbf{U}_{\tau+1} - \mathbf{U}_\tau \rangle + \langle \nabla_{\mathbf{V}_{(i)}} \mathcal{L}_{(i)}(\mathbf{U}_\tau, \mathbf{V}_{(i),\tau}), \mathbf{V}_{(i),\tau+1} - \mathbf{V}_{(i),\tau} \rangle \\
 & + \frac{L}{2} \left( \|\mathbf{V}_{(i),\tau+1} - \mathbf{V}_{(i),\tau}\|_F^2 + \|\mathbf{U}_{\tau+1} - \mathbf{U}_\tau\|_F^2 \right)
 \end{aligned}$$

where  $L$  is defined in (52). Since  $\mathbf{U}_{\tau+1}^T \mathbf{V}_{(i),\tau+1} = 0$  and  $\mathbf{U}_\tau^T \mathbf{V}_{(i),\tau} = 0$ , we know that

$$\mathcal{L}_{(i)}(\mathbf{U}_{\tau+1}, \mathbf{V}_{(i),\tau+1}) = -f_i(\mathbf{U}_{\tau+1}, \mathbf{V}_{(i),\tau+1})$$

and that

$$\mathcal{L}_{(i)}(\mathbf{U}_\tau, \mathbf{V}_{(i),\tau}) = -f_i(\mathbf{U}_\tau, \mathbf{V}_{(i),\tau})$$

Then, summing up both sides for  $n$  from 1 to  $N$ , we have:

$$\begin{aligned}
 & -f(\mathbf{U}_{\tau+1}, \{\mathbf{V}_{(i),\tau+1}\}) \leq -f(\mathbf{U}_\tau, \{\mathbf{V}_{(i),\tau}\}) \\
 & + \left\langle \sum_{i=1}^N \nabla_U \mathcal{L}_{(i)}(\mathbf{U}_\tau, \mathbf{V}_{(i),\tau}), \mathbf{U}_{\tau+1} - \mathbf{U}_\tau \right\rangle + \sum_{i=1}^N \langle \nabla_{\mathbf{V}_{(i)}} \mathcal{L}_{(i)}(\mathbf{U}_\tau, \mathbf{V}_{(i),\tau}), \mathbf{V}_{(i),\tau+1} - \mathbf{V}_{(i),\tau} \rangle \\
 & + \sum_{i=1}^N \frac{L}{2} \left( \|\mathbf{V}_{(i),\tau+1} - \mathbf{V}_{(i),\tau}\|_F^2 + \|\mathbf{U}_{\tau+1} - \mathbf{U}_\tau\|_F^2 \right)
 \end{aligned}$$

From equation (57), we know

$$\begin{aligned}
& \|\mathbf{U}_{\tau+1} - \mathbf{U}_\tau\|_F \\
&= \|\eta_\tau \square \mathbf{U}_\tau + \eta_\tau^2 \mathbf{e}_{1,\tau}\|_F \\
&\leq \eta_\tau \|\square \mathbf{U}_\tau\|_F + \|\eta_\tau^2 \mathbf{e}_{1,\tau}\|_F \\
&\leq \eta_\tau \|\square \mathbf{U}_\tau\|_F + \eta_\tau^2 M_1 \|\square \mathbf{U}_\tau\|_F^2 \\
&\leq \eta_\tau (1 + \frac{M_1}{2}) \|\square \mathbf{U}_\tau\|_F
\end{aligned}$$

Similarly, from Lemma 20, we have:

$$\begin{aligned}
& \|\mathbf{V}_{(i),\tau+1} - \mathbf{V}_{(i),\tau}\|_F \\
&= \|\eta_\tau \square \mathbf{V}_{(i),\tau} + \eta_\tau \mathbf{U}_\tau \square \mathbf{U}_\tau^T \mathbf{V}_{(i),\tau} + \eta_\tau^2 \mathbf{e}_{5,(i),\tau}\|_F \\
&\leq \eta_\tau \|\square \mathbf{V}_{(i),\tau}\|_F + \eta_\tau \|\mathbf{U}_\tau \square \mathbf{U}_\tau^T \mathbf{V}_{(i),\tau}\|_F + \eta_\tau^2 \|\mathbf{e}_{5,(i),\tau}\|_F \\
&\leq \eta_\tau \|\square \mathbf{V}_{(i),\tau}\|_F + \eta_\tau \|\square \mathbf{U}_\tau\|_F + \eta_\tau^2 \|\mathbf{e}_{5,(i),\tau}\|_F \\
&\leq \eta_\tau \|\square \mathbf{U}_\tau\|_F (1 + C_{5,0} \eta_\tau \|\square \mathbf{U}_\tau\|_F) + \eta_\tau \|\square \mathbf{V}_{(i),\tau}\|_F (1 + C_{5,1} \eta_\tau \|\square \mathbf{V}_{(i),\tau}\|_F) \\
&\leq \eta_\tau \|\square \mathbf{V}_{(i),\tau}\|_F \left(1 + \frac{1}{2} C_{5,1}\right) + \eta_\tau \|\square \mathbf{U}_\tau\|_F \left(1 + \frac{1}{2} C_{5,0}\right)
\end{aligned}$$

Combining the two inequalities and Lemma 21, we have:

$$\begin{aligned}
& -f(\mathbf{U}_{\tau+1}, \{\mathbf{V}_{(i),\tau+1}\}) \\
&\leq -f(\mathbf{U}_\tau, \{\mathbf{V}_{(i),\tau}\}) - \eta_\tau \left( N \|\square \mathbf{U}_\tau\|_F^2 + \sum_{i=1}^N \|\square \mathbf{V}_{(i),\tau}\|_F^2 \right) \\
&+ \eta_\tau^2 N C_{6,0} \|\square \mathbf{U}_\tau\|_F^2 + \eta_\tau^2 \sum_{i=1}^N C_{6,1} \|\square \mathbf{V}_{(i),\tau}\|_F^2 \\
&+ \eta_\tau^2 \frac{L}{2} \sum_{i=1}^N \left( \left( \left(1 + \frac{M_2}{2}\right)^2 + 2 \left(1 + \frac{C_{5,0}}{2}\right)^2 \right) \|\square \mathbf{U}_\tau\|_F^2 + 2 \left(1 + \frac{C_{5,1}}{2}\right)^2 \|\square \mathbf{V}_{(i),\tau}\|_F^2 \right) \\
&\leq -f(\mathbf{U}_\tau, \{\mathbf{V}_{(i),\tau}\}) - \frac{\eta_\tau}{2} \left( N \|\square \mathbf{U}_\tau\|_F^2 + \sum_{i=1}^N \|\square \mathbf{V}_{(i),\tau}\|_F^2 \right)
\end{aligned} \tag{62}$$

Summing up both sides for  $\tau$  from 1 to  $R$  and rearranging terms, we have:

$$\frac{\eta_1}{2} \sum_{\tau=1}^R \left( N \|\square \mathbf{U}_\tau\|_F^2 + \sum_{i=1}^N \|\square \mathbf{V}_{(i),\tau}\|_F^2 \right) \leq f^* - f(\mathbf{U}_1, \{\mathbf{v}_{(i),1}\})$$

As a result,

$$\min_{\tau \in \{1, \dots, N\}} \sum_{\tau=1}^R \left( N \|\square \mathbf{U}_\tau\|_F^2 + \sum_{i=1}^N \|\square \mathbf{V}_{(i),\tau}\|_F^2 \right) \leq \frac{2(f^* - f(\mathbf{U}_1, \{\mathbf{v}_{(i),1}\}))}{R\eta_1}$$

This completes the proof of Theorem 8. Notice that  $C_{6,0}$ ,  $C_{6,1}$ , and  $L$  are of the order  $G_{max,op}\sqrt{r}$ , thus the requirement on  $\eta_c$  in equation (61) becomes:

$$\eta_c = C_\eta \frac{1}{G_{max,op}\sqrt{r}}$$

where  $C_\eta$  is a constant that only depends on  $M_1$ ,  $M_2$ , and  $M_3$  from the generalized retraction definition 5. ■

## D. Proof for local exponential convergence

For simplicity, we introduce a few additional notations.

At communication round  $\tau$ , suppose the global and local PCs are  $\{\mathbf{u}_{\tau,k}\}_{k=1,\dots,r}$  and  $\{\mathbf{v}_{(i),\tau,k}\}_{i=1,\dots,N,k=1,\dots,r}$ , and they satisfy the requirement in Theorem 10. Then we can introduce  $\mathbf{U}_\tau^\star$  and  $\mathbf{V}_{(i),\tau}^\star$ 's defined by

$$\mathbf{U}_\tau^\star = \Pi_g \mathbf{U}_\tau ((\mathbf{U}_\tau)^T \Pi_g \mathbf{U}_\tau)^{-1/2} \quad (63)$$

and

$$\mathbf{V}_{(i),\tau}^\star = \Pi_{(i)} \mathbf{V}_{(i),\tau} \left( \mathbf{V}_{(i),\tau}^T \Pi_{(i)} \mathbf{V}_{(i),\tau} \right)^{-1/2} \quad (64)$$

for each  $n = 1, \dots, N$ .

It's easy to verify that

$$\mathbf{U}_\tau^\star (\mathbf{U}_\tau^\star)^T = \Pi_g$$

and that

$$\mathbf{V}_{(i),\tau}^\star (\mathbf{V}_{(i),\tau}^\star)^T = \Pi_{(i)}$$

Notice that  $\mathbf{U}_\tau^\star$  and  $\mathbf{V}_{(i),\tau}^\star$ 's are one global optimal solution, but not the unique global optimal solution. The  $\mathbf{U}_\tau^\star$  and  $\mathbf{V}_{(i),\tau}^\star$ 's are dependent on communication  $\tau$ . We use  $\Delta \mathbf{U}_\tau$  to denote the difference between  $\mathbf{U}_\tau$  and  $\mathbf{U}_\tau^\star$ :

$$\Delta \mathbf{U}_\tau = \mathbf{U}_\tau - \mathbf{U}_\tau^\star \quad (65)$$

and similarly:

$$\Delta \mathbf{V}_{(i),\tau} = \mathbf{V}_{(i),\tau} - \mathbf{V}_{(i),\tau}^\star \quad (66)$$

The following lemma presents a lower bound on the norm of the updates:

**Lemma 22** (*Formal version of Lemma 11*) (*Personalized gradient dominance property*)  
 Suppose  $\mathbf{U}_\tau^\star$  and  $\mathbf{V}_{(i),\tau}^\star$ 's are defined by equation (63) and (64), where  $\mathbf{U}_\tau$  and  $\mathbf{V}_{(i),\tau}$  are the global and local principal vectors at round  $\tau$ , then the following inequality holds:

$$\begin{aligned} & N \left\| \left( \mathbf{I} - \mathbf{P}_{\mathbf{U}_\tau} - \sum_{j=1}^N \frac{1}{N} \mathbf{P}_{\mathbf{V}_{(j),\tau}} \right) \mathbf{U}_\tau^\star \right\|_F^2 + \sum_{i=1}^N \left\| \left( \mathbf{I} - \mathbf{P}_{\mathbf{U}_\tau} - \mathbf{P}_{\mathbf{V}_{(i),\tau}} \right) \mathbf{V}_{(i),\tau}^\star \right\|_F^2 \\ & \geq N \ell(\theta) \zeta_\tau - C_9 \zeta_\tau^{1.5} \end{aligned} \quad (67)$$

where  $\ell(\theta)$  is:

$$\ell(\theta) = \frac{\theta^2}{2 - \theta + \sqrt{(2 - \theta)^2 - \theta^2}} \quad (68)$$

**Proof**

We begin by analyzing the first term in the inequality. By Definitions (65) and (66), for any  $i$ , we know that:

$$\begin{aligned} & \left( \mathbf{I}_d - \mathbf{U}_\tau \mathbf{U}_\tau^T - \mathbf{V}_{(i),\tau} \mathbf{V}_{(i),\tau}^T \right) \mathbf{U}_\tau^* \\ &= \left( \mathbf{I}_d - \mathbf{U}_\tau^* (\mathbf{U}_\tau^*)^T - \mathbf{V}_{(i),\tau}^* (\mathbf{V}_{(i),\tau}^*)^T \right) \mathbf{U}_\tau^* \\ & - \left( \Delta \mathbf{U}_\tau (\mathbf{U}_\tau^*)^T + \Delta \mathbf{V}_{(i),\tau} (\mathbf{V}_{(i),\tau}^*)^T + \mathbf{V}_{(i),\tau}^* (\Delta \mathbf{V}_{(i),\tau})^T \right) \mathbf{U}_\tau^* \\ & - \left( \Delta \mathbf{U}_\tau (\Delta \mathbf{U}_\tau)^T + \Delta \mathbf{V}_{(i),\tau} (\Delta \mathbf{V}_{(i),\tau})^T + \mathbf{U}_{\tau,*} (\Delta \mathbf{U}_\tau)^T \right) \mathbf{U}_\tau^* \end{aligned} \quad (69)$$

The first term is 0 by the definition of  $\mathbf{U}^*$  and  $\mathbf{V}_{(i)}^*$ . The second term is the leading term.

The norm of the third term is bounded as:

$$\begin{aligned} & \left\| \left( \Delta \mathbf{U}_\tau (\Delta \mathbf{U}_\tau)^T + \Delta \mathbf{V}_{(i),\tau} (\Delta \mathbf{V}_{(i),\tau})^T \right) \mathbf{U}_\tau^* \right\|_F \\ & \leq \left( \|\Delta \mathbf{U}_\tau\|_F^2 + \|\Delta \mathbf{V}_{(i),\tau}\|_F^2 \right) \end{aligned}$$

Then

$$\begin{aligned} & \frac{1}{N} \sum_{i=1}^N \left( \mathbf{I}_d - \mathbf{U}_\tau \mathbf{U}_\tau^T - \mathbf{V}_{(i),\tau} \mathbf{V}_{(i),\tau}^T \right) \mathbf{U}_\tau^* \\ & + \frac{1}{N} \sum_{i=1}^N \left( \Delta \mathbf{U}_\tau (\mathbf{U}_\tau^*)^T + \Delta \mathbf{V}_{(i),\tau} (\mathbf{V}_{(i),\tau}^*)^T + \mathbf{V}_{(i),\tau}^* (\Delta \mathbf{V}_{(i),\tau})^T \right) \mathbf{U}_\tau^* \\ & = -\frac{1}{N} \sum_{i=1}^N \left( \Delta \mathbf{U}_\tau (\Delta \mathbf{U}_\tau)^T + \Delta \mathbf{V}_{(i),\tau} (\Delta \mathbf{V}_{(i),\tau})^T + \mathbf{U}_{\tau,*} (\Delta \mathbf{U}_\tau)^T \right) \mathbf{U}_\tau^* \\ & = \boldsymbol{\epsilon}_{1,(0),\tau} \end{aligned}$$

where  $\boldsymbol{\epsilon}_{1,(0),\tau}$  is defined as:

$$\begin{aligned} & \boldsymbol{\epsilon}_{1,(0),\tau} \\ & = -\frac{1}{N} \sum_{i=1}^N \left( \Delta \mathbf{U}_\tau (\Delta \mathbf{U}_\tau)^T + \Delta \mathbf{V}_{(i),\tau} (\Delta \mathbf{V}_{(i),\tau})^T + \mathbf{U}_{\tau,*} (\Delta \mathbf{U}_\tau)^T \right) \mathbf{U}_\tau^* \end{aligned}$$

Its norm is bounded by:

$$\left\| \boldsymbol{\epsilon}_{1,(0),\tau} \right\|_F \leq \frac{1}{N} \sum_{i=1}^N \left( \|\Delta \mathbf{U}_\tau\|_F^2 + \|\Delta \mathbf{V}_{(i),\tau}\|_F^2 \right)$$

The update of  $\mathbf{V}_{(i)}$  can be estimated similarly:

$$\begin{aligned}
 & \left( \mathbf{I}_d - \mathbf{U}_\tau \mathbf{U}_\tau^T - \mathbf{V}_{(i),\tau} \mathbf{V}_{(i),\tau}^T \right) \mathbf{V}_{(i),\tau}^* \\
 &= \left( \mathbf{I}_d - \mathbf{U}_\tau^* (\mathbf{U}_\tau^*)^T - \mathbf{V}_{(i),\tau}^* (\mathbf{V}_{(i),\tau}^*)^T \right) \mathbf{V}_{(i),\tau}^* \\
 &= \left( \Delta \mathbf{U}_\tau (\mathbf{U}_\tau^*)^T + \mathbf{U}_{\tau,*} (\Delta \mathbf{U}_\tau)^T + \Delta \mathbf{V}_{(i),\tau} (\mathbf{V}_{(i),\tau}^*)^T \right) \mathbf{V}_{(i),\tau}^* \\
 &= \left( \Delta \mathbf{U}_\tau (\Delta \mathbf{U}_\tau)^T + \Delta \mathbf{V}_{(i),\tau} (\Delta \mathbf{V}_{(i),\tau})^T + \mathbf{V}_{(i),\tau}^* (\Delta \mathbf{V}_{(i),\tau})^T \right) \mathbf{V}_{(i),\tau}^*
 \end{aligned} \tag{70}$$

Similarly, we can define

$$\boldsymbol{\epsilon}_{1,(i),\tau} = - \left( \Delta \mathbf{U}_\tau (\Delta \mathbf{U}_\tau)^T + \Delta \mathbf{V}_{(i),\tau} (\Delta \mathbf{V}_{(i),\tau})^T \right) \mathbf{U}_\tau^*$$

Its norm is upper bounded by:

$$\|\boldsymbol{\epsilon}_{1,(i),\tau}\| \leq \|\Delta \mathbf{U}_\tau\|_F^2 + \|\Delta \mathbf{V}_{(i),\tau}\|_F^2$$

We define  $\boldsymbol{\nu}_\tau$  as the vectorization of  $\Delta \mathbf{U}_\tau$  and  $\Delta \mathbf{V}_{(i),\tau}$ 's:

$$\boldsymbol{\nu}_\tau = \text{vec} \left( [\Delta \mathbf{U}_\tau, \Delta \mathbf{V}_{(1),\tau}, \dots, \Delta \mathbf{V}_{(N),\tau}] \right) \tag{71}$$

and  $\widetilde{\boldsymbol{\nu}}_\tau$  as:

$$\widetilde{\boldsymbol{\nu}}_\tau = \text{vec} \left( \left[ \sqrt{N} \Delta \mathbf{U}_\tau, \Delta \mathbf{V}_{(1),\tau}, \dots, \Delta \mathbf{V}_{(N),\tau} \right] \right) \tag{72}$$

By Lemma 17, we have:

$$\begin{aligned}
 \|\widetilde{\boldsymbol{\nu}}_\tau\| &= \sqrt{N \|\Delta \mathbf{U}_\tau\|_F^2 + \sum_{i=1}^N \|\Delta \mathbf{V}_{(i),\tau}\|_F^2} \\
 &\geq \sqrt{N \zeta_{(0),\tau} + \sum_{i=1}^N \zeta_{(i),\tau}} \\
 &= \sqrt{N \zeta_\tau}
 \end{aligned}$$

and similarly,  $\|\boldsymbol{\nu}_\tau\| \leq \sqrt{2} \sqrt{\zeta_\tau}$ .

We define  $\boldsymbol{\omega}$  as the vectorization of  $\left( \mathbf{I} - \mathbf{P}_{\mathbf{U}_\tau} - \sum_{j=1}^N \frac{1}{N} \mathbf{P}_{\mathbf{V}_{(j),\tau}} \right) \mathbf{U}_\tau^*$  and  $\left( \mathbf{I} - \mathbf{P}_{\mathbf{U}_\tau} - \mathbf{P}_{\mathbf{V}_{(i),\tau}} \right) \mathbf{V}_{(i),\tau}^*$ 's:

$$\begin{aligned}
 \boldsymbol{\omega} &= \text{vec} \left( \left[ \left( \mathbf{I} - \mathbf{P}_{\mathbf{U}_\tau} - \sum_{j=1}^N \frac{1}{N} \mathbf{P}_{\mathbf{V}_{(j),\tau}} \right) \mathbf{U}_\tau^*, \right. \right. \\
 &\quad \left. \left( \mathbf{I} - \mathbf{P}_{\mathbf{U}_\tau} - \mathbf{P}_{\mathbf{V}_{(1),\tau}} \right) \mathbf{V}_{(1),\tau}^*, \dots, \left( \mathbf{I} - \mathbf{P}_{\mathbf{U}_\tau} - \mathbf{P}_{\mathbf{V}_{(i),\tau}} \right) \mathbf{V}_{(i),\tau}^*, \dots, \left( \mathbf{I} - \mathbf{P}_{\mathbf{U}_\tau} - \mathbf{P}_{\mathbf{V}_{(N),\tau}} \right) \mathbf{V}_{(N),\tau}^* \right] \right)
 \end{aligned} \tag{73}$$

and  $\boldsymbol{\varsigma}$  as the vectorization of  $\boldsymbol{\epsilon}_{1,(0),\tau}$  and  $\boldsymbol{\epsilon}_{1,(i),\tau}$ 's:

$$\boldsymbol{\varsigma} = \text{vec} \left( [\boldsymbol{\epsilon}_{1,(0),\tau}, \dots, \boldsymbol{\epsilon}_{1,(i),\tau}] \right) \tag{74}$$

By Lemma 17, we have:

$$\begin{aligned}
\|\varsigma\| &= \sqrt{\sum_{i=0}^N \|\epsilon_{1,(i),\tau}\|_F^2} \\
&\leq \sum_{i=0}^N \|\epsilon_{1,(i),\tau}\|_F \\
&\leq \frac{N+1}{N} \left( N \|\Delta \mathbf{U}_\tau\|_F^2 + \sum_{i=1}^N \|\Delta \mathbf{V}_{(i),\tau}\|_F^2 \right) \\
&\leq 2(N+1)\zeta_\tau
\end{aligned}$$

Remember that we use  $\mathcal{D}_{a,b,c}$  to denote a  $(b+c) \times (b+c)$  diagonal matrix, whose first  $b$  diagonal entries are  $a$  and remaining  $c$  diagonal entries are 1.

By definition of vectorization, we have:

$$\boldsymbol{\omega}_\tau^T \mathcal{D}_{N,rd,Nrd} \boldsymbol{\omega}_\tau = N \left\| \left( \mathbf{I} - \mathbf{P}_{\mathbf{U}_\tau} - \sum_{j=1}^N \frac{1}{N} \mathbf{P}_{\mathbf{V}_{(j),\tau}} \right) \mathbf{U}_\tau^* \right\|_F^2 + \sum_{i=1}^N \left\| \left( \mathbf{I} - \mathbf{P}_{\mathbf{U}_\tau} - \mathbf{P}_{\mathbf{V}_{(i),\tau}} \right) \mathbf{V}_{(i),\tau}^* \right\|_F^2 \quad (75)$$

With the vectorized matrices, we can rewrite equations (69) and (70) into the following vector form:

$$\boldsymbol{\omega}_\tau = A_\tau \boldsymbol{\nu}_\tau + \boldsymbol{\varsigma}_\tau \quad (76)$$

where  $A_\tau$  is an  $rd(N+1)$  by  $rd(N+1)$  matrix. It has a block structure:

$$A_\tau = \begin{pmatrix} A_{00} & A_{01} & A_{02} & \cdots & A_{0N} \\ A_{10} & A_{11} & 0 & \cdots & 0 \\ A_{20} & 0 & A_{22} & \cdots & 0 \\ \vdots & \vdots & \vdots & \ddots & \vdots \\ A_{N0} & 0 & 0 & \cdots & A_{NN} \end{pmatrix}$$

And the blocks are:

$$A_{00} = \mathbf{I}_r \otimes \mathbf{I}_d \quad (77)$$

For  $i \in \{1, \dots, N\}$ , we have:

$$A_{0i} = \frac{1}{N} \begin{pmatrix} \mathbf{v}_{(i),1}^* (\mathbf{u}_{\tau,1}^*)^T & \mathbf{v}_{(i),2}^* (\mathbf{u}_{\tau,1}^*)^T & \cdots & \mathbf{v}_{(i),r}^* (\mathbf{u}_{\tau,1}^*)^T \\ \mathbf{v}_{(i),1}^* (\mathbf{u}_{\tau,2}^*)^T & \mathbf{v}_{(i),2}^* (\mathbf{u}_{\tau,2}^*)^T & \cdots & \mathbf{v}_{(i),r}^* (\mathbf{u}_{\tau,2}^*)^T \\ \vdots & \vdots & \ddots & \vdots \\ \mathbf{v}_{(i),1}^* (\mathbf{u}_{\tau,r}^*)^T & \mathbf{v}_{(i),2}^* (\mathbf{u}_{\tau,r}^*)^T & \cdots & \mathbf{v}_{(i),r}^* (\mathbf{u}_{\tau,r}^*)^T \end{pmatrix} \quad (78)$$

The diagonal block is also:

$$A_{ii} = \mathbf{I}_r \otimes \mathbf{I}_d \quad (79)$$

The off-diagonal block is defined as:

$$A_{i0} = N A_{0i}^T \quad (80)$$

Therefore:

$$\begin{aligned}
 & \omega_\tau^T \mathcal{D}_{N,rd,Nrd} \omega_\tau \\
 &= \nu_\tau^T A_\tau^T \mathcal{D}_{N,rd,Nrd} A_\tau \nu_\tau \\
 &+ \nu_\tau^T A_\tau^T \mathcal{D}_{N,rd,Nrd} \varsigma_\tau + \varsigma_\tau^T \mathcal{D}_{N,rd,Nrd} A_\tau \nu_\tau + \varsigma_\tau^T \mathcal{D}_{N,rd,Nrd} \varsigma_\tau \\
 &\geq \nu_\tau^T A_\tau^T \mathcal{D}_{N,rd,Nrd} A_\tau \nu_\tau - 2 \|\varsigma_\tau\| \|\mathcal{D}_{N,rd,Nrd}\|_{op} \|A_\tau \nu_\tau\| \\
 &\geq \nu_\tau^T A_\tau^T \mathcal{D}_{N,rd,Nrd} A_\tau \nu_\tau - 2 \|\varsigma_\tau\| \|\mathcal{D}_{N,rd,Nrd}\|_{op} \|A_\tau\|_{op} \|\nu_\tau\| \\
 &\geq \tilde{\nu}_\tau^T \mathcal{D}_{\frac{1}{\sqrt{N}},rd,Nrd} A_\tau^T \mathcal{D}_{N,rd,Nrd} A_\tau \mathcal{D}_{\frac{1}{\sqrt{N}},rd,Nrd} \tilde{\nu}_\tau - 4(N+1)\zeta_\tau N \sqrt{2(N+1)} \sqrt{2\zeta_\tau} \\
 &\geq \|\tilde{\nu}_\tau\|^2 \lambda_{\min} \left( \mathcal{D}_{\frac{1}{\sqrt{N}},rd,Nrd} A_\tau^T \mathcal{D}_{N,rd,Nrd} A_\tau \mathcal{D}_{\frac{1}{\sqrt{N}},rd,Nrd} \right) - C_9 N \zeta_\tau^{1.5}
 \end{aligned} \tag{81}$$

where we applied Lemma 25 in the third inequality.  $C_9$  is a constant defined as:

$$C_9 = 8(N+1)\sqrt{N+1}$$

We can introduce:

$$B = (A_{01} \ A_{02} \ \cdots \ A_{0N})$$

Then  $A_\tau$  satisfies the definition of  $\theta$ -block-arrowhead matrix in Lemma 12. As shown in Lemma 12 and Sec. E, the minimum eigenvalue of  $\mathcal{Q}(A_\tau)$  is lower bounded by  $\lambda_{\min} \left( \mathcal{D}_{\frac{1}{\sqrt{N}},rd,Nrd} A_\tau^T \mathcal{D}_{N,rd,Nrd} A_\tau \mathcal{D}_{\frac{1}{\sqrt{N}},rd,Nrd} \right) \geq \ell(\theta)$ . As a result:

$$\begin{aligned}
 & \omega_\tau^T \mathcal{D}_{N,rd,Nrd} \omega_\tau \\
 &\geq \|\tilde{\nu}_\tau\|^2 \ell(\theta) - C_9 N \zeta_\tau^{1.5} \\
 &\geq N \zeta_\tau \ell(\theta) - C_9 N \zeta_\tau^{1.5}
 \end{aligned}$$

By the application of (75), we prove the inequality (67). ■

Remember that we introduced  $\zeta_{(i),\tau}$ 's and  $\zeta_\tau$  in (30), (31), and (32). Now we define some similar variables:

$$\tilde{\zeta}_{(i),\tau} = 2r - \left\langle \mathbf{P}_{U_\tau} + \mathbf{P}_{V_{(i),\tau}}, \mathbf{\Pi}_g + \mathbf{\Pi}_{(i)} \right\rangle \tag{82}$$

for each  $i = 1, \dots, N$ . We use  $\zeta_\tau$  to denote:

$$\tilde{\zeta}_\tau = \sum_{i=1}^N \zeta_{(i),\tau} \tag{83}$$

From Lemma 2, there exists a relation between  $\zeta_\tau$  and  $\tilde{\zeta}_\tau$ :

$$\frac{\theta}{2} N \zeta_\tau \leq \tilde{\zeta}_\tau \leq N \zeta_\tau \tag{84}$$

The following lemma establishes a Polyak-Lojasiewicz-style inequality for the update.

**Lemma 23** Suppose  $\mu$  is the lowest minimum eigenvalue of  $\{\mathbf{S}_{(i)}\}_{i=1,\dots,N}$ , and  $\square \mathbf{U}_\tau$  and  $\square \mathbf{V}_{(i),\tau}$ 's are defined in (54) and (58), we have:

$$N \|\square \mathbf{U}_\tau\|_F^2 + \sum_{i=1}^N \|\square \mathbf{V}_{(i),\tau}\|_F^2 \geq \mu^2 \ell(\theta) \zeta_\tau - C_{10} \zeta_\tau^{1.5} \quad (85)$$

where  $C_{10}$  is a constant:

$$C_{10} = \mu^2 C_9 + 2\sqrt{2}N(1 + \sqrt{N})G_{max,op}^2 \leq O(N^{1.5}G_{max,op}^2)$$

**Proof** We first calculate  $\square \mathbf{U}_\tau$

$$\begin{aligned} \square \mathbf{U}_\tau &= \frac{1}{N} \sum_{i=1}^N \left( \mathbf{I} - \mathbf{P}_{\mathbf{U}_\tau} - \mathbf{P}_{\mathbf{V}_{(i),\tau}} \right) \mathbf{S}_{(i)} \mathbf{U}_\tau \\ &= \frac{1}{N} \sum_{i=1}^N \left( \mathbf{I} - \mathbf{P}_{\mathbf{U}_\tau} - \mathbf{P}_{\mathbf{V}_{(i),\tau}} \right) \mathbf{S}_{(i)} \mathbf{U}_\tau^* + \frac{1}{N} \sum_{i=1}^N \left( \mathbf{I} - \mathbf{P}_{\mathbf{U}_\tau} - \mathbf{P}_{\mathbf{V}_{(i),\tau}} \right) \mathbf{S}_{(i)} (\mathbf{U}_\tau - \mathbf{U}_\tau^*) \\ &= \square \mathbf{U}_{\tau,1} + \square \mathbf{U}_{\tau,2} \end{aligned}$$

where

$$\square \mathbf{U}_{\tau,1} = \frac{1}{N} \sum_{i=1}^N \left( \mathbf{I} - \mathbf{P}_{\mathbf{U}_\tau} - \mathbf{P}_{\mathbf{V}_{(i),\tau}} \right) \mathbf{S}_{(i)} \mathbf{U}_\tau^*$$

and

$$\square \mathbf{U}_{\tau,2} = \frac{1}{N} \sum_{i=1}^N \left( \mathbf{I} - \mathbf{P}_{\mathbf{U}_\tau} - \mathbf{P}_{\mathbf{V}_{(i),\tau}} \right) \mathbf{S}_{(i)} (\mathbf{U}_\tau - \mathbf{U}_\tau^*)$$

We bound the norm of  $\square \mathbf{U}_{\tau,2}$  as:

$$\begin{aligned} &\|\square \mathbf{U}_{\tau,2}\|_F \\ &= \left\| \frac{1}{N} \sum_{i=1}^N \left( \mathbf{I} - \mathbf{P}_{\mathbf{U}_\tau} - \mathbf{P}_{\mathbf{V}_{(i),\tau}} \right) \mathbf{S}_{(i)} (\mathbf{U}_\tau - \mathbf{U}_\tau^*) \right\|_F \\ &\leq \frac{1}{N} \sum_{i=1}^N \left\| \left( \mathbf{I} - \mathbf{P}_{\mathbf{U}_\tau} - \mathbf{P}_{\mathbf{V}_{(i),\tau}} \right) \mathbf{S}_{(i)} (\mathbf{U}_\tau - \mathbf{U}_\tau^*) \right\|_F \\ &= \frac{1}{N} \sum_{i=1}^N \left\| \left( \mathbf{I} - \mathbf{P}_{\mathbf{U}_\tau} - \mathbf{P}_{\mathbf{V}_{(i),\tau}} \right) (\mathbf{\Pi}_g + \mathbf{\Pi}_{(i)}) \mathbf{S}_{(i)} (\mathbf{\Pi}_g + \mathbf{\Pi}_{(i)}) (\mathbf{U}_\tau - \mathbf{U}_\tau^*) \right\|_F \\ &\leq \frac{1}{N} \sum_{i=1}^N \left\| \left( \mathbf{I} - \mathbf{P}_{\mathbf{U}_\tau} - \mathbf{P}_{\mathbf{V}_{(i),\tau}} \right) (\mathbf{\Pi}_g + \mathbf{\Pi}_{(i)}) \right\|_F \|\mathbf{S}_{(i)}\|_{op} \|(\mathbf{\Pi}_g + \mathbf{\Pi}_{(i)}) (\mathbf{U}_\tau - \mathbf{U}_\tau^*)\|_F \end{aligned}$$

By Lemma 17, we know that:

$$\begin{aligned} &\|(\mathbf{\Pi}_g + \mathbf{\Pi}_{(i)}) (\mathbf{U}_\tau - \mathbf{U}_\tau^*)\|_F \\ &\leq \|\mathbf{\Pi}_g + \mathbf{\Pi}_{(i)}\|_{op} \|\mathbf{U}_\tau - \mathbf{U}_\tau^*\|_F \\ &= \|\Delta \mathbf{U}_\tau\|_F \\ &\leq \|\Delta \mathbf{U}_\tau, \Delta \mathbf{V}_{(i),\tau}\|_F \\ &\leq \sqrt{2} \sqrt{\tilde{\zeta}_{(i),\tau}} \end{aligned}$$

Also,

$$\left\| \left( \mathbf{I} - \mathbf{P}_{U_\tau} - \mathbf{P}_{V_{(i),\tau}} \right) (\mathbf{\Pi}_g + \mathbf{\Pi}_{(i)}) \right\|_F = \sqrt{\tilde{\zeta}_{(i),\tau}}$$

Combining them, we have:

$$\begin{aligned} & \left\| \frac{1}{N} \sum_{i=1}^N \left( \mathbf{I} - \mathbf{P}_{U_\tau} - \mathbf{P}_{V_{(i),\tau}} \right) \mathbf{S}_{(i)} (\mathbf{U}_\tau - \mathbf{U}_\tau^*) \right\|_F \\ & \leq \frac{1}{N} \sum_{i=1}^N \sqrt{2} G_{(i),op} \tilde{\zeta}_{(i),\tau} \\ & \leq \sqrt{2} G_{max,op} \zeta_\tau \end{aligned}$$

where we used Lemma 2 in the second inequality.

Also,

$$\begin{aligned} & \|\square \mathbf{U}_{\tau,1}\|_F \\ & = \left\| \frac{1}{N} \sum_{i=1}^N \left( \mathbf{I} - \mathbf{P}_{U_\tau} - \mathbf{P}_{V_{(i),\tau}} \right) \mathbf{S}_{(i)} \mathbf{U}_\tau^* \right\|_F \\ & \leq \frac{1}{N} \sum_{i=1}^N \left\| \left( \mathbf{I} - \mathbf{P}_{U_\tau} - \mathbf{P}_{V_{(i),\tau}} \right) \mathbf{S}_{(i)} \mathbf{U}_\tau^* \right\|_F \\ & = \frac{1}{N} \sum_{i=1}^N \left\| \left( \mathbf{I} - \mathbf{P}_{U_\tau} - \mathbf{P}_{V_{(i),\tau}} \right) (\mathbf{\Pi}_g + \mathbf{\Pi}_{(i)}) \mathbf{S}_{(i)} (\mathbf{\Pi}_g + \mathbf{\Pi}_{(i)}) \mathbf{U}_\tau^* \right\|_F \\ & \leq \frac{1}{N} \sum_{i=1}^N \left\| \left( \mathbf{I} - \mathbf{P}_{U_\tau} - \mathbf{P}_{V_{(i),\tau}} \right) (\mathbf{\Pi}_g + \mathbf{\Pi}_{(i)}) \right\|_F \|\mathbf{S}_{(i)}\|_{op} \|\mathbf{U}_\tau^*\|_{op} \\ & \leq \frac{1}{N} \sum_{i=1}^N \sqrt{\tilde{\zeta}_{(i),\tau}} G_{op,max} \\ & \leq \sqrt{\frac{1}{N} \sum_{i=1}^N \tilde{\zeta}_{(i),\tau}} G_{op,max} \\ & \leq \sqrt{\zeta_\tau} G_{op,max} \end{aligned}$$

For the update of  $\mathbf{V}_{(i),\tau}$

$$\begin{aligned} \square \mathbf{V}_{(i),\tau} &= \left( \mathbf{I} - \mathbf{P}_{U_\tau} - \mathbf{P}_{V_{(i),\tau}} \right) \mathbf{S}_{(i)} \mathbf{V}_{(i),\tau} \\ &= \left( \mathbf{I} - \mathbf{P}_{U_\tau} - \mathbf{P}_{V_{(i),\tau}} \right) \mathbf{S}_{(i)} \mathbf{V}_{(i),\tau}^* + \left( \mathbf{I} - \mathbf{P}_{U_\tau} - \mathbf{P}_{V_{(i),\tau}} \right) \mathbf{S}_{(i)} \left( \mathbf{V}_{(i),\tau} - \mathbf{V}_{(i),\tau}^* \right) \\ &= \square \mathbf{V}_{(i),\tau,1} + \square \mathbf{V}_{(i),\tau,2} \end{aligned}$$

where the first term is defined as:

$$\square \mathbf{V}_{(i),\tau,1} = \left( \mathbf{I} - \mathbf{P}_{U_\tau} - \mathbf{P}_{V_{(i),\tau}} \right) \mathbf{S}_{(i)} \mathbf{V}_{(i),\tau}^* \quad (86)$$

and the second term is defined as

$$\square \mathbf{V}_{(i),\tau,2} = \left( \mathbf{I} - \mathbf{P}_{\mathbf{U}_\tau} - \mathbf{P}_{\mathbf{V}_{(i),\tau}} \right) \mathbf{S}_{(i)} \left( \mathbf{V}_{(i),\tau} - \mathbf{V}_{(i),\tau}^* \right) \quad (87)$$

We can bound the norm of  $\square \mathbf{V}_{(i),\tau,2}$  as:

$$\begin{aligned} & \|\square \mathbf{V}_{(i),\tau,2}\|_F \\ &= \left\| \left( \mathbf{I} - \mathbf{P}_{\mathbf{U}_\tau} - \mathbf{P}_{\mathbf{V}_{(i),\tau}} \right) \mathbf{S}_{(i)} \left( \mathbf{V}_{(i),\tau} - \mathbf{V}_{(i),\tau}^* \right) \right\|_F \\ &\leq \left\| \left( \mathbf{I} - \mathbf{P}_{\mathbf{U}_\tau} - \mathbf{P}_{\mathbf{V}_{(i),\tau}} \right) (\mathbf{\Pi}_g + \mathbf{\Pi}_{(i)}) \mathbf{S}_{(i)} (\mathbf{\Pi}_g + \mathbf{\Pi}_{(i)}) \left( \mathbf{V}_{(i),\tau} - \mathbf{V}_{(i),\tau}^* \right) \right\|_F \\ &\leq \left\| \left( \mathbf{I} - \mathbf{P}_{\mathbf{U}_\tau} - \mathbf{P}_{\mathbf{V}_{(i),\tau}} \right) (\mathbf{\Pi}_g + \mathbf{\Pi}_{(i)}) \right\|_F \|\mathbf{S}_{(i)}\|_{op} \left\| (\mathbf{\Pi}_g + \mathbf{\Pi}_{(i)}) \left( \mathbf{V}_{(i),\tau} - \mathbf{V}_{(i),\tau}^* \right) \right\|_F \\ &\leq G_{max,op} \sqrt{2\tilde{\zeta}_{(i),\tau}} \end{aligned}$$

and bound the norm of  $\square \mathbf{V}_{\tau,1}$  as:

$$\begin{aligned} \|\square \mathbf{V}_{\tau,1}\|_F &\leq \left\| \left( \mathbf{I} - \mathbf{P}_{\mathbf{U}_\tau} - \mathbf{P}_{\mathbf{V}_{(i),\tau}} \right) \mathbf{S}_{(i)} \mathbf{U}_\tau^* \right\|_F \\ &= \left\| \left( \mathbf{I} - \mathbf{P}_{\mathbf{U}_\tau} - \mathbf{P}_{\mathbf{V}_{(i),\tau}} \right) \mathbf{S}_{(i)} \right\|_F \\ &\leq \left\| \left( \mathbf{I} - \mathbf{P}_{\mathbf{U}_\tau} - \mathbf{P}_{\mathbf{V}_{(i),\tau}} \right) (\mathbf{\Pi}_g + \mathbf{\Pi}_{(i)}) \right\|_F \|\mathbf{S}_{(i)}\|_{op} \\ &\leq G_{max,op} \sqrt{\tilde{\zeta}_{(i),\tau}} \end{aligned}$$

With the decomposition,

$$\square \mathbf{U}_\tau = \square \mathbf{U}_{\tau,1} + \square \mathbf{U}_{\tau,2}$$

and

$$\square \mathbf{V}_{(i),\tau} = \square \mathbf{V}_{(i),\tau,1} + \square \mathbf{V}_{(i),\tau,2}$$

we have:

$$\begin{aligned} & N \|\square \mathbf{U}_\tau\|_F^2 + \sum_{i=1}^N \|\square \mathbf{V}_{(i),\tau}\|_F^2 \\ &= N \|\square \mathbf{U}_{\tau,1} + \square \mathbf{U}_{\tau,2}\|_F^2 + \sum_{i=1}^N \|\square \mathbf{V}_{(i),\tau,1} + \square \mathbf{V}_{(i),\tau,2}\|_F^2 \\ &\geq N \|\square \mathbf{U}_{\tau,1}\|_F^2 - 2N \|\square \mathbf{U}_{\tau,2}\|_F \|\square \mathbf{U}_{\tau,1}\|_F \\ &\quad + \sum_{i=1}^N \|\square \mathbf{V}_{(i),\tau,1}\|_F^2 - 2 \|\square \mathbf{V}_{(i),\tau,1}\|_F \|\square \mathbf{V}_{(i),\tau,2}\|_F \end{aligned}$$

For the leading term, we have:

$$\begin{aligned}
 & N \|\square \mathbf{U}_{\tau,1}\|_F^2 + \sum_{i=1}^N \|\square \mathbf{V}_{(i),\tau,1}\|_F^2 \\
 &= N \text{Tr} \left( \left( \frac{1}{N} \sum_{i=1}^N (\mathbf{I} - \mathbf{P}_{\mathbf{U}_\tau} - \mathbf{P}_{\mathbf{V}_{(i),\tau}}) \right)^2 \mathbf{S}_{(i)} \mathbf{U}_\tau^* (\mathbf{U}_\tau^*)^T \mathbf{S}_{(i)} \right) \\
 &+ \sum_{i=1}^N \text{Tr} \left( \left( \mathbf{I} - \mathbf{P}_{\mathbf{U}_\tau} - \mathbf{P}_{\mathbf{V}_{(i),\tau}} \right)^2 \mathbf{S}_{(i)} \mathbf{V}_{(i),\tau}^* (\mathbf{V}_{(i),\tau}^*)^T \mathbf{S}_{(i)} \right)
 \end{aligned}$$

Since

$$\mathbf{S}_{(i)} \mathbf{U}_\tau^* (\mathbf{U}_\tau^*)^T \mathbf{S}_{(i)} \succeq \mu^2 \mathbf{U}_\tau^* (\mathbf{U}_\tau^*)^T$$

and

$$\mathbf{S}_{(i)} \mathbf{V}_{(i),\tau}^* (\mathbf{V}_{(i),\tau}^*)^T \mathbf{S}_{(i)} \succeq \mu^2 \mathbf{V}_{(i),\tau}^* (\mathbf{V}_{(i),\tau}^*)^T$$

By Lemma 13, we have:

$$\begin{aligned}
 & N \|\square \mathbf{U}_{\tau,1}\|_F^2 + \sum_{i=1}^N \|\square \mathbf{V}_{(i),\tau,1}\|_F^2 \\
 &\geq \mu^2 N \text{Tr} \left( \left( \frac{1}{N} \sum_{i=1}^N (\mathbf{I} - \mathbf{P}_{\mathbf{U}_\tau} - \mathbf{P}_{\mathbf{V}_{(i),\tau}}) \right)^2 \mathbf{U}_\tau^* (\mathbf{U}_\tau^*)^T \right) \\
 &+ \mu^2 \sum_{i=1}^N \text{Tr} \left( \left( \mathbf{I} - \mathbf{P}_{\mathbf{U}_\tau} - \mathbf{P}_{\mathbf{V}_{(i),\tau}} \right)^2 \mathbf{V}_{(i),\tau}^* (\mathbf{V}_{(i),\tau}^*)^T \right) \\
 &\geq \mu^2 (\ell(\theta) N \zeta_\tau - C_9 N \zeta_\tau^{1.5})
 \end{aligned}$$

where we use Lemma 22 in the last inequality with the condition that  $\ell(\theta) \zeta_\tau \geq C_9 \zeta_\tau^{1.5}$ .

For the cross terms, since we know that  $\|\square \mathbf{U}_{\tau,1}\|_F \leq \frac{1}{\sqrt{N}} \sqrt{r \tilde{\zeta}_\tau} G_{\max,F}$ , we can derive:

$$\begin{aligned}
 & 2N \|\square \mathbf{U}_{\tau,2}\|_F \|\square \mathbf{U}_{\tau,1}\|_F + 2 \sum_{i=1}^N \|\square \mathbf{V}_{(i),\tau,1}\|_F \|\square \mathbf{V}_{(i),\tau,2}\|_F \\
 &\leq 2\sqrt{2} N G_{\max,op}^2 \zeta_\tau^{1.5} + 2\sqrt{2} G_{\max,op}^2 \sum_{i=1}^N \tilde{\zeta}_{(i),\tau}^{1.5} \\
 &\leq 2\sqrt{2} N G_{\max,op}^2 \zeta_\tau^{1.5} + 2\sqrt{2} G_{\max,op}^2 N^{1.5} \left( \frac{1}{N} \sum_{i=1}^N \tilde{\zeta}_{(i),\tau} \right)^{1.5} \\
 &\leq 2\sqrt{2} N G_{\max,op}^2 \zeta_\tau^{1.5} + 2\sqrt{2} N^{1.5} G_{\max,op}^2 \zeta_\tau^{1.5} \\
 &= 2\sqrt{2} N (1 + \sqrt{N}) G_{\max,op}^2 \zeta_\tau^{1.5}
 \end{aligned}$$

Combining the inequalities, we have:

$$\begin{aligned} N \|\square \mathbf{U}_\tau\|_F^2 + \sum_{i=1}^N \|\square \mathbf{V}_{(i),\tau}\|_F^2 \\ \geq \mu^2 N \ell(\theta) \zeta_\tau - N C_{10} \zeta_\tau^{1.5} \end{aligned}$$

where  $C_{10} = \mu^2 C_9 + 2\sqrt{2}(1 + \sqrt{N})G_{max,op}^2$

This completes our proof. ■

**Lemma 24** *Suppose the optimal value of objective is  $f^*$ , we have:*

$$G_{max,op} \zeta_\tau \geq f^* - f(\mathbf{U}_\tau, \{\mathbf{V}_{(i),\tau}\})$$

**Proof** The proof is straightforward.

For the objective on client  $i$ , we have:

$$\begin{aligned} f_i^* - f_i &= \text{Tr}(\mathbf{S}_{(i)}(\mathbf{\Pi}_g + \mathbf{\Pi}_{(i)})) - \text{Tr}(\mathbf{S}_{(i)}(\mathbf{P}_{\mathbf{U}_\tau} + \mathbf{P}_{\mathbf{V}_{(i),\tau}})) \\ &= \text{Tr}(\mathbf{S}_{(i)}(\mathbf{\Pi}_g + \mathbf{\Pi}_{(i)})) - \text{Tr}((\mathbf{\Pi}_g + \mathbf{\Pi}_{(i)}) \mathbf{S}_{(i)}(\mathbf{\Pi}_g + \mathbf{\Pi}_{(i)}) (\mathbf{P}_{\mathbf{U}_\tau} + \mathbf{P}_{\mathbf{V}_{(i),\tau}})) \\ &= \text{Tr}(\mathbf{S}_{(i)}(\mathbf{\Pi}_g + \mathbf{\Pi}_{(i)})) - \text{Tr}(\mathbf{S}_{(i)}(\mathbf{\Pi}_g + \mathbf{\Pi}_{(i)}) (\mathbf{P}_{\mathbf{U}_\tau} + \mathbf{P}_{\mathbf{V}_{(i),\tau}}) (\mathbf{\Pi}_g + \mathbf{\Pi}_{(i)})) \\ &= \text{Tr}(\mathbf{S}_{(i)}(\mathbf{\Pi}_g + \mathbf{\Pi}_{(i)}) (\mathbf{I} - \mathbf{P}_{\mathbf{U}_\tau} - \mathbf{P}_{\mathbf{V}_{(i),\tau}}) (\mathbf{\Pi}_g + \mathbf{\Pi}_{(i)})) \\ &\leq G_{(i),op} \text{Tr}((\mathbf{\Pi}_g + \mathbf{\Pi}_{(i)}) (\mathbf{I} - \mathbf{P}_{\mathbf{U}_\tau} - \mathbf{P}_{\mathbf{V}_{(i),\tau}}) (\mathbf{\Pi}_g + \mathbf{\Pi}_{(i)})) \\ &= G_{(i),op} (2r - \text{Tr}((\mathbf{\Pi}_g + \mathbf{\Pi}_{(i)}) (\mathbf{P}_{\mathbf{U}_\tau} + \mathbf{P}_{\mathbf{V}_{(i),\tau}}))) \\ &= G_{(i),op} \tilde{\zeta}_{(i),\tau} \end{aligned}$$

where we apply the result in Lemma 13 and the fact that  $\mathbf{S}_{(i)} \preceq G_{(i),op}(\mathbf{\Pi}_g + \mathbf{\Pi}_{(i)})$ .

Then we can sum the above inequality for  $i$  from 1 to  $N$ :

$$\begin{aligned} \sum_{i=1}^N f_i^* - f_i &\leq \sum_{i=1}^N G_{(i),op} \zeta_{(i),\tau} \\ &\leq N G_{max,op} \zeta_\tau \end{aligned} \tag{88}$$

This completes the proof. ■

Finally we come to the proof of Theorem 10:

**Proof** Combining Lemma 23 and Lemma 24, we know that when  $\zeta_\tau$  is sufficiently small:

$$\sqrt{\zeta_\tau} \leq \frac{\ell(\theta)\mu^2}{2C_{10}} \leq O\left(\frac{\ell(\theta)\mu^2}{N^{1.5}G_{max,op}^2}\right)$$

we have:

$$\begin{aligned}
 & N \|\square \mathbf{U}_\tau\|_F^2 + \sum_{i=1}^N \|\square \mathbf{V}_{(i),\tau}\|_F^2 \\
 & \geq \mu^2 N \ell(\theta) \zeta_\tau - N C_{10} \zeta_\tau^{1.5} \\
 & \geq \frac{1}{2} \mu^2 N \ell(\theta) \zeta_\tau \\
 & \geq \frac{\mu^2 \ell(\theta)}{2 G_{max,op}} (f^* - f(\mathbf{U}_\tau, \{\mathbf{V}_{(i),\tau}\}))
 \end{aligned}$$

Therefore from equation 62, we know:

$$-f(\mathbf{U}_{\tau+1}, \{\mathbf{V}_{(i),\tau+1}\}) \leq -f(\mathbf{U}_\tau, \{\mathbf{V}_{(i),\tau}\}) - \frac{\eta_\tau \mu^2 \ell(\theta)}{4 N G_{max,op}} (f^* - f(\mathbf{U}_\tau, \{\mathbf{V}_{(i),\tau}\}))$$

We add  $f^*$  on both sides:

$$\begin{aligned}
 & f^* - f(\mathbf{U}_{\tau+1}, \{\mathbf{V}_{(i),\tau+1}\}) \\
 & \leq f^* - f(\mathbf{U}_\tau, \{\mathbf{V}_{(i),\tau}\}) - \frac{\eta_\tau \mu^2 \ell(\theta)}{4 G_{max,op}} (f^* - f(\mathbf{U}_\tau, \{\mathbf{V}_{(i),\tau}\})) \\
 & = \left(1 - \frac{\eta_\tau \mu^2 \ell(\theta)}{4 G_{max,op}}\right) (f^* - f(\mathbf{U}_\tau, \{\mathbf{V}_{(i),\tau}\}))
 \end{aligned}$$

This completes the proof of Theorem 10. ■

## E. The spectral analysis on $\theta$ -block-arrowhead matrix $A$

In this section, we will give a lower bound of the minimum eigenvalue of  $\theta$ -arrowhead matrices. The analysis has stand-alone value as no previous works on estimating eigenvalues of matrices can give reasonable results, to our best knowledge.

The lower bound on the minimum eigenvalue is nontrivial because  $A$  is nonsymmetric, and  $\mathcal{Q}(A) = \mathcal{D}_{\frac{1}{\sqrt{N}},rd,Nrd} A^T \mathcal{D}_{N,rd,Nrd} A \mathcal{D}_{\frac{1}{\sqrt{N}},rd,Nrd}$  is not necessarily diagonal dominant. Therefore, a bound given by conventional matrix perturbation theory like Gershgorin's circle theorem, becomes vacuous: the lower bound on the eigenvalue of a positive semidefinite matrix is negative. Our result is novel and applies to a general form of matrices.

The bound (34) is surprisingly tight. In some of our numerical simulations, the difference between  $\ell(\theta)$  and the numerical solution for the minimum eigenvalue is smaller than  $10^{-14}$ . We present the proof of Lemma 12:

**Proof** Remember that:

$$\mathcal{Q}(A) = \mathcal{D}_{\frac{1}{\sqrt{N}},rd,Nrd} A^T \mathcal{D}_{N,rd,Nrd} A \mathcal{D}_{\frac{1}{\sqrt{N}},rd,Nrd} = \begin{pmatrix} \mathbf{I} + N B B^T & 2\sqrt{N} B \\ 2\sqrt{N} B^T & \mathbf{I} + N B^T B \end{pmatrix}$$

Suppose  $\alpha = (\alpha_0^T, \alpha_1^T)^T$  is an eigenvector of matrix  $\mathcal{Q}(A)$  with corresponding eigenvalue  $\lambda$ :

$$\mathcal{Q}(A) \alpha = \lambda \alpha \tag{89}$$

The second block of the eigen-equations (89) is:

$$2\sqrt{N}B^T\alpha_0 + (\mathbf{I} + NB^TB)\alpha_1 = \lambda\alpha_1$$

We can solve for  $\alpha_1$ :

$$\alpha_1 = -2\sqrt{N}((1-\lambda)\mathbf{I} + NB^TB)^{-1}B^T\alpha_0$$

Plugging this into the first block of the eigen-equations (89):

$$(\mathbf{I} + NBB^T)\alpha_0 + 2\sqrt{N}B\alpha_1 = \lambda\alpha_0$$

we have:

$$(\mathbf{I} + NBB^T)\alpha_0 - 4NB((1-\lambda)\mathbf{I} + NB^TB)^{-1}B^T\alpha_0 = \lambda\alpha_0$$

Similarly, we can solve the above equation for  $\alpha_0$ :

$$\alpha_0 = 4N((1-\lambda)\mathbf{I} + N^2BB^T)^{-1}B((1-\lambda)\mathbf{I} + NB^TB)^{-1}B^T\alpha_0$$

By matrix inversion lemma, when  $\lambda < 1$ :

$$((1-\lambda)\mathbf{I} + NB^TB)^{-1} = \frac{1}{1-\lambda} \left( \mathbf{I} - B^T \left( \frac{\mathbf{I}}{N} + \frac{1}{1-\lambda}BB^T \right)^{-1} B \frac{1}{1-\lambda} \right)$$

With some algebra, we have:

$$\begin{aligned} & 4N((1-\lambda)\mathbf{I} + NBB^T)^{-1}B((1-\lambda)\mathbf{I} + NB^TB)^{-1}B^T \\ &= 4N((1-\lambda)\mathbf{I} + NBB^T)^{-1}B\frac{1}{1-\lambda} \left( \mathbf{I} - B^T \left( \frac{\mathbf{I}}{N} + \frac{1}{1-\lambda}BB^T \right)^{-1} B \frac{1}{1-\lambda} \right) B^T \\ &= 4((1-\lambda)\mathbf{I} + C_B)^{-1}C_B((1-\lambda)\mathbf{I} + C_B)^{-1} \end{aligned}$$

where  $C_B$  is a matrix defined as:

$$C_B = NBB^T$$

Note that the second assumption of Lemma 12 requires that

$$0 \preceq C_B \preceq (1-\theta)\mathbf{I}$$

Therefore, we can rewrite the eigen-equation on  $\alpha_0$  as:

$$\alpha_0 = 4((1-\lambda)\mathbf{I} + C_B)^{-1}C_B((1-\lambda)\mathbf{I} + C_B)^{-1}\alpha_0$$

The equation shows that  $\alpha_0$  is an eigenvector of  $4((1-\lambda)\mathbf{I} + C_B)^{-1}C_B((1-\lambda)\mathbf{I} + C_B)^{-1}$  with eigenvalue 1. As a result, the operator norm of the matrix should be no smaller than 1:

$$\lambda_{max} \left( 4((1-\lambda)\mathbf{I} + C_B)^{-1}C_B((1-\lambda)\mathbf{I} + C_B)^{-1} \right) \geq 1 \quad (90)$$

We now show, by contradiction, that  $\forall \lambda \in \mathbb{R}$  that satisfies the inequality (90), it must be lower bounded by  $\ell(\theta)$ :

$$\lambda \geq \ell(\theta) = \frac{\theta^2}{2 - \theta + \sqrt{(2 - \theta)^2 - \theta^2}} \quad (91)$$

Suppose there exists a  $\tilde{\lambda}$  such that:

$$0 \leq \tilde{\lambda} < \ell(\theta) \quad (92)$$

Since  $C_B$  is real symmetric positive semidefinite, by spectral theorem, it has eigen-decomposition

$$C_B = \sum_{i=1}^{rd} \lambda_{C_B,i} \vartheta_i \vartheta_i^T \quad (93)$$

with all eigenvalues bounded by:

$$0 \leq \lambda_{C_B,i} \leq 1 - \theta$$

Then,

$$4((1 - \lambda)\mathbf{I} + C_B)^{-1} C_B ((1 - \lambda)\mathbf{I} + C_B)^{-1} = 4 \sum_{i=1}^{rd} \frac{\lambda_{C_B,i}}{(1 - \lambda + \lambda_{C_B,i})^2} \vartheta_i \vartheta_i^T$$

The operator norm of  $4((1 - \lambda)\mathbf{I} + C_B)^{-1} C_B ((1 - \lambda)\mathbf{I} + C_B)^{-1}$  is defined as:

$$\begin{aligned} & \max_{\boldsymbol{\beta}} \boldsymbol{\beta}^T 4((1 - \lambda)\mathbf{I} + C_B)^{-1} C_B ((1 - \lambda)\mathbf{I} + C_B)^{-1} \boldsymbol{\beta} \\ & \text{such that } \|\boldsymbol{\beta}\| = 1 \end{aligned}$$

We can write the objective in summation form:

$$\begin{aligned} & \boldsymbol{\beta}^T 4((1 - \lambda)\mathbf{I} + C_B)^{-1} C_B ((1 - \lambda)\mathbf{I} + C_B)^{-1} \boldsymbol{\beta} \\ & = 4 \sum_{i=1}^{rd} \frac{\lambda_{C_B,i}}{((1 - \lambda) + \lambda_{C_B,i})^2} (\vartheta_i^T \boldsymbol{\beta})^2 \\ & \leq 4 \max_{i=1, \dots, rd} \frac{\lambda_{C_B,i}}{((1 - \lambda) + \lambda_{C_B,i})^2} \sum_{j=1}^{rd} (\vartheta_j^T \boldsymbol{\beta})^2 \\ & = 4 \max_{i=1, \dots, rd} \frac{\lambda_{C_B,i}}{((1 - \lambda) + \lambda_{C_B,i})^2} \end{aligned}$$

When  $\tilde{\lambda}$  satisfies the assumption (92),  $\tilde{\lambda} \leq \ell(\theta) \leq \theta$ , it is easy to verify that  $\frac{\lambda_{C_B,i}}{((1 - \tilde{\lambda}) + \lambda_{C_B,i})^2}$  is an increasing function of  $\lambda_{C_B,i}$  on  $[0, 1 - \theta]$ , therefore:

$$\frac{\lambda_{C_B,i}}{((1 - \tilde{\lambda}) + \lambda_{C_B,i})^2} \leq \frac{1 - \theta}{((1 - \tilde{\lambda}) + 1 - \theta)^2}$$

Since the right hand side is an increasing function of  $\tilde{\lambda}$  in the range specified by (92), we have:

$$\frac{1 - \theta}{\left((1 - \tilde{\lambda}) + 1 - \theta\right)^2} < \frac{1 - \theta}{\left((1 - \ell(\theta)) + 1 - \theta\right)^2} = \frac{1}{4}$$

which contradicts equation (90). This completes the proof. ■

Next we give an upper bound of the operator norm of  $A$ .

**Lemma 25** *The operator norm of a  $\theta$ -arrowhead matrix  $A$  is bounded by:*

$$\|A\|_{op} \leq \sqrt{2(N+1)} \quad (94)$$

**Proof** By decomposition

$$A = \mathbf{I} + \begin{pmatrix} 0 & B \\ NB^T & 0 \end{pmatrix}$$

we have:

$$A^T A = \begin{pmatrix} \mathbf{I} + N^2 BB^T & (N+1)B \\ (N+1)B^T & \mathbf{I} + B^T B \end{pmatrix}$$

Therefore,

$$\|A^T A\|_{op} = \left\| \begin{pmatrix} \mathbf{I} + N^2 BB^T & 0 \\ 0 & \mathbf{I} + B^T B \end{pmatrix} \right\|_{op} + \left\| \begin{pmatrix} 0 & (N+1)B \\ (N+1)B^T & 0 \end{pmatrix} \right\|_{op}$$

For the first term, since  $\|NBB^T\|_{op} \leq 1 - \theta \leq 1$ , and  $\|B^T B\|_{op} = \|BB^T\|_{op}$ , we know:

$$\left\| \begin{pmatrix} \mathbf{I} + N^2 BB^T & 0 \\ 0 & \mathbf{I} + B^T B \end{pmatrix} \right\|_{op} \leq 1 + N$$

For the second term, we have:

$$\left\| \begin{pmatrix} 0 & B \\ B^T & 0 \end{pmatrix} \right\|_{op}^2 = \left\| \begin{pmatrix} BB^T & 0 \\ 0 & B^T B \end{pmatrix} \right\|_{op} \leq \frac{1}{N}$$

Thus:

$$\|A^T A\|_{op} \leq 1 + N + (1 + N) \frac{1}{N} \leq 2(N+1)$$

We thus complete the proof. ■